

# **Identification and Characterization of Novel mTOR Splicing Isoforms**

**Zeyad Mohammad S Alharbi**

A thesis submitted to the University College of London in  
fulfilment with the requirements for the degree of Doctor of  
Philosophy

London, January 2015



**Research Department of Structural and Molecular Biology**

**University College London**

**Gower Street, London WC1E 6BT, United Kingdom**

## **Declaration**

I, Zeyad M. Raddadi Alharbi, declare that all work presented in this thesis is the result of my own work. The work presented here does not constitute part of any thesis. Where information has been derived from other sources, I confirm that this has been indicated in the thesis. The work herein was carried out while I was a graduate student at the University College London, Research Department of Structural and Molecular Biology under the supervision of Professor Ivan Gout.

Zeyad Alharbi

## Abstract

mTOR (mammalian target of rapamycin) is a serine/threonine protein kinase which belongs to the family of phosphoinositide 3-kinase related kinases (PIKK), which also includes ATR, ATM, DNA-PK, SMG1 and TRRAP. mTOR contains several conserved protein-protein interaction modules at the N-terminus and a protein kinase domain at the C-terminus. The regulatory interactions of mTOR are mainly mediated by HEAT (Huntingtin, Elongation factor 3, protein phosphatase 2A, and TOR1) repeats and FAT (FRAP, ATM and TRRAP) domains. In contrast to other PIKK family members, mTOR possesses a unique FRB (FKBP12/Rapamycin Binding) domain which mediates the interaction with the FKBP12/rapamycin inhibitory complex.

mTOR is a key component of two distinct multi-protein complexes in mammalian cells, termed mTOR complex 1 (TORC1) and mTOR complex 2 (TORC2). A diverse range of extracellular and intracellular signals stimulate both mTOR complexes to regulate cell growth, survival and proliferation. Dysregulation of mTOR signalling has been implicated in various human pathologies, including cancer, inflammation, neurodegenerative and metabolic disorders. Therefore, mTOR is an attractive target for drug discovery. In cancer research, mTOR inhibitors have shown a potent anti-proliferative activity in pre-clinical studies and several of these are currently being evaluated in clinical trials.

There is only one mTOR gene in higher vertebrates, which is known to encode two splicing isoforms: mTOR $\alpha$  and mTOR $\beta$ . In contrast to the full length mTOR $\alpha$  protein, mTOR $\beta$  lacks most of its protein-protein interaction modules, HEAT and FAT, but retains domains responsible for FKBP12/rapamycin binding, protein kinase activity and regulation. Importantly, mTOR $\beta$  was shown to shorten considerably the G1 phase of the cell cycle, to

stimulate cell proliferation and to possess oncogenic potential in cell-based and xenograft studies.

Like other PIKK family members, there is increasing evidence of the presence of mTOR splicing isoforms. The main aim of this study was to identify new mTOR splicing isoforms and to determine their molecular characterization. In addition we aim to explore the ability of these isoforms to phosphorylate known mTOR targets such as 4E-BP1. Furthermore, we aim to study the role of the new isoforms in the mTOR-mediated cellular processes, such as cell proliferation, and the contribution of the identified isoforms in the oncogenic characteristics of cells.

In this study, we have employed bioinformatics, biochemical, cell and molecular techniques to identify and characterize two novel mTOR splicing isoforms, denoted mTOR $\delta$  and mTOR $\gamma$ . When compared to mTOR $\alpha$ , the mTOR $\delta$  splice variant contains only the N-terminal HEAT repeats and a unique C-terminal region, while the mTOR $\gamma$  isoform possesses a 12 amino acid deletion in the kinase domain. The existence of the mTOR $\delta$  isoform was confirmed at mRNA and protein levels by identifying corresponding EST clones and detecting the splice variant with specific anti-mTOR $\delta$  antibodies. Furthermore, we have found several EST clones corresponding to the mTOR $\gamma$  splicing variant. In contrast to mTOR $\alpha$ , the stably expressed mTOR $\delta$  and mTOR $\gamma$  lack the kinase activity *in vitro*. It was also found that stable overexpression of mTOR $\delta$  and mTOR $\gamma$  splice variants in HEK293 cells inhibits cell proliferation and colony formation in soft agar. These findings suggest that identified novel isoforms have the potential to regulate the mTOR signalling pathway in a dominant-negative manner.

## **Acknowledgments**

I would like to express my sincere gratitude to my supervisor Professor Ivan Gout whose passion for science is truly inspiring, for offering me this PhD position, for the continuous support of my study, as well as for all his help and guidance during the production of my PhD thesis. His guidance helped me in all the time of research and writing of this thesis. I would also like to thank my committee members, Professor Elizabeth Shephard and Professor John Christodoulou for their advice on both research as well as on my career.

My sincere thanks also goes to Dr. Alexander Zhyvoloup for enlightening me the first glance of research.

My friends and colleagues made the time during the research unforgettable. Special thanks to Ahmed, Pascale, Lena, Yugo, Kamil and Mahmoud for all their help, humour and support. Also, thanks to all the girls and guys I met around the department and shared a joke with from time to time. You all made life more enjoyable. I would also like to thank all of my friends who supported me and encouraged me to strive towards my goal.

Last but not the least a special thanks to my family for spurring me on to complete this thesis and for all their support during my studies and in particular my mother who spent sleepless nights praying for me and was always my support in the moments where I needed support.

## Table of contents

Declaration .....	2
Abstract .....	3
Acknowledgments .....	5
List of Figure .....	12
Abbreviations .....	17
Chapter 1: General Introduction .....	24
1.1 mTOR, an overview .....	24
1.1.1 The mTOR Structure .....	25
1.1.2 mTOR Complexes in mammalian cells .....	28
1.1.2.1 mTORC1 .....	30
1.1.2.2 mTORC2 .....	31
1.1.2.3 Regulation of mTOR .....	32
1.1.2.3.1 mTORC1 regulation .....	32
1.1.2.3.2 mTORC2 Regulation .....	35
1.2 Role of mTOR in cellular functions .....	35
1.2.1 mTOR signalling in the regulation of protein synthesis .....	38
1.2.2 Implication of mTOR signalling in the regulation of cell survival .....	39
1.2.3 Role of mTOR signalling in mitochondrial biogenesis .....	42
1.2.4 Regulation of ribosomal biogenesis via the mTOR signalling pathway .....	42
1.2.5 Role of mTOR signalling in autophagy .....	43
1.2.6 mTOR signalling and lipid biosynthesis .....	43

1.2.7	Other roles of mTOR in regulating cellular processes.....	46
1.3	FKBP12 – Rapamycin Complex .....	46
1.3.1	Overview of Rapamycin.....	46
1.3.2	Overview of FKBP12.....	47
1.4	Initial evidence for the existence of mTOR splicing isoforms.....	48
1.5	Aim of the study.....	50
1.6	Methods of isolating mTOR.....	50
Chapter 2:	Methodology .....	54
2.1	Materials.....	54
2.1.1	Common laboratory reagents .....	54
2.1.2	Molecular cloning materials.....	54
2.1.3	Proteins.....	55
2.1.4	Antibodies .....	56
2.1.5	Mammalian cell lines .....	56
2.1.6	Bacteria.....	57
2.2	Methods.....	57
2.2.1	Molecular methods.....	57
2.2.1.1	Primers design.....	57
2.2.1.2	DNA digestion .....	58
2.2.1.3	DNA ligation.....	58
2.2.1.4	Polymerase chain reaction .....	58
2.2.1.5	Electrophoresis and DNA purification.....	59

2.2.1.6	DNA sequencing .....	59
2.2.1.7	Transformation and plasmid amplification .....	60
2.2.1.7.1	Plasmid DNA Purification .....	60
2.2.2	Mammalian cell culture .....	61
2.2.2.1	Maintenance of cell lines .....	61
2.2.2.2	Cell counting .....	62
2.2.2.3	Serum and nutrient starvation and stimulation .....	62
2.2.2.4	DNA transfection .....	62
2.2.2.5	Generation of stable cell lines .....	63
2.2.2.6	Cryopreservation .....	64
2.2.2.7	Cell line defrosting .....	64
2.2.3	Protein isolation methods .....	65
2.2.3.1	Mammalian cell lysis for protein analysis .....	65
2.2.3.2	Measuring protein concentration .....	65
2.2.3.3	Immunoprecipitation .....	65
2.2.3.4	Affinity Purification .....	66
2.2.3.5	SDS-PAGE .....	67
2.2.3.5.1	Protein sample preparation .....	68
2.2.3.5.2	Preparation of SDS-PAGE .....	68
2.2.3.6	Protein Visualisation .....	69
2.2.3.6.1	Coomassie Staining .....	69
2.2.3.6.2	Silver Staining .....	70

2.2.3.6.3	Western Blotting.....	70
2.2.3.6.3.1	Proteins transfer to membrane.....	70
2.2.3.6.3.2	Immunoblotting.....	71
2.2.3.6.3.3	Developing Immunoblots.....	71
2.2.3.6.3.4	Stripping and re-probing.....	72
2.2.3.7	Bacteria Cell Lysis and Purification GST-fusion Proteins.....	72
2.2.4	Bioinformatics methods.....	73
2.2.5	Functional analysis.....	74
2.2.5.1	<i>In Vitro</i> Kinase Assay.....	74
2.2.5.2	MTT proliferation assay.....	75
2.2.5.3	Colony Forming Assay.....	75
2.2.6	Statistical analysis.....	76
Chapter 3:	Chapter Three: Identification of novel mTOR isoforms.....	78
3.1	Evidence of the existence of a novel mTOR isoforms.....	78
3.2	Different approaches to identify novel isoforms.....	81
3.2.1	Protein analysis.....	81
3.2.1.1	Results of the protein purification approach.....	82
3.2.1.1.1	GST-FKBP12 Purification.....	82
3.2.1.1.2	Preparation of the affinity Matrix.....	83
3.2.1.1.3	The affinity matrix sensitivity (optimisation).....	84
3.2.1.1.3.1	The effect of rapamycin concentration.....	85
3.2.1.1.3.2	The effect of buffer.....	86

3.2.1.1.3.3	The effect of beads on protein binding .....	86
3.2.1.1.3.4	The effect of GST-FKBP12.....	88
3.2.1.1.3.5	Different purification isolates of the protein .....	88
3.2.1.1.3.6	The effect of different GST-FKBP12 concentrations.....	90
3.2.1.1	Patterns of mTOR immuno-reactive bands from different tissues and cell lines	91
3.2.1.2	Summary of protein analysis approach.....	98
3.2.2	Bioinformatics and molecular approaches .....	99
Chapter 4:	Molecular characterisation and functional analysis of mTOR $\delta$ .....	104
4.1	Molecular characteristics of the mTOR $\delta$ isoform.....	104
4.1.1	Introduction .....	104
4.1.2	Generation of Flag-tagged mTOR $\alpha$ and mTOR S2215Y plasmids .....	108
4.1.3	Generation of the pcDNA3-Flag-mTOR $\delta$ plasmid .....	113
4.1.4	DNA sequence analysis of the generated plasmids.....	115
4.1.5	Generation of stable cell lines expressing mTOR $\delta$ .....	118
4.2	Functional Analysis.....	122
4.2.1	mTOR $\delta$ kinase activity.....	123
4.2.2	MTT assay – cell proliferation assay .....	124
4.2.3	Colony formation assay.....	127
4.2.4	Discussion and conclusions.....	130
Chapter 5:	Molecular characterisation and functional analysis of mTOR $\gamma$ .....	135
5.1	Molecular characteristics of the mTOR $\gamma$ isoform .....	135

5.1.1	Introduction .....	135
5.1.2	Generation of a Flag-tagged mTOR $\gamma$ plasmid .....	138
5.1.3	DNA sequence analysis of the constructed pcDNA3 – Flag – mTOR $\gamma$ plasmid.....	145
5.1.4	Generation of HEK 293T cells stably expressing the mTOR $\gamma$ isoform.....	146
5.2	Functional Analysis.....	149
5.2.1	mTOR kinase assay .....	150
5.2.2	MTT assay – cell proliferation assay .....	152
5.2.3	Colony formation assay.....	155
5.2.4	Discussion and conclusions.....	158
Chapter 6:	Discussion .....	161
6.1	mTOR protein .....	161
6.2	Discussion .....	165
6.3	Conclusion.....	169
6.4	Future directions for mTOR $\delta$ and mTOR $\gamma$ .....	170
6.4.1	The effect of the mTOR $\delta$ and the mTOR $\gamma$ on the cell cycle and cell size.....	170
6.4.2	Cellular localization of the mTOR $\delta$ and the mTOR $\gamma$ .....	171
6.4.3	The effect of the mTOR $\delta$ and the mTOR $\gamma$ on the progression of tumour in a xenograft model in nude mice .....	171
6.4.4	Binding partners of the mTOR $\delta$ and the mTOR $\gamma$ .....	172
Appendices	.....	174
References	.....	176

## List of Figure

Figure 1.1: Diseases linked to dysregulated mTOR signalling and the corresponding affected organs (Dazert and Hall 2011) .....	26
Figure 1.2: Schematic diagram of mTOR domains with phosphorylation sites noted (Harris and Lawrence, Jr. 2003) .....	28
Figure 1.3: Schematic diagram of mTOR complexes. a) mTOR complex 1 and its targets. b) mTOR complex 2 and its targets.....	29
Figure 1.4: Regulation of mTORC1 by hormones, growth factors and nutrients. Processes that up regulate signaling are shown in black; those that down regulate signaling are shown in red.....	34
Figure 1.5: Schematic diagram of downstream targets of mTORC1 and its role in cellular functions.....	37
Figure 1.6: Regulation of cap-dependent translation initiation by mTORC1 via 4E-BP. ....	39
Figure 1.7: Role of mTORC2 in cellular survival. The mTORC2 promotes cellular survival by activating Akt and via SGK1 phosphorylation (Laplante and Sabatini 2012).....	41
Figure 1.8: Regulation of lipid synthesis by mTOR. ....	45
Figure 1.9: Modular representation of mTOR isoforms .....	50
Figure 3.1: Northern blotting of human tissues indicates the presence of several potential mTOR splicing forms.....	79

Figure 3.2: Western blot of Gel filtration analysis of mTOR splicing forms in MCF7 cells	
indicates the presence of several potential mTOR splicing forms .....	79
Figure 3.3: Western blotting examples of commercially available antibodies targeting mTOR	
(280 kDa).....	80
Figure 3.4: Coomassie stain of affinity purification of GST-FKBP12. ....	83
Figure 3.5: Schematic diagram of the affinity matrix mTOR and identify a new mTOR	
splicing isoform.....	84
Figure 3.6: Affinity purification of mTOR $\alpha$ and mTOR $\beta$ from HEK 293 cells over-expressing	
mTOR $\alpha$ and mTOR $\beta$ .....	85
Figure 3.7: Western blotting to study the effect of buffer on GST-FKBP12 binding efficiency	
to Glutathione Sepharose beads. ....	86
Figure 3.8: Western blotting to study the effect of Beads on FKBP12 binding efficiency. ....	87
Figure 3.9: Western blotting to study the effect of bead volume and protein concentration on	
the amount of mTOR purified using the affinity matrix. ....	88
Figure 3.10: Western blotting to study the effect of GST-FKBP12 concentration on the	
binding efficiency of mTOR to affinity matrix.....	90
Figure 3.11: Western blotting of affinity purified mTOR from Rats' Heart.....	92
Figure 3.12: Western blotting of affinity purified mTOR from Starved and starved stimulated	
HEK 293.....	93

Figure 3.13: Western blotting of affinity purified mTOR from HEK 293 using the modified procedure, after the 3D structure has been revealed (15 min incubation with rapamycin). .....	94
Figure 3.14: Commercially available antibodies against different mTOR epitope.....	97
Figure 3.15: Western blotting of affinity purified mTOR against different antibodies. ....	99
Figure 3.16: Schematic domain organization of mTOR splicing forms .....	101
Figure 3.17: Western blotting analysis testing the expression of mTOR $\delta$ in different cell lines. .....	102
Figure 4.1: Schematic representation of the domain organisation of the mTOR $\delta$ splice isoform. ....	107
Figure 4.2: Schematic representation of the domain organisation of the mTOR $\beta$ mutant.....	107
Figure 4.3: Plan for the generation of the pcDNA3–Flag–mTOR $\alpha$ and pcDNA3–Flag–mTOR S2215Y isoforms.....	109
Figure 4.4: Agarose gel image of the DNA fragments used for the construction of pcDNA3–Flag–mTOR $\alpha$ and pcDNA3–Flag–mTOR S2215Y. ....	110
Figure 4.5: Agarose gel image of colonies selected for digestion and sequencing analysis..	111
Figure 4.6: Agarose gel image of the results of the digestion analysis of the pcDNA3–Flag–mTOR $\alpha$ and pcDNA3–Flag–mTOR S2215Y plasmids for the first selection which showed negative results.....	112

Figure 4.7: Agarose gel image of the results of the digestion analysis of the pcDNA3–Flag–mTOR $\alpha$ and pcDNA3–Flag–mTOR S2215Y plasmids for the second selection which demonstrated positive results. ....	113
Figure 4.8: Plan to generate pcDNA3–Flag–mTOR $\delta$ . ....	114
Figure 4.9: Agarose gel image of the DNA fragments used for the construction of pcDNA3–Flag–mTOR $\delta$ . ....	115
Figure 4.10: Sequencing analysis of pcDNA3–Flag–mTOR S2215Y. ....	116
Figure 4.11: mTOR $\delta$ COOH-terminal sequence highlighted in red. ....	117
Figure 4.12: Nucleotide sequence alignment of the mTOR $\delta$ fragment. ....	118
Figure 4.13: Western blot confirming the expression of Flag–mTOR $\delta$ , Flag–mTOR $\alpha$ and Flag–mTOR S2215Y in transfected HEK 293 cells. ....	120
Figure 4.14: Parental HEK 293 cells demonstrate a higher proliferation potential than HEK 293 cells over–expressing the mTOR $\delta$ isoform. ....	126
Figure 4.15: The mTOR $\delta$ protein stably enhances either cell cycle arrest or cell death. ....	129
Figure 5.1: A schematic representation of the domain organisation of the mTOR $\gamma$ splicing isoform. ....	137
Figure 5.2: A schematic diagram demonstrating the location of the 12–amino acid deletion in mTOR $\beta$ . ....	138
Figure 5.3: The plan for the construction of the pcDNA3–Flag–mTOR $\gamma$ isoform. ....	140

Figure 5.4: Agarose gel image of the DNA fragments used for the construction of pcDNA3–Flag–mTOR $\gamma$ .....	141
Figure 5.5: Agarose gel image of the pcDNA3–Flag–mTOR $\gamma$ colonies selected for digestion analysis.....	142
Figure 5.6: Agarose gel image of the results of the digestion analysis of the constructed pcDNA3–Flag–mTOR $\gamma$ plasmid showing the absence of the insert band (negative result). .....	143
Figure 5.7: Agarose gel image of the resultant of the digestion analysis of the constructed pcDNA3–Flag–mTOR $\gamma$ plasmid confirming the presence of the insert band. ....	144
Figure 5.8: Sequencing analysis of pcDNA3–Flag–mTOR $\gamma$ . ....	146
Figure 5.9: Western blot confirming the high expression of Flag–mTOR $\gamma$ in parallel with the other mTOR isoforms in HEK 293 cell lines. ....	148
Figure 5.10: <i>In vitro</i> kinase assay for mTOR $\gamma$ . ....	152
Figure 5.11: mTOR $\gamma$ negatively regulates cellular proliferation. ....	154
Figure 5.12: mTOR $\gamma$ down–regulates the anchorage-independent growth of HEK 293 in soft agar. ....	157

## Abbreviations

3D	Three-dimensional
4E-BP	Eukaryotic initiation factor 4E binding protein
A549	Human lung carcinoma
AB	Antibody
Akt/PKB	Protein Kinase B
AMPK	AMP-activated protein kinase
APS	Ammonium persulphate
ATCC	American Type Culture Collection
ATG13	Autophagy-related 13
ATG13	Autophagy-related protein 13
ATP	Adenosine Triphosphate
BAD	Pro-apoptotic protein
BLAST	Basic Local Alignment Search Tool
Cdc42	Cell division control protein 42
CO <sub>2</sub>	Carbon dioxide
Cos7	Monkey kidney fibroblast-like
CREMt	Polyvinylidene difluoride

cryo-EM	Cryo-electron microscopy
DMEM	Dulbecco's Modified Eagle's medium
DMSO	Dimethyl Sulfoxide
DNA	Deoxyribonucleic Acid
DNA-PK	DNA-dependent protein kinase
DTT	Dithiothreitol
E.Coli	Escherichia coli
ECL	Chemiluminescence
EDTA	Ethylenediaminetetraacetic acid
eEF2K	Elongation factor 2 kinase
eIF4E	Eukaryotic translation initiation factor 4E
FAT	FRAP, ATM, and TRRAP
FATC	FRAP-ATM-TRRAP-C-terminal domain
FATN	FRAP-ATM-TRRAP-N-terminal domain
FBS	Foetal bovine serum
FIP200	FAK family kinase-interacting protein 200kDa
FKPB12	FK506-binding protein of 12 kDa
FOXO1	Forkhead box protein O1

FOXO3	Forkhead box protein O3
FRAP	FKBP12-rapamcyin associated protein
FRB	FKBP12 Rapamycin Binding domain
FTS	Farnesylthiosalicylic acid
GSK	Glycogen synthase kinase 3
HEAT	Huntingtin, elongation factor 3, protein phosphatase 2A, and TOR1
HEK 293	Human Embryonic Kidney 293 Cells
HELA	Human cervical epithelial carcinoma cell line
HepG2	Hepatocellular carcinoma
HRP	Horseradish peroxidase-linked
IPMK	Identified inositol polyphosphate multikinase
IPTG	Isopropyl- 1 -thio- $\beta$ -D-galactopyranoside
LB	Luria Broth
MAPK	Mitogen-activated protein kinase
MAPKAP1	Mitogen-activated protein kinase-associated protein1
MCF7	Human breast adenocarcinoma cell line
MDM2	Mouse double minute 2 homolog
mLST8/G $\beta$ L	Mammalian LST8/G-protein $\beta$ -subunit like protein

mRNA	Messenger Ribonucleic Acid
mSin1	Mammalian stress activated protein kinase – interacting protein
mTOR	Mammalian Target of Rapamycin and recently known as Mechanistic Target of Rapamycin
mTORC1	mTOR Complex 1
mTORC2	mTOR complex 2
MW	Molecular Weight
NITE	National institute of technology and evaluation
PCR	Polymerase chain reaction
PDB	Protein Data Bank
PGC1 $\alpha$	Peroxisome proliferator–activated receptor gamma coactivator 1-alpha
PI3K	Phosphatidylinositol-3-kinase
PIKK	Phosphatidyl inositol 3' kinase-related kinases
PKC	Protein kinase C
PP2A	Protein Phosphatase 2
PPAR- $\gamma$	Peroxisome proliferator-activated receptor- $\gamma$
PPAR $\gamma$	Peroxisome proliferator–activated receptor gamm
PRAS40	Proline-rich AKT substrate 40 kDa

protor	Protein observed with Rictor
PVDF	Polyvinylidene difluoride
Rac1	Ras-related C3 botulinum toxin substrate 1
RAFT	Rapamycin and FKBP12 target
Rag	Recombination Activation protein
RAPT	Rapamycin target
raptor	Regulatory associated protein of mTOR
RD	Regulatory domain
Rheb	Ras homolog enriched in brain
RhoA	Ras homolog gene family, member A
rictor	Rapamycin insensitive companion of mTOR
RPM	Revolutions per minute
rRNA	Ribosomal RNA
S6K	S6 Kinase
SDS-PAGE	SDS-polyacrylamide gel electrophoresis
SEP	Sirolimus effector protein
SGK1	Serum/glucocorticoid regulated kinase 1
SOC	Super Optimal broth with Catabolite repression

SREBP1	Sterol regulatory element-binding protein 1
SREBP-1	Sterol regulatory element binding protein-1
STAT3	Signal transducer and activator of transcription 3
STAT3	Signal transducer and activator of transcription 3
TBST	Tris-Buffered Saline and Tween 20
TEMED	Tetramethylethylenediamine
TIF-IA	Transcription initiation factor IA
T <sub>m</sub>	Temperatures
tRNA	Transfer RNA
UCL	University College London
ULK1	Unc51-like kinase 1
ULK1	Unc-51-like kinase 1
UV	Ultra-violet
YY1	Yin Yang 1

# **Chapter 1**

## **General Introduction**

## Chapter 1: General Introduction

---

### 1.1 mTOR, an overview

The mammalian Target of Rapamycin (mTOR), but now officially mechanistic TOR, also known as FRAP, RAFT, or RAPT, is an evolutionarily conserved, 280 kDa serine/threonine protein kinase. mTOR belongs to the phosphatidyl-inositol 3-kinase-related kinase (PIKKs) protein family. The mTOR protein plays a critical role in regulating cellular processes, such as cellular growth, proliferation, cytoskeletal organization, survival, protein transcription and protein synthesis (Corradetti and Guan 2006; Hay and Sonenberg 2004)

The mTOR protein lies in the centre of intersecting signalling pathways. Due to its position, mTOR plays a critical role in regulating these pathways, therefore mTOR regulates key cellular processes. Dysregulation of the mTOR pathway has been implicated in many diseases, such as tumorigenesis, metastasis (Graff and Zimmer 2003), metabolic diseases including diabetes (Schaeffer and Abrass 2010), cardiac hypertrophy (Young and Nickerson-Nutter 2005), sepsis (Kimball et al. 2003; Lang and Frost 2007) and after traumatic brain injury (Chen et al. 2007 (Adapted from Dazert and Hall, 2011) (Figure 1.1).

Growth factors, nutrients and hormones activate mTOR and magnify its activity. In different forms of cancer, this activity is dysregulated (Choo et al. 2006; Hardie

2008; Inoki et al. 2003; Laplante and Sabatini 2009). Amplified mTOR activity will in turn accelerate protein synthesis and stimulate multiple proteins promoting tumour progression. Amplified mTOR-mediated processes may increase cell growth, proliferation, cellular metabolism and energy utilization. In addition, mTOR may increase tumour angiogenesis through the production of pro-angiogenic factors and also by directly driving vascular cell proliferation (Fingar and Blenis 2004). mTOR is known as a vital regulator of gene expression at the level of transcription and translation, and consequently is an excellent intracellular target for anti-cancer therapy.

The aim of this study is to elucidate the regulation of mTOR signalling in health and cancer, by identifying different splicing isoforms of mTOR and defining their roles in mTOR mediated cellular processes. In this study, I focus on providing evidence for the existence of a new mTOR splicing isoform, identifying its domain structure and expression pattern in cell lines and tissues, as well as elucidating its contribution to cellular processes in health and disease.

### **1.1.1 The mTOR Structure**

The mTOR protein consists of 2,549 amino acids, composing multiple highly conserved domains. Similar to other PIKK family members, mTOR contains a protein kinase domain at the COOH-terminus and a long stretch of protein-protein interaction modules within its NH<sub>2</sub>-terminus.

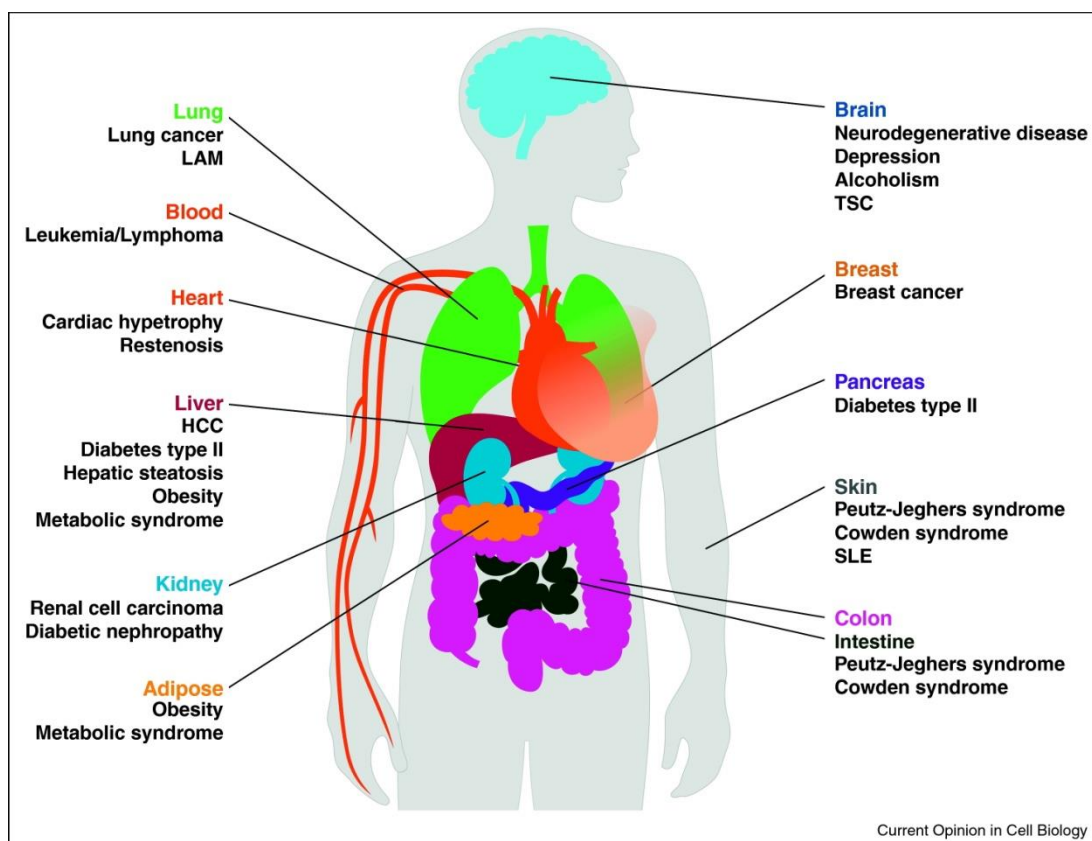


**Figure 1.1: Diseases linked to dysregulated mTOR signalling and the corresponding affected organs (Adapted from Dazert and Hall, 2011)**

The NH<sub>2</sub>-terminal includes a chain of HEAT (Huntingtin, elongation factor 3, protein phosphatase 2A, and TOR1) repeats, which form a helical structure. These HEAT repeats enable protein–protein interactions. Therefore, it is important for mediating mTOR interaction with other proteins in the mTOR complexes (Perry and Kleckner 2003). The crystal structure of other proteins which contain HEAT repeats, such as human DNA-dependent protein kinase (DNA-PK), show that the large number of alpha-helical HEAT repeats are vital for protein-protein interactions (Sibanda et al. 2010).

The HEAT repeats are followed by a moderately conserved FAT (FRAP, ATM, and TRRAP) domain. There is also a short FATC at the COOH-terminal. The FAT and FATC domains are found in all PIKK family members. It has been proposed that these two domains interact with each other, thus concealing the kinase domain until mTOR is activated by phosphorylation in response to diverse extracellular stimuli and cellular metabolites. In addition, deletion of 20 amino acids (amino acids 2,430–2,450) just upstream of the FATC domain, resulted in an increase in mTOR kinase activity, thus magnifying the stimulation toward downstream targets *in vitro* and *in vivo* (Sekulic et al. 2000). Between the FAT and FATC domains there are three domains: a) FKBP12 Rapamycin Binding (FRB) domain, which is the target of the inhibitory rapamycin–FKBP12 complex; b) adjacent to the FRB domain lies a highly conserved serine-threonine kinase domain; c) Regulatory domain (RD) is located downstream of the kinase domain (Figure 1.2).

Several activating mutations have been recently identified in mTOR, but their detailed analysis indicated that none of them possesses an oncogenic potential (Brown et al. 1995; Kim et al. 2002; Peterson et al. 1999; Vilella-Bach et al. 1999).

The crystal structure of mTOR has not yet been determined, but molecular modelling suggests that most of the protein consists mainly of helical structures (Perry & Kleckner 2003).

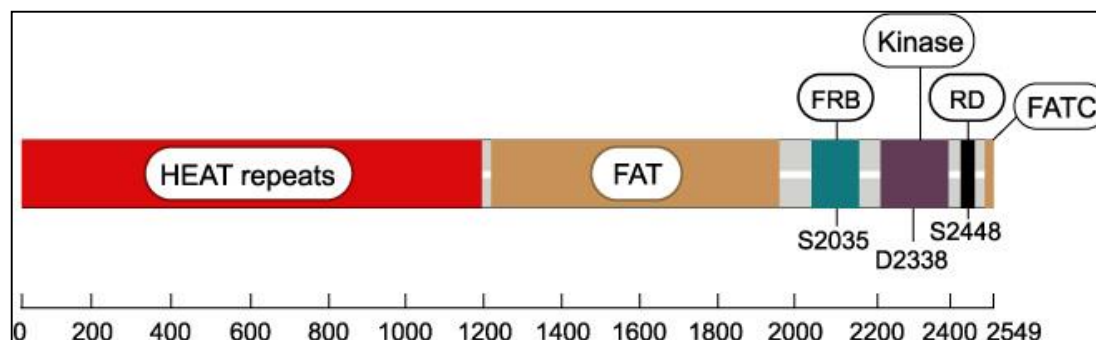


**Figure 1.2: Schematic diagram of mTOR domains with phosphorylation sites noted (Adapted from Harris and Lawrence, Jr. 2003).**

The mTOR protein primarily localized in the cytosol. However it has also been associated with the membranes of several organelles such as the Golgi, endoplasmic reticulum, mitochondria and nucleus (Desai et al. 2002; Drenan et al. 2004; Liu and Zheng 2007; Sabatini et al. 1999; Tirado et al. 2003; Withers et al. 1997).

### 1.1.2 mTOR Complexes in mammalian cells

mTOR has been shown to localize in the cytoplasm in two multiprotein complexes, mTOR Complex 1 (mTORC1) and mTOR complex 2 (mTORC2) (Guertin and Sabatini 2005a) (Figure 1.3).

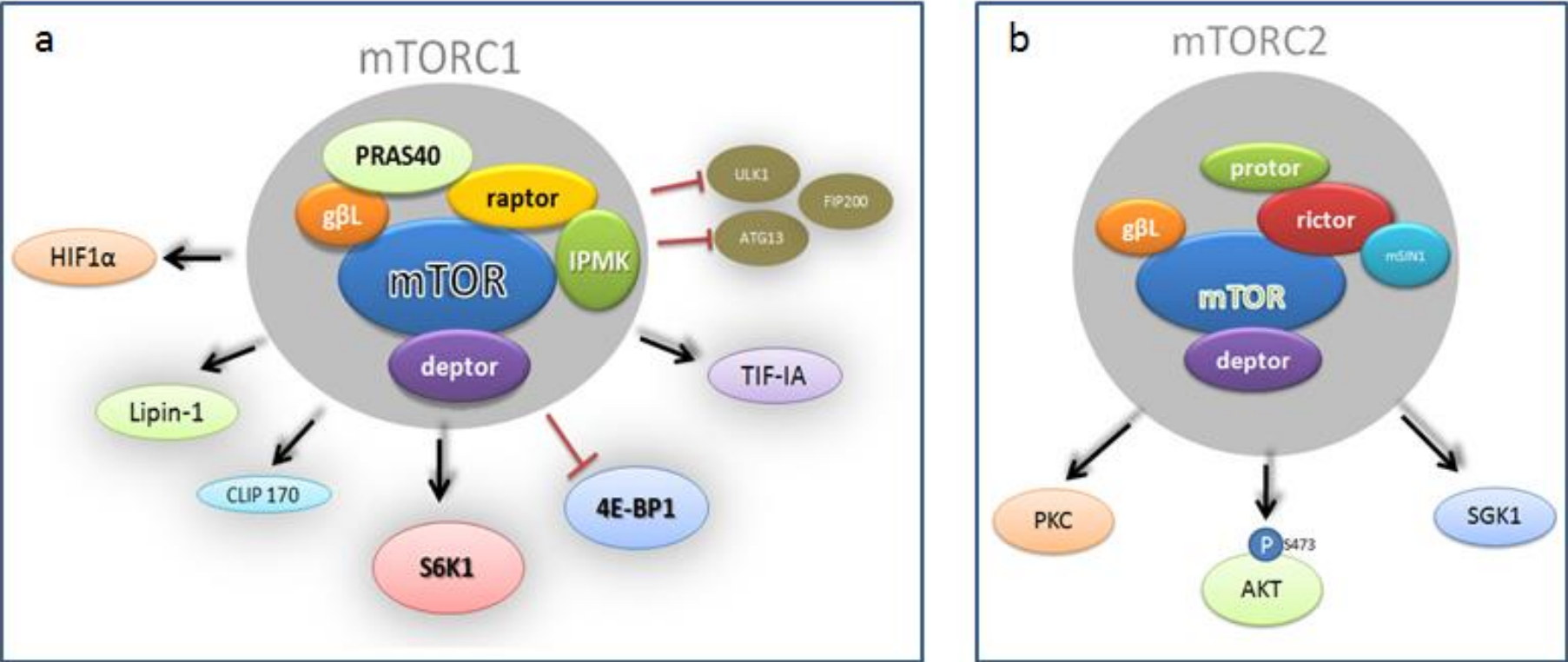


Figure 1.3: Schematic diagram of mTOR complexes. a) mTOR complex 1 and its targets. b) mTOR complex 2 and its targets

### 1.1.2.1 mTORC1

The multi-protein mTORC1 is composed of mTOR, regulatory associated protein of mTOR (raptor), mammalian LST8/G-protein  $\beta$ -subunit like protein (mLST8/G $\beta$ L), Proline-rich AKT substrate 40 kDa (PRAS40), and the newly identified inositol polyphosphate multikinase (IPMK) (Hara et al. 2002; Kim et al. 2002; Kim et al. 2003; Kim et al. 2011; Vander et al. 2007).

Indeed, some proteins in mTORC1 are known to be essential for mTOR to perform mTORC1 activities (Hara et al. 2002; Kim et al. 2002; Sancak et al. 2007). Raptor (150 kDa) has been reported to play critical roles in mediating mTORC1 assembly and consequently mTORC1 function. In addition, it helps to recruit mTORC1 substrates, as well as regulate its activity and subcellular localization. Raptor interacts with mTOR via a strong NH<sub>2</sub>-terminal interaction and a weaker COOH-terminal interaction (Hara et al. 2002; Kim et al. 2002; Sancak et al. 2008).

The function of mLST8 (36 kDa) in mTORC1 is ambiguous, since lack of this protein does not show any effect on mTORC1 activity *in vivo* (Guertin et al. 2006).

PRAS40 (40 kDa) has been recognised as a negative regulator of mTORC1. It was identified as a raptor-interacting protein. Later in this text we will discuss that, *in vitro*, Akt phosphorylate PRAS40, which prevents it from inhibiting mTORC1 in cells (Sancak et al. 2007; Vander et al. 2007; Wang et al. 2007).

IPMK is an inositol phosphate multiple kinase, which catalyses the formation of higher phosphorylated inositols, InsP<sub>5</sub> and InsP<sub>6</sub>. IPMK stabilizes mTOR-raptor interaction through the NH<sub>2</sub>-terminal sequence of IPMK. The IPMK NH<sub>2</sub>-terminal sequence is a specific binding site of mTOR. Depletion of IMPK resulted in reduced

mTORC1 activity and reduced mTORC1 response to stimulation by amino acids. IMPK regulates amino acid signaling to mTOR, independently of its catalytic function. (Kim et al. 2011).

The three-dimensional (3D) structure of human mTORC1 has been determined by cryo-electron microscopy (cryo-EM). The cryo-EM revealed the shape of mTORC1, however, it was not possible to define the inter-molecular and inter-subunit boundaries at the available resolution (Yip et al. 2010).

### **1.1.2.2 mTORC2**

mTORC2 like mTORC1 contains mTOR and mLST8/GβL, but instead of raptor, PRAS40, and IPMK, it contains rapamycin insensitive companion of mTOR (riCTOR), mammalian stress activated protein kinase – interacting protein (mSin1), and the protein observed with Rictor (protor) (Frias et al. 2006; Jacinto et al. 2004; Pearce et al. 2007; Sarbassov et al. 2004; Yang et al. 2006).

mLST8 is a component of both mTORC1 and mTORC2. Although mLST8 is not required for mTORC1, it is required for mTORC2 function. Moreover, lack of mLST8 can disrupt the assembly of mTORC2 and its functions (Guertin et al. 2006).

Rictor (200 kDa), also known as mAVO3, is rapamycin insensitive companion of mTOR, and it is critical for mTORC2 activity. It might also help in protein-protein interactions (Sarbassov et al. 2004).

mSin1 (70 kDa), also known as mitogen-activated protein kinase-associated protein1 (MAPKAP1), is critical for the assembly of mTORC2 and consequently for phosphorylation of its target, Akt/PKB (Frias et al. 2006).

Protector (42 kDa) increase the mTORC2-mediated activation of SGK1 (Pearce et al. 2007; Pearce et al. 2011).

### 1.1.2.3 Regulation of mTOR

#### 1.1.2.3.1 mTORC1 regulation

The regulation of mTORC1 activity appears to be complex and is likely to be dependent on the organization of the various subunits in the mTORC1 (Yip et al. 2010a).

The activity of mTORC1 is stimulated by the integration of many signals, including growth factors, insulin, nutrients and energy availability (Figure 1.4). In addition mTORC1 could be regulated by cellular stresses such as hypoxia, osmotic stress, reactive oxygen species and viral infection (Avruch et al. 2005; Corradetti & Guan 2006; Fang et al. 2001; Hay & Sonenberg 2004; Kim et al. 2002).

Ras homolog enriched in brain (Rheb) binds near the mTOR kinase domain, and plays a critical role in stimulating mTORC1 activity (Long et al. 2005a; Long et al. 2005). Insulin activates Rheb through Phosphatidylinositol-3-kinase (PI3K) pathway, whereas, growth factors activate Rheb through mitogen-activated protein kinase (MAPK) signaling pathway and accelerate insulin signaling activity. Growth factors, insulin, and amino acids can keep Rheb in its active form, and therefore stimulate mTORC1 activity (Guertin and Sabatini 2007; Shaw and Cantley 2006).

In contrast, PRAS40 inhibits Rheb-dependent mTORC1 activation in a dose-dependent manner *in vitro* (Sancak et al. 2007; Vander et al. 2007). Akt/PKB is a serine/threonine protein kinase, activated by growth factors. Akt has two main roles in mTORC1 activation. First, Akt inhibits TSC1/2, which prevents Rheb from

activating mTORC1. Secondly, it phosphorylates PRAS40, hence preventing its function as a Rheb inhibitor (Sancak et al. 2007; Vander et al. 2007).

Another method for mTORC1 activation, independent of Rheb, is via amino acids and Rag. Lack of amino acids from the medium resulted in inhibition of mTORC1 activity. Amino acids activate Rag on the lysosomal surface. This activation allows it to recruit and bind to mTORC1, where Rheb-GTP is also situated, leading to activation of mTORC1 (Sancak et al. 2008; Sancak et al. 2010). The underlying mechanism of this process is still not clearly understood.

The activity of mTORC1 is inhibited by low nutrient levels, growth factor deprivation, energy stress, caffeine, rapamycin, farnesylthiosalicylic acid (FTS), and curcumin (Beevers et al. 2006; Kim et al. 2002; McMahon et al. 2005).

The kinase domain in mTOR is relatively similar to the one in PI3K. mTOR activity can be inhibited *in vitro* with high concentrations of PI3K inhibitors, LY92900 and Wortmannin (Brunn et al. 1996a; Hay & Sonenberg 2004). There are many known compounds which compete with ATP binding to mTOR kinase domain, suppressing its activity. These compounds are known as ATP competitive mTOR inhibitors and include PP242, Torin1, WYE-354, AP23573 and Ku-0063794. In contrast to Rapamycin, they inhibit both mTORC1 and mTORC2 activity. These inhibitors have a significant selectivity over PI3K (Feldman et al. 2009; Garcia-Martinez et al. 2009; Mita and Tolcher 2007; Thoreen et al. 2009; Yu et al. 2009).

Although relatively short exposure to FKBP12-rapamycin did not affect the structural integrity of mTORC1, extended incubation (more than 20 minutes) resulted in disassembly of mTORC1 (Yip et al. 2010a)

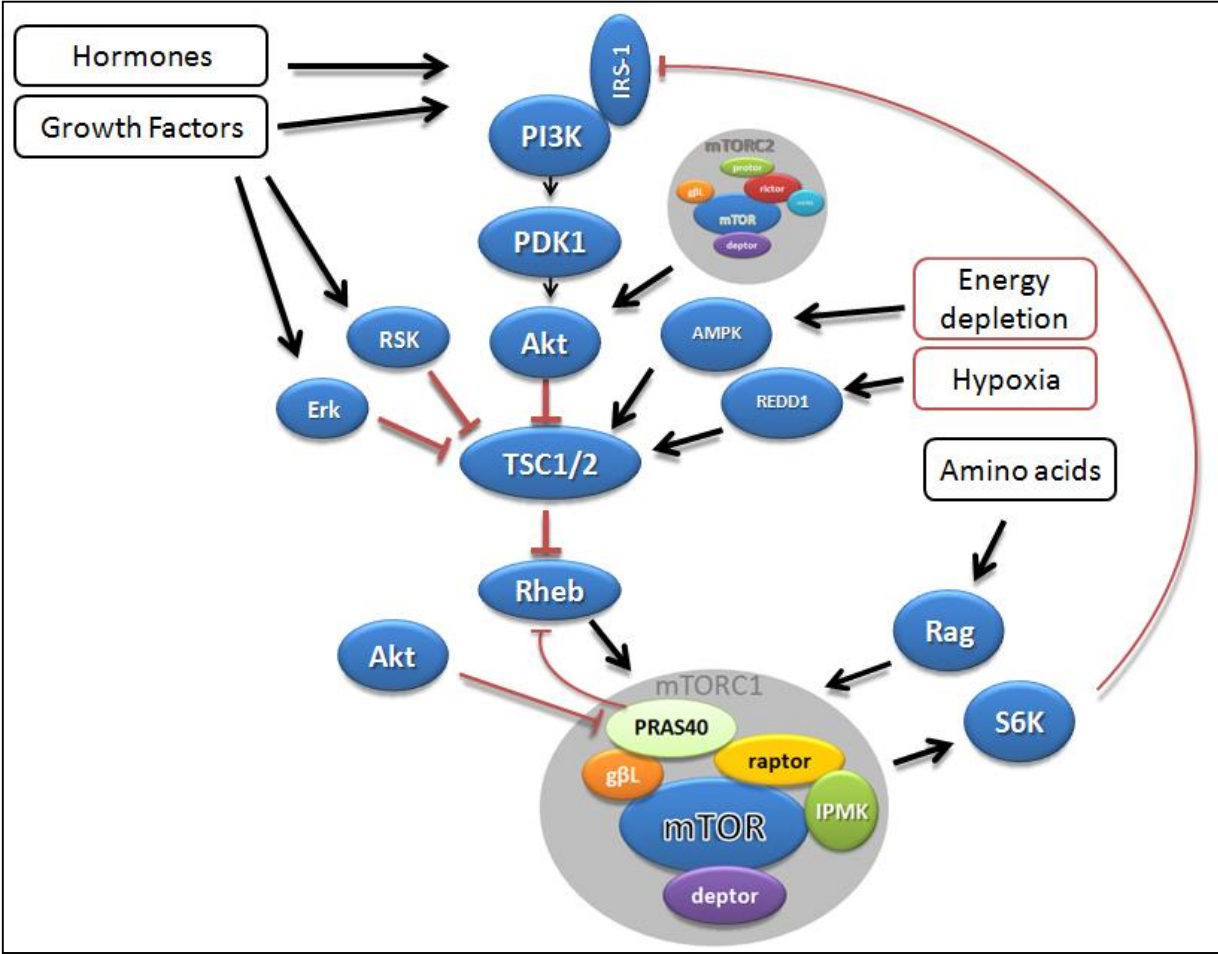


Figure 1.4: Regulation of mTORC1 by hormones, growth factors and nutrients. Processes that up regulate signaling are shown in black; those that down regulate signalling are shown in red.

### 1.1.2.3.2 mTORC2 Regulation

Compared to mTORC1, there is limited information about mTORC2 regulation. mTORC2 has been shown to be growth factor sensitive but nutrient insensitive (Jacinto et al. 2004; Loewith et al. 2002; Sarbassov et al. 2004). After growth factor stimulation, mTORC2 is activated in numerous cell lines and tissues. The underlying mechanism of this activation is still unknown (Frias et al. 2006; Sarbassov et al. 2004; Sarbassov et al. 2005; Yang et al. 2006).

Rapamycin is known to inhibit mTORC1 activity. In contrast, mTORC2 was identified as a rapamycin-insensitive mTOR complex. Subsequent studies have shown that prolonged exposure to rapamycin treatment can disrupt mTORC2 assembly, consequently inhibiting its activity. In addition, prolonged exposure promotes rapamycin binding to free mTOR molecules, thus inhibiting the formation of new mTORC2 (Sarbassov et al. 2005; Sarbassov et al. 2006).

Some proteins in the mTORC2, such as mLST8, are required to maintain the rictor-mTOR, but not the raptor-mTOR, lack of mLST8 can disrupt the assembly of mTORC2, thus affecting mTORC2 function (Guertin et al. 2006).

## 1.2 Role of mTOR in cellular functions

The mTOR pathway has been shown to control multiple cellular processes, including cell growth, cell cycle progression, nutrient plasticity, cellular survival, metabolism and translation initiation. Translation initiation is the most studied function of mTOR and is the rate-limiting step in protein synthesis (Gingras et al. 2004) (Figure 1.5).

mTORC1 has been shown to interact, direct or indirect, with many targets include S6K, 4E-BP, ATG13, ULK1, TIF-IA, Lipin-1, SREBP1, PPAR $\gamma$ , PGC1 $\alpha$ , and

STAT3. These targets are responsible for regulation of many cellular processes, including protein and lipid synthesis, mitochondrial and ribosomal biogenesis and autophagy.

The mTORC2 plays a critical role in cell survival, metabolism, and proliferation. The mTORC2 phosphorylates and activates its downstream effectors Akt/PKB, serum/glucocorticoid regulated kinase 1 (SGK1), and protein kinase C (PKC). Akt plays a critical role in multiple cellular processes including glucose metabolism, apoptosis, cell proliferation, transcription and cell migration (Frias et al. 2006; Guertin and Sabatini 2005; Guertin & Sabatini 2007; Hresko and Mueckler 2005; Lee et al. 2005; Sarbassov et al. 2005; Yang et al. 2006).

mTORC2 functions as an important regulator of the cytoskeleton, via its organisation and stimulation of F-actin stress fibres, by enhancing the phosphorylation of protein kinase C  $\alpha$  (PKC $\alpha$ ) and paxillin, and also by the addition of GTP to RhoA, Rac1 and Cdc42 (Sarbassov et al. 2004).

Despite all the differences between lower and higher eukaryotic organisms, budding yeast and *Drosophila* can still be considered as models when studying the mammalian TOR. TOR is a highly conserved protein kinase, with high sequence identity and functional similarity between yeast, *Drosophila* and mammals. Also cellular processes in lower and higher eukaryotes are more likely to be conserved. TOR in budding yeast and *Drosophila* participates in a variety of cellular processes (Crespo and Hall 2002; Rohde et al. 2001) and some of these roles have not yet been proven in mammals. The implication of mTOR in many diseases suggests that it has unidentified targets and roles in mammalian cells.

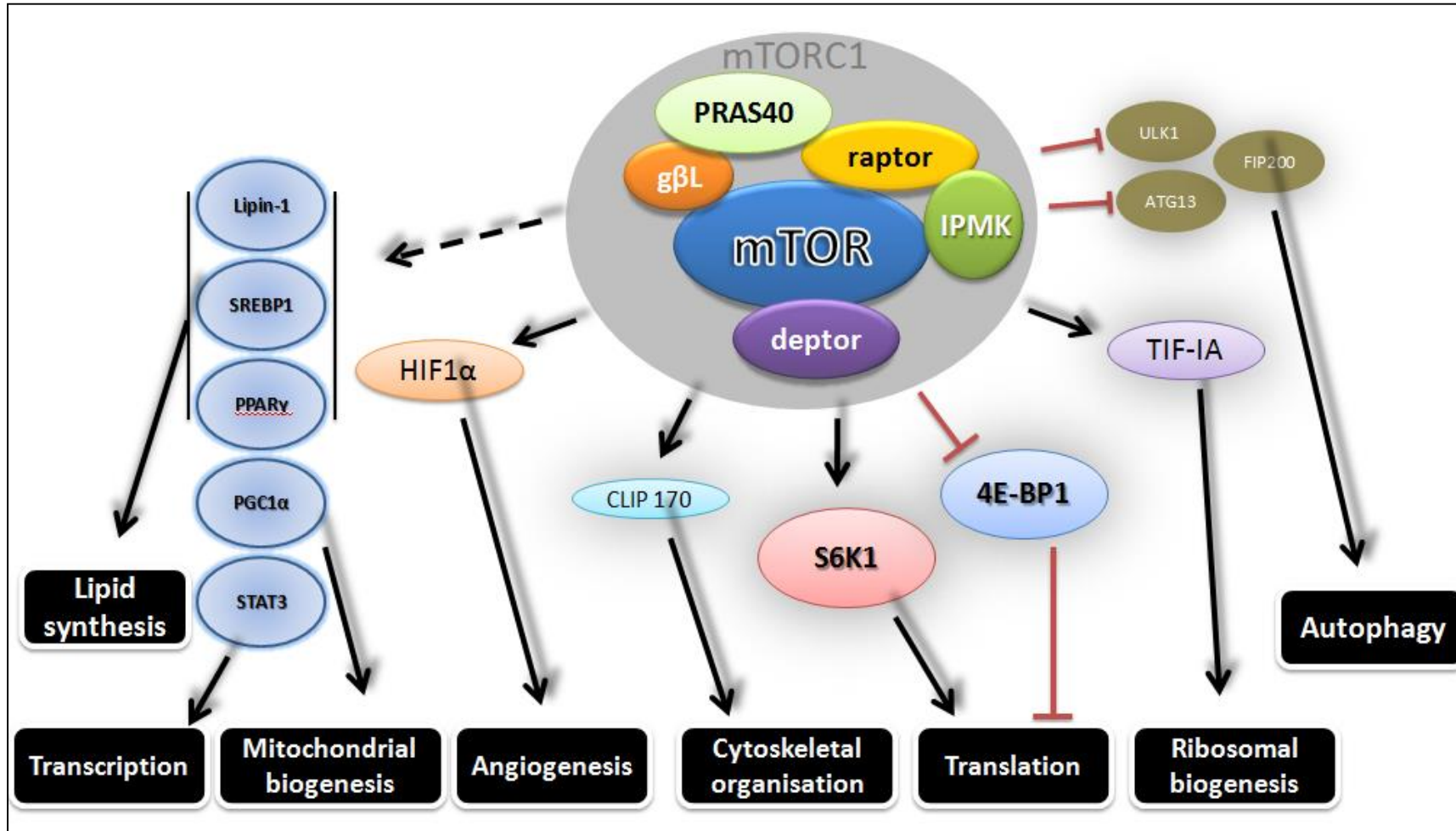


Figure 1.5: Schematic diagram of downstream targets of mTORC1 and its role in cellular functions.

### 1.2.1 mTOR signalling in the regulation of protein synthesis

mTORC1 controls cell growth by phosphorylating the key regulators of protein synthesis, including S6 Kinase 1 (S6K1) and the eukaryotic translation initiation factor 4E binding protein 1 (4E-BP1). S6K1 and 4E-BP1 are the two best characterized targets of mTORC1 (Hay & Sonenberg 2004; Ma and Blenis 2009; Richter and Sonenberg 2005).

4E-BP1 binds tightly to the eukaryotic translation initiation factor 4E (eIF4E), preventing it from performing its translation initiation roles. eIF4E binds to 5'-capped mRNAs and recruits them to the ribosomal initiation complex for translation (Pause et al. 1994). To initiate translation, eIF4E needs to be released from 4E-BP1. The mTORC1 phosphorylates two sites in 4E-BP1 *in vitro* (Brunn et al. 1997; Burnett et al. 1998; Gingras et al. 2001). This phosphorylation initiates subsequent phosphorylation of Thr-70 followed by Ser-65 (Gingras et al. 2001; Heesom and Denton 1999; Mothe-Satney et al. 2000). Moreover, mTORC1 has been shown to phosphorylate at least four residues of 4E-BP1 in a hierarchical manner (Gingras et al. 1999; Huang and Houghton 2001; Mothe-Satney et al. 2000) (Figure 1.6).

S6K has been known to regulate cell growth (Shima et al. 1998). mTORC1 phosphorylates S6K1 on the hydrophobic-motif residue Thr-389 (Pullen and Thomas 1997; Saitoh et al. 2002), followed by subsequent phosphorylation by PDK1 (Pullen et al. 1998; Pullen & Thomas 1997). Activation of S6K1 augments cell growth by stimulating the initiation of protein synthesis, through phosphorylation of Ribosomal protein S6 and other components which participate in protein synthesis (Peterson and Schreiber 1998). S6K1 participates in a positive feedback loop with mTORC1 by

phosphorylating mTOR at two sites, stimulating mTOR activity (Chiang and Abraham 2005; Holz and Blenis 2005).

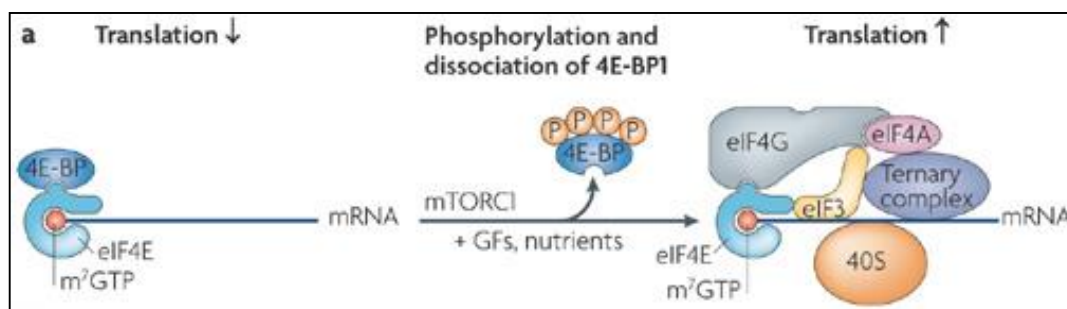


**Figure 1.6: Regulation of cap-dependent translation initiation by mTORC1 via 4E-BP.** Unphosphorylated 4E-binding proteins bind tightly to eIF4E, preventing it from interacting with eIF4G and thus inhibiting translation. The mTORC1 phosphorylates 4E-BPs in a hierarchical manner, releasing the 4E-BP from eIF4E. This results in the recruitment of eIF4G to the 5' cap and allows translation initiation to proceed (Adapted from Ma & Blenis 2009).

### 1.2.2 Implication of mTOR signalling in the regulation of cell survival

In normal cells, there is a balance between survival and apoptotic signals. If these signals are dysregulated, cells might either recover or enter the programme of cell death. PI3K signalling pathway plays a critical role in mediating pro-survival processes. Pro-survival signalling pathways are often dysregulated in cancer cells. Suppression of these survival signals promotes apoptotic processes. Therefore survival signals are known to be excellent targets for anti-cancer therapy (Foster 2004).

The mTOR plays a critical role in cell survival in the following ways. Firstly, mTORC2 promotes Akt activity. Akt then phosphorylates and inactivates several pro-apoptotic factors, promoting cellular growth and survival. These factors include

GSK3b, BAD, forkhead family transcription factors and MDM2 (Vivanco and Sawyers 2002). Akt phosphorylates the forkhead box proteins FOXO1 and FOXO3, preventing their translocation to the nucleus. FOXO1 and FOXO3 are transcription factors that promote gene expression of proteins responsible for apoptosis (Guertin et al. 2006) (Figure 1.7).

Secondly, mTOR, via Akt, mediates the stabilization of cell surface amino acid transporters, protecting cells from apoptosis (Edinger and Thompson 2002).

Thirdly, mTORC1 phosphorylates and activates S6K1 which generates a negative feedback loop to suppress PI3K activity, resulting in reduced survival signals.

Fourthly, mTOR, via S6K1, has been shown to inhibit the pro-apoptotic protein BAD (Harada et al. 2001).

mTORC1 phosphorylates 4E-BP1 and S6K1, promoting mRNA translation, ribosome biogenesis, and down-regulate autophagy. This allows mTOR to regulate cell growth, proliferation and survival (Hara et al. 2002; Kim et al. 2002; Kim et al. 2003; Ruggero and Pandolfi 2003).

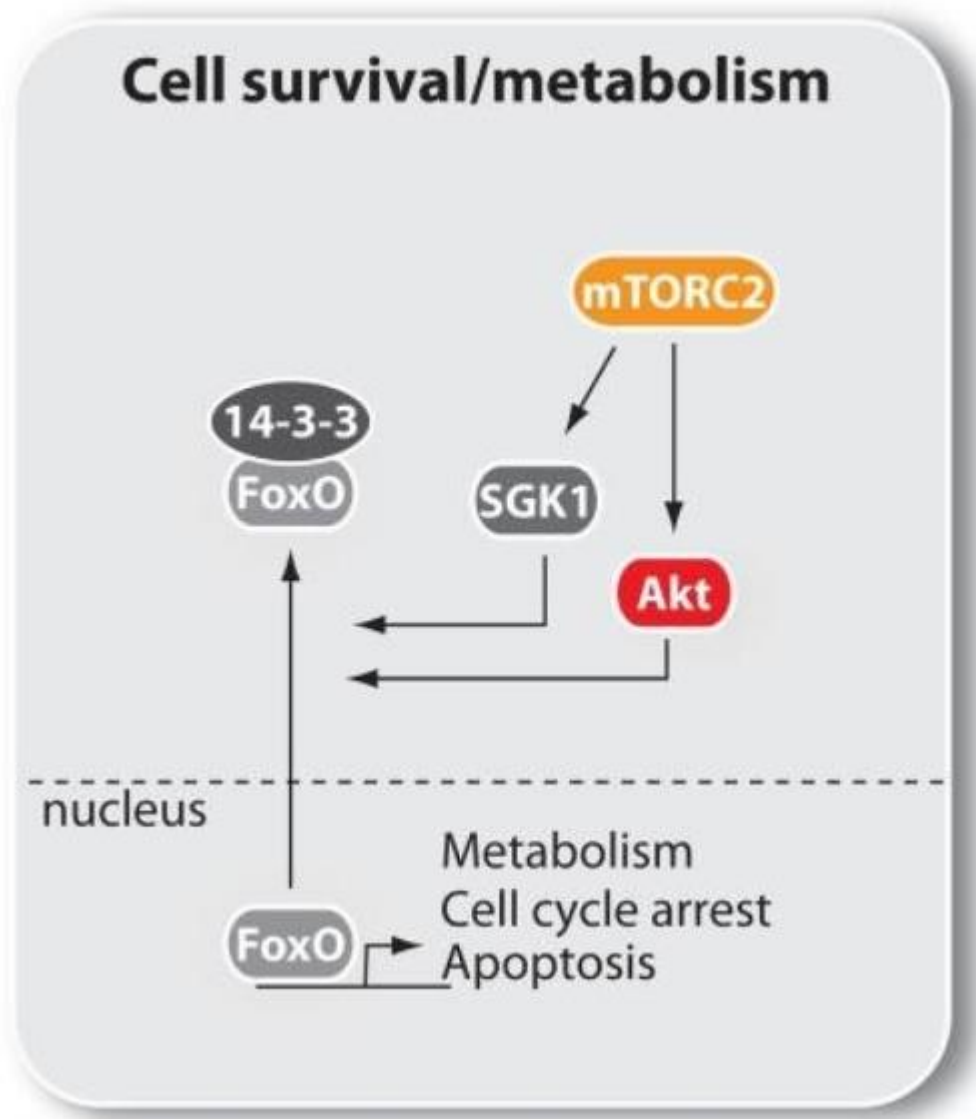


**Figure 1.7: Role of mTORC2 in cellular survival. The mTORC2 promotes cellular survival by activating Akt and via SGK1 phosphorylation (Adapted from Laplante and Sabatini 2012).**

### 1.2.3 Role of mTOR signalling in mitochondrial biogenesis

In mammalian cells, mTOR activity positively correlates with mitochondrial activity (Schieke et al. 2006). mTORC1 inhibition by rapamycin has been shown to down-regulate the rate of oxygen consumption and mitochondrial oxidative capacity (Cunningham et al. 2007). The mTOR appears to regulate peroxisome-proliferator-activated receptor coactivator (PGC1 $\alpha$ ). In addition to the role of PGC1 $\alpha$  in regulating the expression of many mitochondrial genes, PGC1 $\alpha$  also acts as transcriptional coactivator for Yin Yang 1 (YY1) in an mTOR-dependent manner. YY1 belongs to the zinc-finger GLI-Kruppel class of transcription factors. Knockdown of YY1 resulted in a significant decrease in mitochondrial gene expression (Cunningham et al. 2007; Dunlop and Tee 2009; Schieke and Finkel 2006).

### 1.2.4 Regulation of ribosomal biogenesis via the mTOR signalling pathway

The rate of protein synthesis can be regulated by increasing the translation efficiency of existing ribosomes and by the production of new ribosomes. mTOR is a key regulator of both processes, either directly or indirectly, via several components. These include eIF4B, eIF4G, and eIF4E (Hay & Sonenberg 2004). In addition, mTORC1 phosphorylates 4E-BP preventing its activity, as a translational repressor (Brunn et al. 1997; Burnett et al. 1998; Gingras et al. 2001).

Moreover, S6K and its targets, the ribosomal protein S6 and elongation factor-2 kinase (eEF2K), also contribute to ribosome biogenesis. mTOR, via S6K, regulates ribosome biogenesis by controlling the expression of ribosomal protein mRNAs and

the transcription of ribosomal RNA (rRNA) and tRNA, a major limiting step in ribosome biogenesis (Crespo & Hall 2002; Rohde et al. 2001).

Transcription machinery for ribosomal RNA synthesis is regulated by RNA polymerase I (Pol I). This process is mediated by the transcription factor TIF-IA. TIF-IA is also known as regulatory factor that regulate the formation of the transcription initiation complex. mTOR activates TIF-IA, consequently mTOR regulate transcription of ribosomal RNA (Mayer et al. 2004).

### **1.2.5 Role of mTOR signalling in autophagy**

mTOR inhibits autophagy, a catabolic process involving the degradation of cellular components to constituent amino acids. Conversely, in the case of cellular stress, mTOR is inhibited and autophagy is activated (Crespo & Hall 2002; Rohde et al. 2001). In mammalian cells, autophagy-related 13 (ATG13), Unc-51-like kinase 1 (ULK1), FAK family kinase-interacting protein 200kDa (FIP200), and ATG101 forms a complex, which regulates autophagy (Ganley et al. 2009; Hosokawa et al. 2009; Jung et al. 2010). mTORC1 phosphorylates ATG13 and ULK1, inhibiting the complex ability to initiate autophagy (Hosokawa et al. 2009a; Hosokawa et al. 2009). The mTOR-mediated autophagy inhibition allows cells to survive in extreme conditions. Although mTOR has been known as a key regulator of autophagy, the underlying regulatory mechanisms are not clearly understood (Blommaert et al. 1995; Shigemitsu et al. 1999).

### **1.2.6 mTOR signalling and lipid biosynthesis**

The mTOR has been known to regulate cell growth and proliferation via its role in protein synthesis. However, there is growing evidence showing that mTOR controls

cell growth and proliferation by lipid synthesis, a process which is required for cell membrane synthesis and storage of lipid as a source of energy.

The mTORC1 controls lipid synthesis by regulating the transcription factor sterol regulatory element binding protein-1 (SREBP-1). SREBP-1 regulates the expression of genes required for cholesterol, fatty acid, triglyceride and phospholipid synthesis (Horton et al. 2002). The mechanism of SREBP-1 regulation by mTOR is still not well understood.

Activated Akt positively regulates the expression of genes involved in lipid synthesis and nuclear accumulation of SREBP-1 (Manning and Cantley 2007). Inhibition of mTOR by rapamycin, inhibits the Akt mediated SREBP-1 activation and the expression of genes responsible for lipid synthesis. In mammalian cells, SREBP-1 depletion inhibits cell growth (Porstmann et al. 2008).

mTORC1 also controls adipogenesis by regulating the expression and activation of peroxisome proliferator-activated receptor- $\gamma$  (PPAR- $\gamma$ ). PPAR- $\gamma$  is a nuclear receptor which regulates the expression of genes involved in fatty acid uptake, synthesis, esterification, and storage in the newly formed adipocytes.

Lipin1, a phosphatidic acid phosphatase, plays an essential role in adipogenesis. Lipin-1 promotes triglyceride synthesis and acts as coactivator for PPAR- $\gamma$ . Lipin1 is phosphorylated in response to insulin and nutrients in a rapamycin-sensitive manner (Koh et al. 2008; Laplante and Sabatini 2009). A diagram illustrating the regulation of lipid synthesis by mTORC1 is shown in Figure 1.8

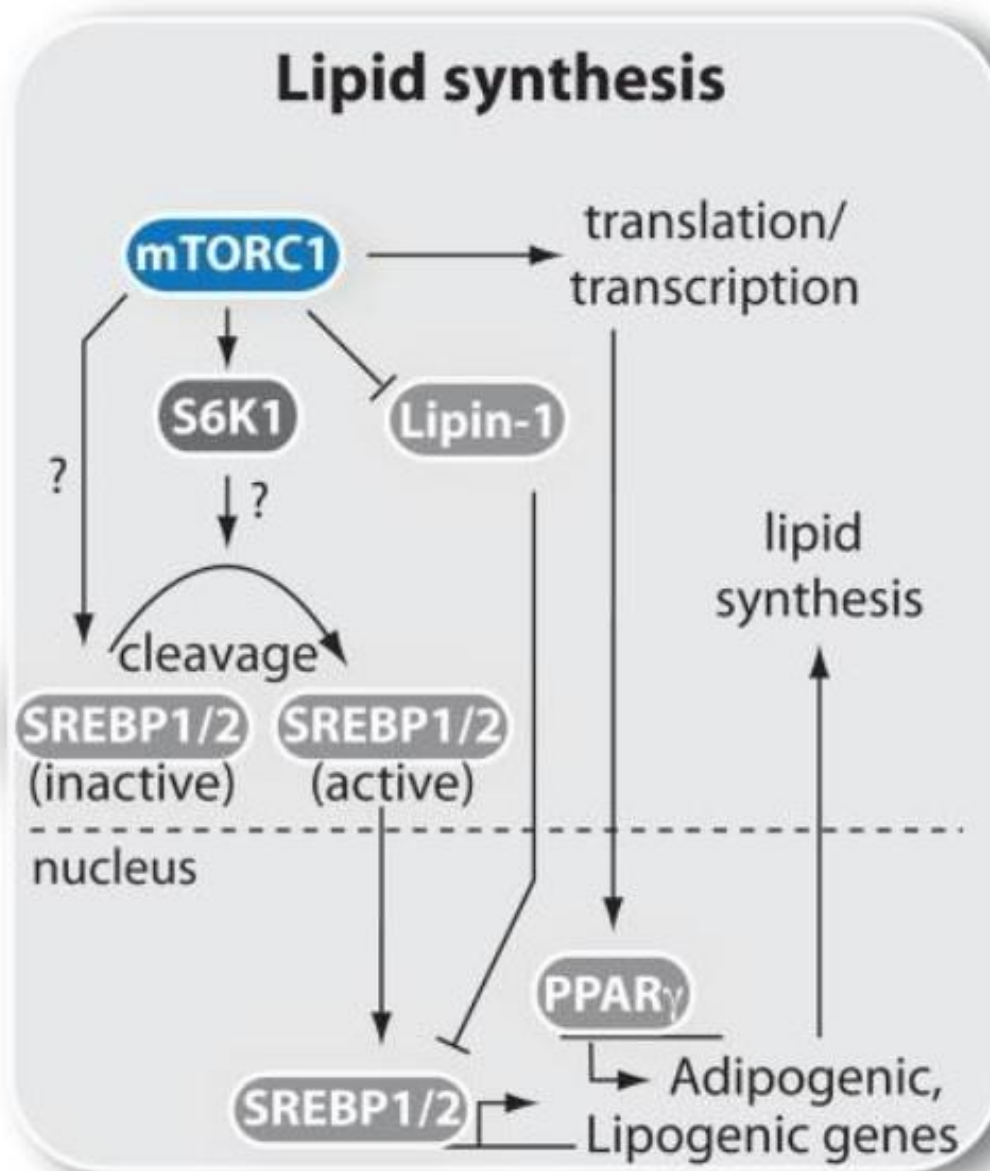


**Figure 1.8: Regulation of lipid synthesis by mTOR.**

The mTORC1 mediates the cleavage of the transcription factor SREBP-1, resulting in its translocation to the nucleus. SREBP-1 induces the expression of several genes that are required by lipogenesis. The mTORC1 also activates PPAR $\gamma$  via several mechanisms, which enhance the expression of lipogenic genes (Adapted from Laplante and Sabatini 2012).

### 1.2.7 Other roles of mTOR in regulating cellular processes

mTOR also regulates gene expression by playing a role in the subcellular localization of transcription factors (Beck and Hall 1999). mTOR has been shown to directly phosphorylate the signal transducer and activator of transcription 3 (STAT3) transcription factor (Yokogami et al. 2000), and S6K1 phosphorylates CREMt, another transcription factor (de Groot et al. 1994). Microarray RNA analysis has shown that mTOR affects the expression of genes responsible for many metabolic and biosynthetic pathways (Peng et al. 2002).

mTOR may also regulate post-transcriptional processes by modulating the activity of some proteins directly involved in post-transcriptional processes of mRNA biogenesis (Wilson and Cerione 2000).

In yeast, protein phosphatases are important downstream targets of TOR. Phosphatase activity in yeast helps the transcriptional and translational processes required for ribosome biogenesis (Crespo & Hall 2002). These phosphatase activities have not yet been identified in mammals.

## 1.3 FKBP12 – Rapamycin Complex

### 1.3.1 Overview of Rapamycin

Rapamycin was identified as an antifungal agent from extracts of the soil bacterium, *Streptomyces hygroscopicus*. The bacterium was found on Easter Island in the 1970s (Sehgal 2003). Subsequent studies on rapamycin revealed impressive tumour- and immuno-suppressive activities (Sehgal et al. 1975; Sehgal 2003; Vezina et al. 1975).

Rapamycin is an mTOR inhibitor that can be administered either orally or intravenously. It enters the tumour cell, where it forms a complex with FK506-binding protein of 12 kDa (FKBP12). This complex binds the FRB domain of mTOR, suppressing its activity (Chen et al. 1995; Sabatini et al. 1994; Sarbassov et al. 2006). The inhibition of mTOR activity suppresses mTOR mediated protein synthesis, eventually resulting in anticancer effects (Dancey 2005). It suppresses tumour cell growth and proliferation and angiogenesis. mTOR inhibition as an anti cancer therapy has been investigated in number of tumour types including renal cancer, breast cancer, lung cancer, colorectal Islet cells cancer. In addition to other mTOR inhibitors, Rapamycin has been helpful in studying mTORC1 activities.

Rapamycin as a drug specifically inhibits mTOR, resulting in reduced cell growth, cell cycle progression and proliferation. Rapamycin was proven to be efficient as antifungal, immunosuppressant and anticancer. However, resistance to rapamycin has been reported (Brunn et al. 1996b; Gingras et al. 2001b; Schmelzle and Hall 2000).

### **1.3.2 Overview of FKBP12**

FKBP12 is a peptidyl-prolyl isomerase, abundantly found in many eukaryotes and ubiquitously, that may function as a protein–folding chaperone for proteins containing proline residues (Schreiber 1991). Rapamycin inhibits the isomerase activity of FKBP12 (Heitman et al. 1991; Koltin et al. 1991; Wiederrecht et al. 1991). Although, mTOR is able to bind to rapamycin-FKBP12 complex, it is unable to bind to either rapamycin or FKBP12 separately (Chen et al. 2007; Gingras et al. 2001; Schmelzle & Hall 2000; Stan et al. 1994). The crystal structure of FKBP12-rapamycin in complex with the FRB domain of mTOR did not reveal how this

interaction prevents phosphorylation of direct mTORC1 substrates and the mechanism of mTOR inhibition by rapamycin remains unclear (Choi et al. 1996). Previous biochemical studies indicated that binding of FKBP12-rapamycin to mTORC1 may result in a conformational change and cause the dissociation of mTOR complex1 proteins (Kim et al. 2002).

Recent studies of mTORC1 by cryo-EM reveals that relatively short exposure to FKBP12-rapamycin does not affect the structural integrity of mTORC1, while extended incubations resulted in disassembly of mTORC1. No intact mTORC1 particles could be detected after one hour incubation (Yip et al. 2010).

It was proposed that FKBP12-rapamycin binds to mTORC1 and this binding blocks access to the active site for mTOR substrates, S6K1 and 4E-BP1 (Yip et al. 2010a). It has been shown that within cells, rapamycin does not completely inhibit 4E-BP1 phosphorylation (Choo et al. 2008; Feldman et al. 2009; Thoreen and Sabatini 2009) or mTORC1 stability (Kim et al. 2002) suggesting that cells contain buffering mechanisms that counter the effects of rapamycin on mTORC1 and that these are lost when mTORC1 is purified (Yip et al. 2010a).

#### **1.4 Initial evidence for the existence of mTOR splicing isoforms**

Since mTOR has been identified and studied based on rapamycin sensitivity, it is possible that mTOR is participating in non-rapamycin related processes, which have not yet been identified. In addition, TOR in budding and fission yeast shows some signaling activity in a rapamycin insensitive manner. It is unknown whether mTOR can also signal in a completely rapamycin-insensitive manner in humans (Fingar et al. 2002; Fingar & Blenis 2004).

Like other PIKK family members, there is an increasing evidence of the presence of mTOR splicing isoforms. Data from our laboratory suggests the existence of several potential splicing isoforms of mTOR. Northern blotting of human tissues as well as western blotting of gel filtration fraction analysis of mTOR from MCF7 cell lysates, indicate the presence of several potential mTOR splicing forms. Our laboratory has also provided evidence for the existence of the mTOR splicing isoform, mTOR $\beta$ , which lacks most of HEAT and FAT domains (Panasyuk et al. 2009) (Figure 1.9). *In vivo*, mTOR $\beta$  could form complexes with Raptor and Rictor. *In vitro*, mTOR $\beta$  has been shown to phosphorylate the same substrates, as originally reported for the full length mTOR (mTOR $\alpha$ ). The mTOR $\beta$  has also been shown to accelerate cell cycle progression and to stimulate cell proliferation. Moreover, mTOR $\beta$  overexpression in cells was shown to have oncogenic potentials, when tested *in vitro* (colony formation assay) and *in vivo* (tumour formation in nude mice) (Panasyuk et al. 2009).

There are numerous commercially available mTOR specific antibodies which recognise different regions in mTOR. When tested in western blotting, they recognise the full length mTOR (280kDa) and a number of immunoreactive bands with lower molecular weight in total cell lysates from different cell lines and tissues. These bands may represent the product of mTOR degradation, non-specific binding or potential splicing isoforms of mTOR.

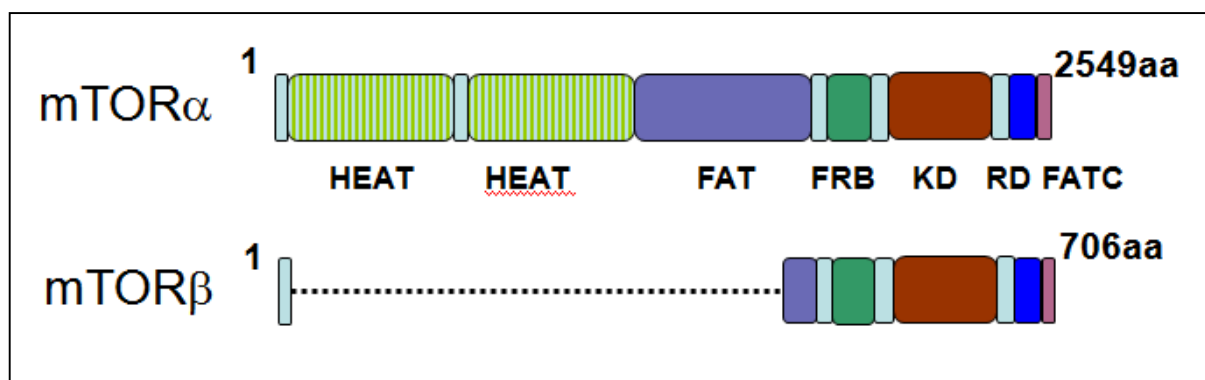


**Figure 1.9: Modular representation of mTOR isoforms**

## 1.5 Aim of the study

In the course of identification and characterization of mTOR $\beta$  in our laboratory, preliminary experimental evidence was obtained in support for the existence on novel mTOR splicing isoforms. Therefore, the initial aim of this study is to search for novel mTOR splicing isoforms by applying bioinformatics, biochemical and molecular biology approaches. The identification of additional mTOR splice variants will inspire us to investigate their ability to form regulatory signalling complexes mTORC1 and mTORC2, and to phosphorylate known downstream substrates. Furthermore, our efforts will be focused on studying the role of the novel isoforms in the mTOR-mediated cellular processes, such as cell proliferation, cell survival and oncogenic transformation.

## 1.6 Methods of isolating mTOR

In order to find novel mTOR splicing isoforms, we looked at how previous researchers had identified mTOR. TOR was discovered as a target of FKBP12-

rapamycin complex, which was known to arrest cell cycle progression. Mammalian TOR was first identified and reported in 1994, and given different names: FKBP12-rapamycin associated protein (FRAP), rapamycin and FKBP12 target (RAFT), rapamycin target (RAPT), or sirolimus effector protein (SEP) (Brown et al. 1994; Chen et al. 1994; Chiu et al. 1994; Sabatini et al. 1994; Sabers et al. 1995).

Brown et al. isolated mTOR, designated FRAP, using a fusion protein of Glutathione-S transferase with the FKBP12, in complex with rapamycin, to identify the binding partner from MG-63 cells (Brown et al. 1994).

Sabatini et al. isolated mTOR, designated RAFT, using cross-linking and affinity purification procedures for proteins interacting with FKBP12 in the presence of rapamycin. They identified two proteins, RAFT1 245 kDa and RAFT2 35 kDa (Sabatini et al. 1994). RAFT1 was described as TOR, while RAFT2 has never been mentioned again.

Chen et al. isolated mTOR from Molt 4 cells, BJAB cells and from normal human T cells, using the GST-FKBP12:Rapamycin affinity matrix method. The identified protein was designated SEP and when tested in complex with FKBP12-rapamycin, exhibited immunosuppressive activity (Chen et al. 1994).

Chiu et al. isolated mTOR, designated RAPT, using a two-hybrid system to screen a mouse cDNA library. The isolated mammalian clones, which interact with FKBP12 in the presence of rapamycin, were further expressed in yeast for protein-protein interaction studies (Chiu et al. 1994).

Sabers et.al. isolated mTOR as a protein target of FKBP12-rapamycin complex in mammalian cells. Their strategies depending on affinity purification technique, by

incubating the tissue extract with GST-FKBP12 in the presence of rapamycin (Sabers et al. 1995).

In our laboratory, a novel mTOR $\beta$  isoform was originally identified in cell lines and tissues by immunoblot analysis with in-house developed anti-mTOR mABs (Figure 1.9). Subsequently, molecular cloning of a cDNA corresponding to mTOR $\beta$  was carried out using a panel of specific primers and the polymerase chain reaction (PCR) approach (Panasyuk et al. 2009).

# **CHAPTER 2**

## **Experimental procedures**

## Chapter 2: Methodology

---

### 2.1 Materials

#### 2.1.1 Common laboratory reagents

All the general purpose chemicals were purchased from Sigma-Aldrich, Thermo Fisher Scientific UK limited, BDH Analar, and Melford Laboratories Ltd. UK unless otherwise stated. General cell culture reagents were purchased from PAA Laboratories GmbH. Pre-stained protein molecular weight markers, DNA Markers, and restriction enzymes were obtained from Fermentas. All solution and buffers summarized in Appendix A

#### 2.1.2 Molecular cloning materials

To purify a good amount of GST-FKBP12 to be used to prepare the affinity matrix, pGEX-FKBP12 plasmid was generated within the lab.

To carry out experiments for mTOR functional analysis, I employed in these studies wild type and activated forms of mTOR. A single amino acid mutation in mTOR, S2215Y resulted in nutrient-independent activation of mTORC1 (Sato et al. 2010). Cells expressing Flag-mTOR $\alpha$  and S2215Y were used as positive controls. In the other hand, cells transfected with a vector and cells transfected with an empty vector will be used as negative controls.

The pcDNA3 Flag-mTOR $\delta$ , pcDNA3 Flag-mTOR $\gamma$ , pcDNA3 Flag-mTOR wild type and pcDNA3 Flag-mTOR S2215Y mutants were generated. Generated expression vectors have been confirmed by restriction analysis and sequencing. These expression vectors were used for generation of stable cell lines.

The pME18SFL3 mTOR $\delta$  plasmid was obtained courtesy from the National institute of technology and evolution (NITE). All other plasmids were obtained from Invitrogen.

### 2.1.3 Proteins

GST-FKBP12 was purified from bacteria using recombinant GST fusion protein, which was over-expressed in *E.Coli Rosetta* cells. The bacteria containing the vector was induced by IPTG, lysed, sonicated, centrifuged, and GST-FKBP12 protein was purified using Glutathione-Sepharose, and dialysed by desalting column.

Affinity matrix was prepared by coupling GST-FKBP12 in complex with Rapamycin to Glutathione Sepharose beads, and tested using lysates of cells over-expressing mTOR $\alpha$  (280kDa) and mTOR $\beta$  (80kDa). GST-FKBP12 purification was repeated 4 different times to test different reaction conditions, which could affect the affinity of mTOR to bind to the affinity matrix. These conditions and factors include Rapamycin, GST-FKBP12, buffers, and beads.

His-tagged S6K1 were purified from Sf9 insect cells and provided by Alexander Zhyvoloup. 4EBP1 and Akt Were purified within the laboratory by previous PhD student in our Laboratory.

### 2.1.4 Antibodies

The monoclonal anti-Flag antibody was purchased from Sigma-Aldrich. Horseradish peroxidase-linked (HRP) secondary antibodies, anti-rabbit and anti-mouse, were purchased from Promega. Monoclonal antibodies against actin, myc and polyclonal Anti-F11 mTOR antibody were generated in the lab by previous students for other purposes. Anti Phospho-Akt (#4051) and anti Phospho-4E-BP1 (#2855) were obtained from Cell Signalling. Anti-S6K1 (phosphoT389) (ab2571) were acquired from Abcam. Anti-Phospho-mTOR (Ser2448) (09-213) and polyclonal antibodies towards the C-terminal peptides of anti-mTOR (07-231) antibodies were obtained from Millipore. The antibody targeting the N-terminal N-19 (sc-1549) of mTOR was purchased from Santa Cruz. The mTOR $\delta$  sequence was sent to our collaborators in Ukraine to generate anti-mTOR $\delta$  C-terminal antibody. The Polyclonal antibodies targeting the mTOR $\delta$  were produced by immunizing a mouse with a synthetic peptide corresponding to residues 28 – 59 of human mTOR $\delta$ . Antibodies are purified by protein A and peptide affinity chromatography (further details about anti-mTOR $\delta$  discussed in chapter four).

### 2.1.5 Mammalian cell lines

HEK 293 (human kidney embryonic cells), MCF-7 (breast adenocarcinoma), Cos7 (monkey kidney fibroblast-like), HepG2 (hepatocellular carcinoma), A549 (human lung carcinoma), MCF7 (human breast adenocarcinoma cell line) and HELA (human cervical epithelial carcinoma) cell lines were obtained from the American Type Culture Collection (ATCC). All other cell lines were kindly provided by Dr. Mina (Institute of structural and molecular biology, University College London). The rat heart tissue was extracted in the lab.

### 2.1.6 Bacteria

*Escherichia coli* XL-10 Blue competent cells, Genotype: supE44 hsdR17 recA1 endA1 gyrA46 thi relA1 lac-F [proAB:acI9 lacZ $\Delta$ M15 Tn10(tet<sup>r</sup>)]. These cells were used in the amplification of plasmid DNA.

*Escherichia coli* BL21(DE3) pLysS cells. Genotype: F<sup>-</sup> ompT hsdS<sub>B</sub> (r<sub>B</sub> - m<sub>B</sub> -) gal dsm (DE3) pLysS (Cam<sup>R</sup>). The DE3 designation means the strains contain the  $\lambda$  DE3 lysogen that carries the gene for T7 RNA polymerase under control of the lacUV5 promoter. Isopropyl- $\beta$ -D-thio-galactopyranoside (IPTG) is required to induce expression of the T7 RNA polymerase. These cells were used in the expression of GST fusions.

## 2.2 Methods

### 2.2.1 Molecular methods

#### 2.2.1.1 Primers design

Primers were designed using the known DNA sequence of the template. Primers were checked for the absence of potential DNA secondary structure formation and annealing of primers to itself or within primer pairs, potential self-complementarity and GC content of the primers to insure similar melting temperatures of the primers. Annealing temperatures (T<sub>m</sub>) for each primer were calculated using Equation 2-1:

$$T_m(^{\circ}\text{C}) = 2(A+T) + 4(G+C) \quad \text{Equation 2-1}$$

All primers were ordered from MWG-Biotech. To check primers were correctly designed and also whether DNA had been correctly inserted into a vector, 10-50 ng/ $\mu$ L DNA samples in 30  $\mu$ L H<sub>2</sub>O were sent off for sequencing analysis as discussed in section (2.2.1.6).

#### **2.2.1.2 DNA digestion**

All restriction endonucleases were purchased from Fermentas and digests were carried out in the manufacturer's recommended digestion buffer. As per the manufacturer's recommendations, five units of restriction enzyme were used to digest 1 $\mu$ g of DNA in a total volume of 20 $\mu$ L. The reaction mixtures were incubated at 37°C for 1hr.

#### **2.2.1.3 DNA ligation**

A rapid DNA ligation kit from Fermentas was used to ligate DNA fragments to linearised vector. In order to reduce the risk of self-ligation of the plasmids, at least a 1:3 molar ratio of vector: insert was utilised in the ligation reactions. The reactions were conducted at room temperature using 1 $\mu$ L of T4 DNA Ligase and 5 $\mu$ L of Rapid Ligation Buffer in a total reaction volume of 20 $\mu$ L. The reaction mixture was used for transformation.

#### **2.2.1.4 Polymerase chain reaction**

The polymerase chain reaction (PCR) was used to amplify specific DNA sequences from DNA templates, using specific DNA primer oligonucleotides. PCR was performed using 2 ng DNA template in a 20  $\mu$ L total volume containing 0.2 mM dNTPs, 2  $\mu$ M of each primer, and 0.5 U DNA polymerase (Thermo Scientific) in 1x reaction buffer as supplied. The reaction was carried out for 30 cycles, consisting of a denaturing stage (98°C for 30s), a primer annealing stage

(56-59° for 30s), and finally a polymerase extension stage (72°C for 1 minutes). After completion of the cycling amplification, a final extension stage (72°C for 3 minutes) was applied. Reactions were carried out in a thermal cycler (Labnet Multigene II).

#### **2.2.1.5 Electrophoresis and DNA purification**

DNA fragments were visualised by separation on an agarose based gel. 0.6 to 1 % w/v agarose gels were used throughout this thesis for DNA purification and analysis. The required weight of agarose was added to TAE buffer (40 mM Tris-Acetate, 1 mM EDTA, pH 7.0) and heated in order to dissolve the agarose. After cooling the solution to approximately 50°C, Gel-Red dye supplied by Biotium was added in a 10,000x dilution. The liquid agarose solution was then poured into a mould containing a well-forming comb and left at room temperature so that it could solidify. DNA samples were prepared and mixed with 6X DNA loading buffer supplied by Fermentas, and then they were loaded into the wells in the gel. The samples were then electrophoresed at 80V in TAE buffer to achieve separation. Standard molecular weight markers (1kb Gene Ruler from Fermentas) were used to ascertain the sizes of the various fragments. The DNA was observed by exposing the gel to long-wave UV light. Purification of the requisite DNA fragments from the gel was performed by excising the bands of interest and using DNA Gel Extraction kit (QIAGEN) to obtain the DNA.

#### **2.2.1.6 DNA sequencing**

Minimum of three grams of plasmid DNA was air dried and sent for sequencing by MWG Biotech, GATC Biotech or by Wolfson Institute for Biomedical Research, UCL.

### 2.2.1.7 Transformation and plasmid amplification

The *XL-10 E.Coli* competent cells, initially stored at  $-70^{\circ}\text{C}$  were thawed on ice and 50  $\mu\text{l}$  cell suspensions were mixed with 1  $\mu\text{l}$  ligation mixture or 50 ng of plasmid DNA. After 20 minutes incubation on ice, the cells were induced to take up the DNA by heat-shock at  $42^{\circ}\text{C}$  for 45 seconds, followed by immediate cooling on ice for 2 minutes and allowed to recover in 1 ml of warm SOC (Super Optimal broth with Catabolite repression) medium or 1 ml of LB medium for 45-60 minutes at  $37^{\circ}\text{C}$  in shaking incubator (220 rpm). The bacterial cells were then briefly centrifuged (3000 rpm for 5 minutes) and the pellet resuspended in 100 $\mu\text{l}$  of LB medium. Bacterial suspension was spread onto pre-warmed LB agar plates containing the appropriate selective antibiotic and incubated overnight at  $37^{\circ}\text{C}$ .

#### 2.2.1.7.1 Plasmid DNA Purification

Plasmid DNA was purified using QIAGEN mini- or midi- Plasmid Purification kit (QIAGEN) according to the manufacturer's instructions. The QIAGEN plasmid purification protocol is based on alkaline lysis of the bacterial cells, followed by binding of plasmid DNA to anion-exchange resin under appropriate low salt and pH conditions. Bacterial pellet from overnight shaker-culture of *XL-10 E. coli* was re-suspended in the provided P1 buffer. The suspension was subsequently lysed by P2 buffer and neutralised with buffers N3 respectively. Cellular debris was removed by centrifugation and the supernatant containing the circular plasmid DNA was collected. The supernatant was applied to a QIAGEN spin column. Further centrifugation through the column results in the plasmid DNA binding to the column. The plasmid DNA was then washed by centrifugation with PB and PE buffers and eluted using TE buffer (10 mM Tris-HCl, pH 8.0, 1 mM EDTA) or ddH<sub>2</sub>O.

The plasmid DNA can be desalted and concentrated by isopropanol precipitation. To precipitate the DNA, an equal volume of 100% isopropanol was added to the DNA solution and immediately centrifuged at 13000 rpm for 30 minutes. The DNA pellet was washed with 70% ethanol, air-dried for 5-10 min and dissolved in an appropriate volume of ddH<sub>2</sub>O or TE buffer. The quality and purity of plasmid DNA was checked by DNA agarose gel alongside a comparative DNA ladder (1 kb GeneRuler, Fermentas). The plasmid DNA concentration was determined by nano-drop analysis.

## **2.2.2 Mammalian cell culture**

### **2.2.2.1 Maintenance of cell lines**

HEK 293 cells were maintained in a high glucose Dulbecco's Modified Eagle's medium (DMEM, from PAA). Media were supplemented with 10% v/v foetal bovine serum (FBS, from Hyclone) and 1% penicillin/streptomycin v/v antibiotics. Cells were grown in 37°C humidified incubators at 10% CO<sub>2</sub>. At about 60-80% confluency, cells were passaged. The media was aspirated and the cells were washed once with Dulbecco's phosphate buffered saline (PBS from PAA). The 1X trypsin-EDTA (supplied by PAA) was then added to detach cells from the plates. The cells were then incubated at 37°C for 1-2 minutes in order to fully detach the cells. The cellular suspension was pipetted up and down continuously to break up any clumps of cells. A fresh media was then added to neutralise the trypsin. The volume of cellular suspension required to achieve a desired confluency was then added with a fresh medium into new plates. All culturing procedures were carried out in a sterile laminar flow hood. All media and reagents used had been previously pre-warmed to 37°C.

#### 2.2.2.2 Cell counting

To count cells, DMEM was removed from plated cells, which were then washed with 1X PBS and trypsin as described for maintenance of cell lines (2.2.2.1). Undetached cells were mixed with DMEM and spun at 1000 RPM for 5 minutes. The cell pellet was re-suspended in fresh PBS, a 2  $\mu$ L aliquot of which was added to a vial containing 10 ml CASYTON Buffer solution (Innovatis). The cells were thoroughly mixed with the buffer and then analysed using the CASY Model TT cell counter (Innovatis), which relies on electronic pulse area analysis for measurements. The CASY machine enables the measurement of total and viable cell numbers, cell size, percentage viability and cell aggregation factors.

#### 2.2.2.3 Serum and nutrient starvation and stimulation

HEK 293 cells were serum starved at about 70% confluency using Dulbecco's modified Eagle's medium (DMEM) High Glucose containing L-glutamine and penicillin/streptomycin for 36 hours. The complete DMEM medium was aspirated and was replaced with serum-free DMEM medium. The cells were then incubated at 37°C overnight in this medium. Serum stimulation is carried out by the addition of 10% fetal bovine serum for 1 hour followed by harvesting the cells. For nutrient starvation, next morning, the serum-free media was removed and the PBS was added into the plates. The cells were then incubated at 37°C for 1 hour to achieve nutrient starvation. At this point, the cells were used for analysis.

#### 2.2.2.4 DNA transfection

When a 10cm plate had reached 80% confluency it was split (1/3) into three new 10cm plates with 8mL of fresh DMEM complete medium. 24hrs later, the media was aspirated and 10mL of new DMEM complete medium was added to each plate. 10 $\mu$ g of plasmid DNA was then mixed with 200 $\mu$ L of sterile 150mM NaCl.

The DNA and NaCl were mixed very well by pipette action. 35 $\mu$ L of Exgen500 transfection reagent supplied by Fermentas was then added and the solution was immediately mixed by pipette action for 10 seconds. The tubes were then incubated at room temperature for 10 minutes before being added drop wise to the previously prepared plates of HEK 293 cells with refreshed medium. The transfected cells were then placed in an incubator at 37°C for 48 hours before being used for experiments or frozen at -80°C.

#### 2.2.2.5 Generation of stable cell lines

Mammalian expression vectors encoding FLAG-mTOR for different isoform have been generated. These constructs contain the neomycin resistance gene which allows selection of transfected cells with Geneticin (G-418). Before Geneticin treatment HEK 293 cell were tested for the Geneticin resistance and the optimum concentration for selection were obtained. HEK 293 cells were transfected with each vector, and transient transfected cells showed good level of expression of these mTOR isoforms. 48 hours after transfection, cells were split 1/20 into complete medium containing 1200  $\mu$ g/ml of G-418. Selective medium was changed every 2-3 days and cell survival was monitored over the period of two weeks to identify colonies that had integrated a gene construct. Selected colonies were mixed and screened for protein expression. Those cell clones that tested positive for expression were frozen in DMEM medium containing 50% FBS and 10% dimethyl sulfoxide (DMSO) and stored in liquid nitrogen.

To maintain HEK 293 stable cell lines, the vial of cells was removed from the liquid nitrogen and thawed quickly at 37°C. Immediately before the cells were completely thawed, the outside of the vial was decontaminated with 70% ethanol, and the contents transferred to a 10 cm plate containing 10 ml of complete medium

without antibiotic [DMEM (high glucose), 10% FBS, 2 mM L-glutamine]. The plate was incubated at 37°C for 2-4 hours to allow the cells to attach to the bottom of the plate. The cells were maintained in a complete medium [DMEM (high glucose), 10% FBS and 1% Penicillin-Streptomycin] containing the selective antibiotic G-418 at a final concentration of 200 ug/ml.

#### **2.2.2.6 Cryopreservation**

Healthy cells of a low passage number (passage 2-5) were grown to about 80% confluency in DMEM, supplemented with 10% FBS and 1% penicillin/streptomycin at 37°C, 10% CO<sub>2</sub>. After media was removed, the cells were washed with PBS and treated with Trypsin-EDTA as described for the maintenance of cell lines (2.2.2.1). Cells were resuspended in fresh DMEM and spun for 5 minutes at 1000 RPM. The medium was removed and cells were re-suspended in 90% FBS, 10% Dimethyl Sulphoxide (DMSO). The cell suspension was placed in freezing vials and stored at -80°C overnight in a box containing isopropanol, which allows the vials containing the cells to slowly come to temperature, preventing cell death. Cells were then placed in liquid nitrogen storage tanks for future use.

#### **2.2.2.7 Cell line defrosting**

To maintain cell lines, the vial containing cells was thawed quickly in a 37°C water bath. The outside of the vial was decontaminated with 70% ethanol just before cells were completely thawed, and the contents were transferred to DMEM supplemented with 10% v/v FBS and 1% penicillin/streptomycin v/v antibiotics. The cells were spun at 1000 RPM for 5 minutes and the pellet of cells were re-suspended in fresh media and transferred to a new plate, which also contained

fresh media. The cells were incubated in a humidified, 37°C, 10% CO<sub>2</sub> incubator and checked daily until they reached 70-90% confluence.

### **2.2.3 Protein isolation methods**

#### **2.2.3.1 Mammalian cell lysis for protein analysis**

Cells were washed twice with ice-cold PBS and extracted with lysis buffer (0.3% v/v CHAPS, 50 mM Tris-HCl pH 6.8, 100 mM NaCl, 2 mM EDTA, 50 mM NaF, 25 mM 2-glycerophosphate, EDTA-free protease inhibitor cocktail (Roche), final pH 7.5). Cells were scraped from the dishes and transferred to micro-centrifuge tubes. Tubes were incubated on ice for 30 minutes prior to centrifugation at 14000 rpm at 4°C for 30 minutes to remove insoluble material. Supernatants were transferred into fresh tubes and the total protein concentrations of cellular extracts were determined by Bradford protein assay.

#### **2.2.3.2 Measuring protein concentration**

The total protein concentration in cell lysates was determined using the Coomassie (Bradford) protein reagent (Pierce). The reagent was diluted 1:1 with ddH<sub>2</sub>O to give the working solution. Samples were made up by adding 1 µl of each lysate sample to 1 ml of reagent solution and standards were prepared by diluting appropriate amounts of 2 mg/ml Bovine Serum Albumin (BSA) to give a range from 0.5-8 µg/ml. All absorbance measurements were taken on an Eppendorf BioPhotometer at 595 nm using plastic 1ml cuvettes.

#### **2.2.3.3 Immunoprecipitation**

Immunoprecipitation of particular proteins was achieved by using antibodies that were specific for the protein of interest. Antibody was added to Protein A

sepharose beads followed by the total cell lysate in a microcentrifuge tube. The sample tubes were then placed on a rotating wheel for 2hrs at 4°C. Following incubation on the wheel, the tubes were washed 3x prior to loading on a SDS-PAGE gel.

#### 2.2.3.4 Affinity Purification

GST-FKBP12 was purified from bacteria using recombinant GST fusion protein, which was over-expressed in *E.Coli Rosetta* cells. The bacteria containing the vector was induced by IPTG, lysed, sonicated, centrifuged, and GST-FKBP12 protein was purified using Glutathione-Sepharose, and dialysed by desalting column.

The GST fusion proteins were then batch-purified from the supernatant by binding to Glutathione-Sepharose beads (Amersham Pharmacia Biotech) for 3 hours at 4°C. Beads were washed in ice cold lysis buffer (2 times). GST fusion proteins were eluted by competition with 20mM glutathione in 100 mM Tris-HCl pH 8.0, 150 mM NaCl (elution buffer). Elution was repeated three times, eluted fractions were subjected to dialysis against dialysis buffer 1 (50 mM Tris-HCl pH 7.5, 150 mM NaCl, 1mM DTT) overnight 4°C, and then against dialysis buffer 2 (buffer 1 containing 50 % glycerol) for three hours at 4°C to remove free glutathione and to concentrate the protein. Dialysis into 50 % glycerol allows long term storage at -20°C while avoiding damage to the protein caused by repetitive freeze-thaw cycles. The quality of the purified proteins was analysed by SDS-PAGE

Affinity matrix was prepared by coupling GST-FKBP12 in complex with Rapamycin to Glutathione Sepharose, and tested using lysates of cells over-expressing mTOR $\alpha$ , (280kDa), and mTOR $\beta$ , (80kDa). GST-FKBP12 purification

was repeated 4 different times to test different reaction conditions, which could affect the affinity of mTOR to bind to the affinity matrix. These conditions and factors include Rapamycin, GST-FKBP12, buffers, and beads.

### 2.2.3.5 SDS-PAGE

Cellular proteins were separated based on their molecular weight (MW). This was done using either the discontinuous SDS-polyacrylamide gel electrophoresis (SDS-PAGE) system as described by Laemmli (Laemmli, 1970), or the mini-PROTEAN® TGX™ (Tris-Glycine eXtended) precast gels (BIO-RAD laboratories, Inc.).

When proteins are mixed and boiled with Laemmli sample buffer, the SDS detergent present in the buffer binds to the proteins. This results in the linearization of the protein as well as the formation of a uniform negative charge across the length of the protein. Consequently, the proteins samples separation based solely upon their size. During electrophoresis, movement of the larger proteins is physically retarded by the matrix, whilst smaller proteins meet with less opposition and move further more quickly.

The home made system gels were run using the Hoefer SE400 electrophoresis system (Hoefer instruments, San Francisco, Ca.). The gel plates were thoroughly cleaned with water and 70% ethanol prior to use and assembled using 0.75 mm spacers as instructed by the manufacturer.

Gels were made fresh on the day of the experiment and consisted of 7.5 to 15 % acrylamide resolving gel and 10 % ammonium persulphate (APS) and Tetramethylethylenediamine (TEMED) which catalyse the polymerisation of the gels.

The Mini-PROTEAN TGX precast gels system retains Laemmli-like separation characteristics, however have an increased gel matrix stability. Gels with gradient concentrations of 4-20% polyacrylamide concentration were typically used and were run using the Mini-PROTEAN Tetra Cell electrophoresis system (BioRad).

#### **2.2.3.5.1 Protein sample preparation**

Samples were prepared for SDS-PAGE analysis by adding the appropriate amount of 5X Laemmli sample buffer to a final concentration of 1X (250mM Tris pH 6.7, 50% glycerol, 0.5% bromophenol blue, 500mM DTT, 10% SDS). Proteins immobilized on sepharose beads (from immunoprecipitations) were denatured by addition of Laemmli buffer. All samples were boiled for 5 minutes then briefly centrifuged prior to loading onto the polyacrylamide gel.

#### **2.2.3.5.2 Preparation of SDS-PAGE**

The resolving gel mixture (Table 2-1) was poured into the space between the glass plates by pipette. The mixture was then overlaid with 1ml of ddH<sub>2</sub>O to avoid a curved meniscus forming on the top of the gel which leads to distortion of protein bands. The polymerization of the resolving gel typically takes around 30 minutes and can be visualized by a clear rounding of the gel corners at the edges beneath the water layer. Once polymerization was complete, the water was removed and any un-polymerized acrylamide was washed from the top of the cassette with water. The stacking gel was then cast with a comb to form the desired number of wells. Following polymerisation of the stacking gel, the comb was removed and wells were washed with tris-glycine running buffer (0.25mM Tris, 250mM glycine, 0.1% SDS) to remove any unpolymerised acrylamide. Wells were refilled with running buffer and samples were loaded using a Hamilton syringe (Hamilton, Reno, Nevada) or disposable

tips. After loading the samples the upper and lower buffer chamber were filled with running buffer. In case of homemade system, Gels were run at 25mA until samples pass the stacking gel then the current is raised to 40mA until the dye front reached the end of the gel. Pre-cast gel where run according to the manufacturer's recommendations.

<i>Concentration</i>	20 ml (one gel)			Mini gels, 5 ml		Stacking Gel	
	7.5%	10%	15%	10%	15%	3ml	5ml
ddH <sub>2</sub> O	9.63	7.9	4.6	1.9	1.1	2.1	3.4
30% Acrylamide mix	4.97	6.7	10.0	1.7	2.5	0.5	0.83
1.5M Tris HCl pH 8.8	5.0	5.0	5.0	1.3	1.3	0.38	0.63
10 SDS	0.2	0.2	0.2	0.05	0.05	0.03	0.05
10 % APS	0.2	0.2	0.2	0.05	0.05	0.03	0.05
TEMED	0.012	0.008	0.008	0.002	0.002	0.003	0.005

**Table 2-1: preparation of poly acrylamide gel**

### 2.2.3.6 Protein Visualisation

Following electrophoresis proteins were visualised by staining or western blotting.

Gels were stained by Coomassie or silver staining systems.

#### 2.2.3.6.1 Coomassie Staining

For Coomassie staining gels were immersed in Coomassie Blue. Two Coomassie stain systems have been used. The InstantBlue is a ready-to-use Coomassie stain that is specially formulated for fast (15 – 60 minutes) and sensitive detection of proteins. Protein gels can be stained in minutes without the need to wash, fix or de-stain.

The second system was the home made Coomassie Blue stain [0.5% (w/v) Coomassie brilliant blue R-250, 50% (v/v) methanol and 10% (v/v) acetic acid]. Gels stained by immersion in Coomassie Blue stain with gentle agitation for 20 minutes, followed by de-staining in 20% (v/v) methanol, 10% (v/v) acetic acid

for several hours. The gel was then dried under vacuum at 80°C for 1 hour. Coomassie brilliant blue binds to proteins stoichiometrically. The relative amounts of protein can be measured by densitometry.

#### **2.2.3.6.2 Silver Staining**

When more sensitive staining was required, gels were silver stained using a silver staining kit from Fermentas (PageSilver). The gel was first fixed in a fixative solution (50% ethanol, 10% acetic acid) for 10 minutes. The fixed gel was washed two times in 30% ethanol for 10 minutes, followed by two washing cycles with ddH<sub>2</sub>O for 20 seconds. The gel was agitated with sensitizing solution (0.4% sensitizer concentrate) for 1 minute, and after the sensitizing solution was removed, it was washed twice with ddH<sub>2</sub>O for 20 seconds. The gel was stained with staining solution (4% stainer, 0.054% formaldehyde) for 20 minutes. After two wash cycles with ddH<sub>2</sub>O, developing solution (10% sensitizer concentrate, 10% developing reagent, 0.027% formaldehyde) was added. The gel was left to develop for 4 minutes, or until the required intensity of bands was reached. Staining was stopped by the addition of stopping solution (8% stop reagent), with gentle agitation for 5 minutes. After the stopping solution was discarded, the gel was stored in ddH<sub>2</sub>O.

#### **2.2.3.6.3 Western Blotting**

##### **2.2.3.6.3.1 Proteins transfer to membrane**

After SDS-PAGE, the proteins were transferred from gels using the wet and semi-wet protein transfer methods. The Trans-Blot™ (Biorad) and The Trans-Blot Turbo transfer systems were utilised to perform the semi-dry transfer. Once the gel cassettes were opened, superfluous parts of the gel were cut off and the gel

was placed on a sheet of PVDF membrane. The membrane and gel were sandwiched between four sheets of pre-soaked 3MM filter paper and air bubbles were removed. Transfer was then conducted at constant currents.

#### **2.2.3.6.3.2 Immunoblotting**

Following transfer, membranes were washed with TBST (10mM Tris-HCl pH7.5, 150mM NaCl, 0.1% Tween 20) before they were blocked for 1 hour in TBST containing 5% (w/v) non-fat dried milk powder or 2% BSA. Blocking seeks to minimise non-specific binding of the antibodies to the membrane. Primary antibodies were diluted according to the manufacturer's guidelines in TBST containing 2% BSA and 0.02% sodium azide. The membranes were then incubated with the primary antibody solutions overnight at 4°C. The following morning, the membranes were washed 3 times for 10 minutes per wash in fresh TBST buffer. The membranes were then incubated for 1 hour at room temperature with the relevant HRP-linked secondary antibody, which was diluted in TBST with 5% milk powder. TBST was then used to wash the membranes 3 times, 10 minutes per wash prior to development by enhanced chemiluminescence (ECL).

#### **2.2.3.6.3.3 Developing Immunoblots**

An equal volumes of ECL solution 1 (coumaric acid, luminol, 50mM Tris-HCl) and ECL solution 2 (0.02% H<sub>2</sub>O<sub>2</sub>, 50mM Tris-HCl) were mixed and incubated with the membrane for 1 and a half minutes at room temperature. The membrane was then encased in Saran wrap and excess ECL solution was removed by blotting. The bands were then detected either by exposing the membrane to an X-ray film in a dark room for different durations, or using the Fujifilm LAS-1000 imaging system. Densitometry analysis was performed using either the Quantity

One™ image processing software (BioRad) or Image J, a public domain Java image processing program.

#### **2.2.3.6.3.4 Stripping and re-probing**

In some cases, membranes were required for re-probing with a different antibody. Antibodies were first stripped from the membrane by incubating in stripping buffer. Two stripping buffer were used, the commercially available Restore Western Blot Stripping Buffer (Thermo Scientific) and a freshly prepared Stripping buffer (62.5mM Tris-HCl, pH 6.7; 2% SDS; 100mM 2-mercaptoethanol). The membrane was incubated for 5 to 15 minutes at room temperature, and 50°C for 30 minutes respectively. Extensive washes in TBST buffer were required before blocking and then re-blotting with another primary antibody.

#### **2.2.3.7 Bacteria Cell Lysis and Purification GST-fusion Proteins**

BL21 (DE3) cells were pelleted by centrifugation at 5000 rpm for 20 minutes at 4°C, washed with ice cold PBS and lysed in 10 volumes of lysis buffer (20mM Tris-HCl pH 7.5, 150mM NaCl, 50mM NaF, 5mM EDTA pH 8.0, 1% Triton, and 1X protease inhibitor cocktail from Roche) and left on ice for 30 minutes. Lysates were subjected to mild sonication by three 45-s pulses (25% duty; 80s on/off) on ice and cleared by centrifugation at 18000 rpm for 30 minutes at 4°C. Small aliquots were collected prior to and following centrifugation and boiled with Laemmli sample buffer to assess the solubility of the recombinant protein by SDS PAGE and coomassie staining. The GST fusion proteins were then purified from the supernatant by binding to Glutathione–Sepharose 4B beads (Amersham Pharmacia Biotech) for 2 hours at 4°C. Beads are washed in ice cold lysis buffer (4 times) and finally with 50mM Tris pH 7.5 (2 times) at 4°C.

GST fusion proteins were either retained on beads in the storage buffer (20mM Tris pH 7.5, 150mM NaCl, protease inhibitor cocktail (Roche), and 50% glycerol) or eluted by competition with elution buffer (20mM glutathione in 100 mM Tris-HCl pH 8.0, 150 mM NaCl). Elution was repeated three times, 5 minutes each, at 4°C on a rotating wheel and the eluted fractions were subjected to dialysis against dialysis buffer 1 (50 mM Tris-HCl pH 7.5, 150 mM NaCl, 1mM DTT) overnight 4°C, and then against dialysis buffer 2 (buffer 1 containing 50 % glycerol) for three hours at 4°C to remove free glutathione and to concentrate the protein. Dialysis into 50 % glycerol allows long term storage at -20°C while avoiding damage to the protein caused by repetitive freeze-thaw cycles. The quality of the purified proteins was analysed by SDS-PAGE and coomassie staining.

#### 2.2.4 Bioinformatics methods

The mTOR gene (156973 nucleotides) and the cDNA (7554 nucleotides) were analysed for exon-intron structure, for alternative starting codons and potential alternative splicing isoforms. The protein domains were analysed using Pfam. The initial alignment produced by the basic local alignment searching tool (BLAST). The BLAST alignment was then manually amended to test for the presence of any cDNA for potential mTOR isoforms. The EST alignment was extended to include different exon deletion or potential start or end codons along the C-terminal and N-terminal regions of mTOR.

Extensive bioinformatics analysis allowed me to identify several potential alternative starting codons and potentially novel splicing isoforms. One was revealed by searching the protein databases. This clone (**EAW71681.1**) was reported by Celera Genomics WGS human genome sequencing project which was generated by the

whole-genome shotgun sequencing method. Another extensive bioinformatics search of EST and RNA analysis resulted in the identification of two cDNA clones coding two potential mTOR splicing isoforms ([AK302863.1](#)).

### 2.2.5 Functional analysis

Investigation of the identified mTOR isoforms *in vivo* and *in vitro*

#### 2.2.5.1 *In Vitro* Kinase Assay

*in vitro* kinase assay was performed to assess the mTOR kinase activity. HEK 293 cells were transfected with pcDNA3–Flag–mTOR $\alpha$ , pcDNA3–Flag–mTOR $\delta$ , pcDNA3–Flag–mTOR $\gamma$  or pcDNA3–Flag–mTOR S2215Y. Cells were lysed using lysis buffer (0.3% v/v CHAPS, 10 mM Tris-Base pH7.5, 150 mM NaCl, 5 mM EDTA, 50 mM NaF, 10 mM Na<sub>4</sub>P<sub>2</sub>O<sub>7</sub>, 1 mM NaVO<sub>3</sub>, EDTA-free protease inhibitor cocktail (Roche)). Protein from transiently transfected cells or stable cell line was immuno-precipitated with protein-G beads coated with anti-Flag antibody. IP was washed twice with Lysis Buffer, once with Wash Buffer (lysis buffer, 300 mM KCl) and once with Kinase Buffer (25 mM HEPES-KOH (pH7.4), 50 mM KCl, 10 mM MgCl<sub>2</sub>, 4 mM MnCl<sub>2</sub>, 5% v/v Glycerol).

The kinase assays with 4EBP1 was performed in kinase buffer containing about 1  $\mu$ g of a 4EBP1 (Calbiochem), 25 mM HEPES-KOH (pH 7.4), 50 mM KCl, 5% glycerol, 10 mM MgCl<sub>2</sub>, 4 mM MnCl<sub>2</sub>, and 100 mM ATP. Kinase reactions were resolved by SDS-PAGE and analyzed by Western blot analysis. The reaction was carried out at 37°C for 60 min and terminated by addition of SDS-PAGE sample buffer and boiling for 10 min. Proteins were resolved by SDS-PAGE either on 10% gels or on 4-12%

precast gradient NuPAGE gels (Invitrogen). The levels of immune-precipitated Flag-mTOR isoforms were measured by Western blotting with anti – Flag antibody.

### **2.2.5.2 MTT proliferation assay**

The MTT assay is a colorimetric assay for measuring the activity of live cells. In viable cells, cellular enzymes reduce the tetrazolium dye, MTT, to produce a strongly pigmented formazan product (Promega). The amount of formazan is directly proportional to cell number. The absorbance of the pigmented product was measured using a micro-plate absorbance plate reader (Tecan).

HEK 293 cells expressing mTOR $\alpha$ , mTOR $\delta$ , mTOR $\gamma$  or mTOR S2215Y were seeded into 96-well plate (5000 cells/well) and grown under standard conditions. After two days, medium was changed with serum free DMEM and time-lapse analyzed for 7 days. MTT dye (Sigma) was added to wells and incubated for 3 hours, and optical density determined at 490 nm (as per manufacturers recommendation).

### **2.2.5.3 Colony Forming Assay**

A clonogenic assay is a technique to study the effectiveness of specific agents on the survival and proliferation of cells. Any anchorage-independent growth of tumour cells is estimated by a soft-agar colony formation assay. To monitor the capacity of mTOR stable cell lines to grow in semisolid medium in vitro. Soft agar assays were performed in 6cm tissue culture plates in triplicate. For each dish, 3 ml of 0.8% agarose containing 1X DMEM and 10 % FBS was used as the bottom layer. This Mixture was maintained at 60 degree Celsius until immediately prior to pouring. After the bottom layer was poured it was allowed to solidify at room temperature. Following stabilization of the bottom agarose layer, the desired number of cells (2000 or 4000) of the cell lines included in the research model were diluted into 3

millilitre of 0.4% agarose containing 1X DMEM and 10%FBS. This model contains parental HEK 293 and HEK 293 over-expressing mTOR $\delta$ , mTOR $\gamma$ , mTOR $\alpha$  and mTOR S2215Y. This mixture was then poured on top of the solid bottom 0.8% agarose layer. Cultures were maintained for 2 weeks at 37 degrees Celsius in a tissue culture incubator in 5% CO<sub>2</sub> humidified atmosphere. Every three days cells were feed by the additions of 0.5 millilitre culture medium. This will also prevent agarose gel dehydration. All soft agar cultures were examined on one day for the number of colonies to eliminate possibility for interfering factors. Colonies were stained 3 weeks later with 0.005% crystal violet-2% ethanol in PBS and counted manually.

### 2.2.6 Statistical analysis

The data were analyzed using SPSS (SPSS Inc., Chicago, USA) software, version 18.0 for Windows. For the colony formation assay, the number of colonies was expressed as mean  $\pm$  S.E.M and the statistical test used was one-way ANOVA, followed by Bonferroni post-hoc test. Whereas for MTT data points were presented as mean  $\pm$  S.E.M and the statistical test used was two-way repeated measures ANOVA, followed by Bonferroni post-hoc test. The statistical significance was fixed at  $P < 0.05$ .

# **Chapter 3**

## **Identification of novel mTOR isoforms**

## Chapter 3: **Chapter Three: Identification of novel mTOR isoforms**

---

### **3.1 Evidence of the existence of a novel mTOR isoforms**

Like other PIKK family members, there is increasing evidence for the presence of mTOR splicing isoforms. Data from our laboratory suggest the existence of several potential splicing isoforms of mTOR. Panasyuk et al. 2009, provided evidence for the existence of the mTOR splicing isoform, mTOR $\beta$ , which lacks most of the HEAT and FAT domains. In addition, Northern blotting of human tissues indicated the presence of several potential mTOR splicing forms (Figure 3.1). Moreover, Western blot analysis of gel filtration fractions from MCF7 cells with anti-mTOR COOH-term antibody revealed the presence of several potential mTOR splicing forms (Figure 3.2).

There are numerous commercially available mTOR specific antibodies, which recognise different regions in mTOR. When the manufacturers tested these antibodies using the Western blot analysis, they recognised the full-length mTOR (280 kDa) and a number of immuno-reactive bands with lower molecular weights in total cell lysates from different cell lines and tissues. These bands may represent the product of mTOR degradation, non-specific binding or potential splicing isoforms of mTOR (Figure 3.3). The initial aim of this study was to identify novel mTOR isoforms. This was attempted using protein, molecular and bioinformatics analysis.



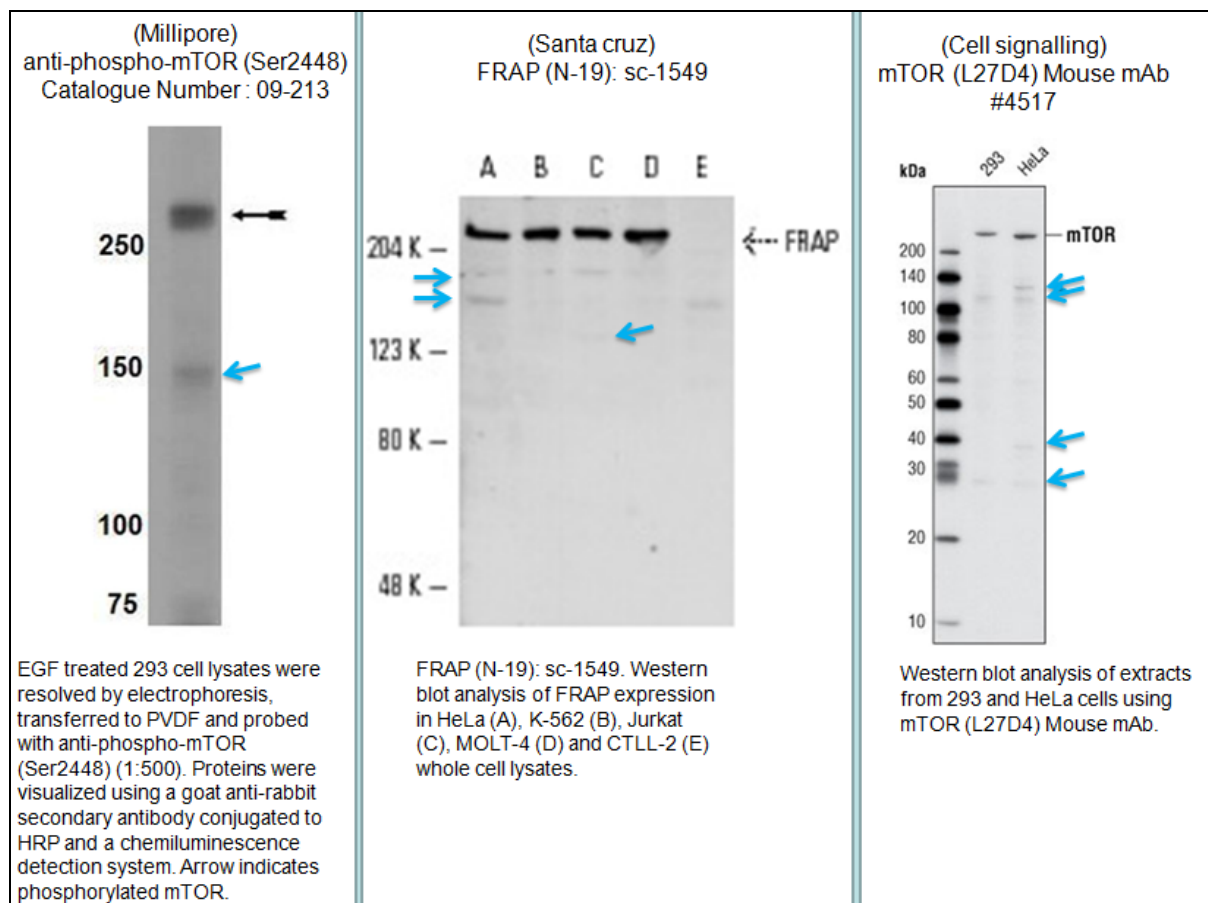


**Figure 3.3: Western blotting examples of commercially available antibodies targeting mTOR (280 kDa).**

There are immuno-reactive bands with lower molecular weight in total cell lysates from different cell lines and tissues. These bands may represent the product of mTOR degradation, non-specific binding or potential splicing isoforms of mTOR (these results were performed by manufacturers and posted in their websites as a real results for their antibodies targeting mTOR).

## 3.2 Different approaches to identify novel isoforms

Different approaches to identify novel isoforms of mTOR were used, including protein, molecular and bioinformatics analysis.

### 3.2.1 Protein analysis

Purification of the protein of interest followed by mass-spectrometry analysis is the most reliable approach to identify a novel binding/regulatory partner or isoform. Therefore, in this study, the identification process was initiated using the protein analysis approach. mTOR protein binds with high specificity to the FKBP12-Rapamycin complex, thus mTOR has been identified as a target of Rapamycin. This complex was used in this study to purify mTOR from different cell lines and tissues. An affinity matrix was generated which consisted of GST-FKBP12-Rapamycin on Glutathione Sepharose beads. The GST-FKBP12 coupled to glutathione sepharose without rapamycin was used as a negative control. It is known that the GST-FKBP12 alone does not bind mTOR, but interacts specifically with FKBP12-Rapamycin complex. The work for the protein approach was carried out using the following steps:

**Stage 1**, Purification of GST-FKBP12 from bacteria and testing the quality of the purified protein.

**Stage 2**, Preparation of the affinity matrix, by coupling GST-FKBP12 in complex with Rapamycin to Glutathione Sepharose Beads.

**Stage 3**, Testing of the affinity matrix using lysates of cells over-expressing Flag-mTOR $\alpha$  and Flag-mTOR $\beta$ . Flag-mTOR $\alpha$  and Flag-mTOR $\beta$  were

expected to bind specifically to GST-FKBP12-Rapamycin, but not to GST-FKBP12-without Rapamycin.

**Stage 4**, Analysis of the pattern of mTOR splicing forms from cell lines or rat tissues (liver and heart), which specifically associate with GST-FKBP12-Rapamycin, but not to GST-FKBP12 without Rapamycin. Followed by analyse of the binding partners by silver or Coomassie stain.

**Stage 5**, Examination of specifically associated proteins with mass-spectrometry analysis.

### **3.2.1.1 Results of the protein purification approach**

#### **3.2.1.1.1 GST-FKBP12 Purification**

GST-FKBP12 protein was used in the preparation of the affinity matrixes. These affinity matrixes were used for the isolation of mTOR splicing isoform from cell extracts of different tissues and cell lines. The recombinant GST-FKBP12 protein was expressed in bacteria and purified using the Glutathione-S Transferase (GST) gene fusion system. Aliquots were taken from each purification step for gel electrophoresis and Coomassie staining, including, before and after sonication, soluble fractions, washes and elutes after affinity purification on Glutathione-Sepharose 4B (Amersham Pharmacia Biotech). The GST-FKBP12 fusion protein was highly expressed and acceptable yields of the fusion proteins was obtained in a soluble form (Figure 3.4).

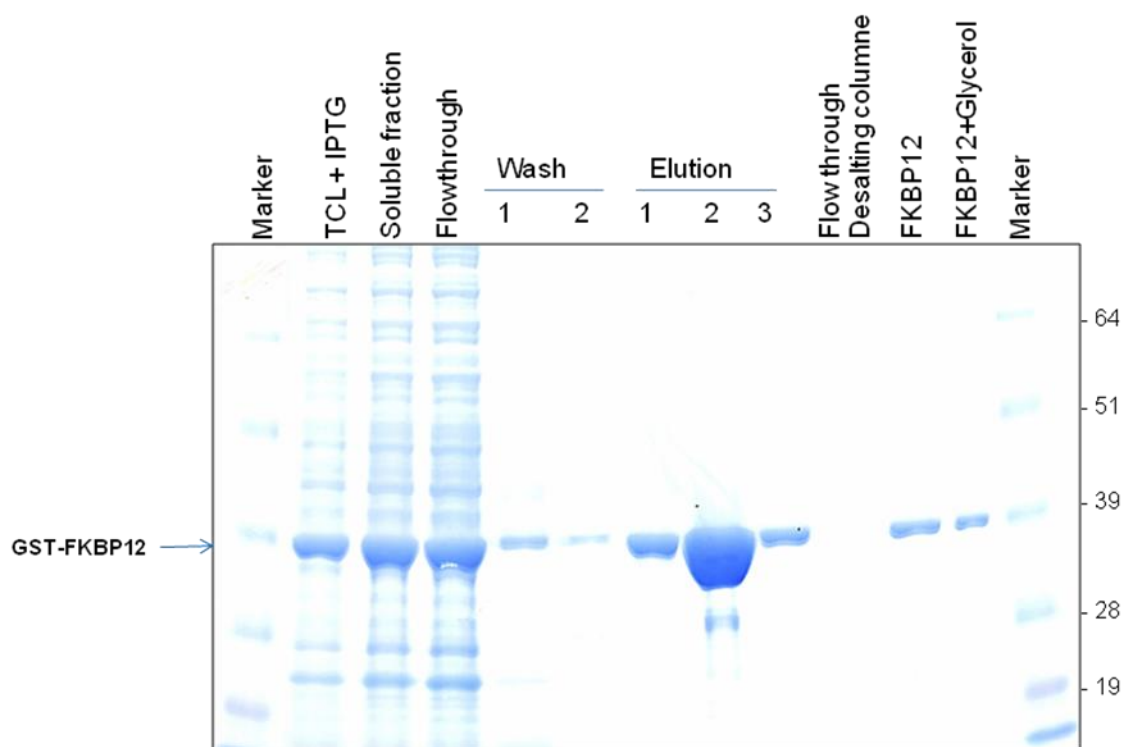


**Figure 3.4: Coomassie stain of affinity purification of GST-FKBP12.**

Coomassie stain of affinity purified GST-FKBP12, expressed in *E.coli*. Recombinant GST fusion proteins were over-expressed in Rosetta cells with IPTG induction, lysed, sonicated, centrifuged, and purified by Glutathione-Sepharose beads, and dialyzed by desalting column

### 3.2.1.1.2 Preparation of the affinity Matrix

The purified recombinant GST-FKBP12 protein was used to prepare the affinity matrix by coupling GST-FKBP12/rapamycin complex with Glutathione Sepharose Beads (Figure 3.5).

The affinity matrix was tested for its ability to bind specifically to mTOR using lysates of cells over-expressing Flag-mTOR $\alpha$  and Flag-mTOR $\beta$ . The Flag-mTOR $\alpha/\beta$  binds specifically to GST-FKBP12- Rapamycin, but not to GST-FKBP12-without Rapamycin (negative control). The Western blot analysis using antibody targeting

mTOR (anti FRAP C-terminal generated by Millipore) from cell lysates, indicating that the affinity matrix binds specifically to mTOR (Figure 3.6). The mTOR band intensity was not enough to indicate a good amount of mTOR, indicating that optimisation was needed.

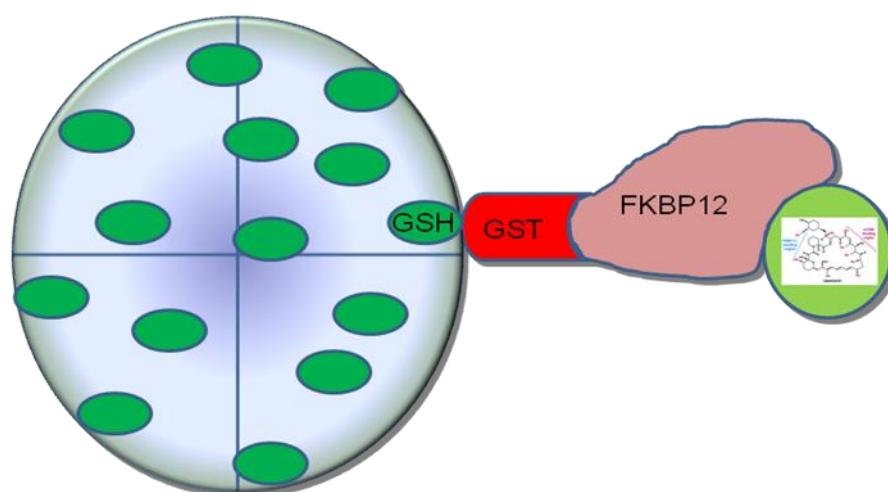


**Figure 3.5: Schematic diagram of the affinity matrix for mTOR protein to identify a new mTOR splicing isoform.**

The affinity matrix consists of Glutathione beads in complex with GST-FKBP12 and rapamycin. The FRB domain of mTOR binds specifically to FKBP12-rapamycin complex.

### 3.2.1.1.3 The affinity matrix sensitivity (optimisation)

To improve the efficiency of the affinity matrix and to minimise the interfering factor and to achieve the maximum affinity of the matrix for mTOR binding, different conditions were analysed. These factors included rapamycin concentration, buffering conditions, beads from different sources, different GST-FKBP12 concentrations and purification methods and different approaches of coupling GST-FKBP12 to Glutathione beads.

### 3.2.1.1.3.1 The effect of rapamycin concentration

Different concentrations of rapamycin resulted in a range of immune-reactivity bands with various intensity. Western blot analysis indicated that mTOR binds to the affinity matrix with rapamycin concentrations of 0.1  $\mu\text{M}$  and 1  $\mu\text{M}$  better than 10  $\mu\text{M}$  (Figure 3.6).

The presence of an additional hazy band of about 60 kDa with 1  $\mu\text{M}$  rapamycin from cells over-expressing mTOR  $\beta$  suggested that this is a potential splicing isoform of mTOR, which was able to bind to the affinity matrix in these conditions.

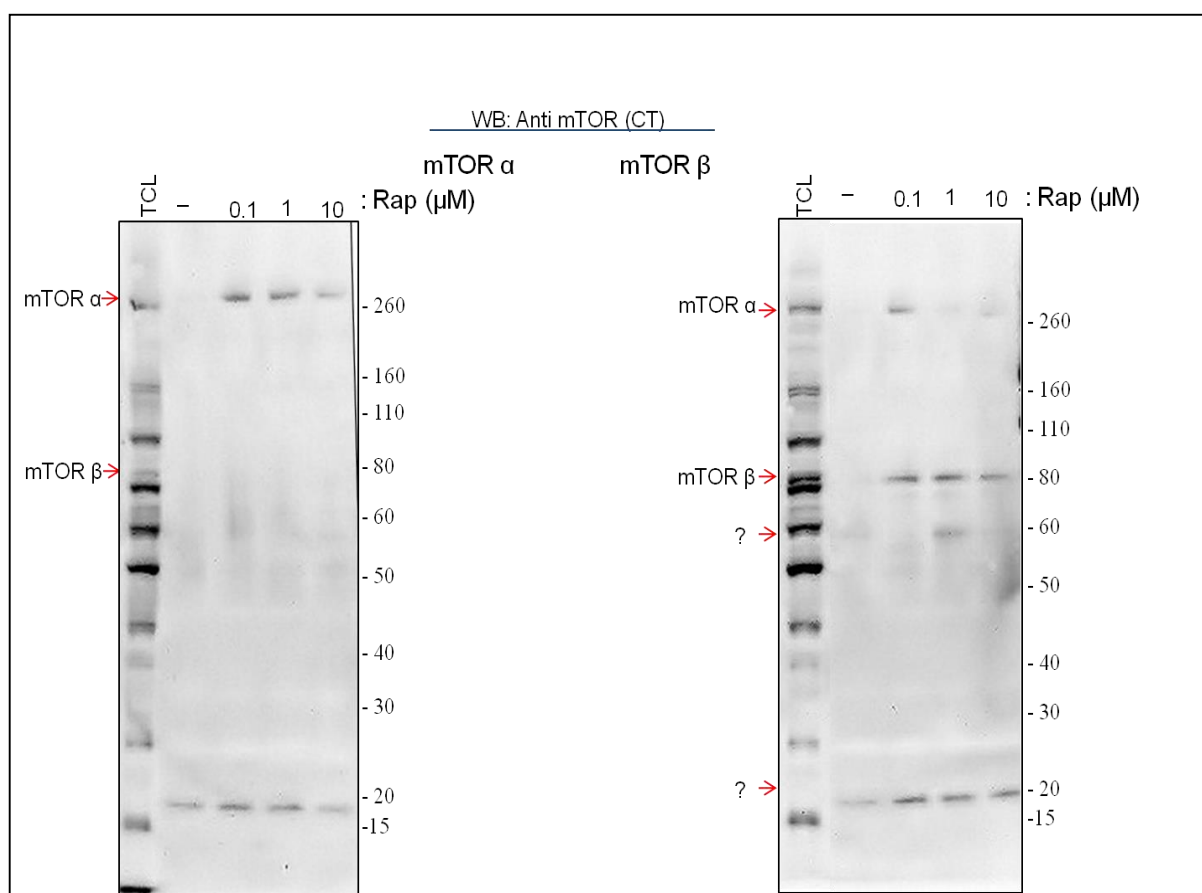


**Figure 3.6: Affinity purification of mTOR $\alpha$  and mTOR $\beta$  from HEK 293 cells over-expressing mTOR $\alpha$  and mTOR $\beta$ .**

Cells were lysed, centrifuged and purified using GST-FKBP12-Rapamycin affinity complex. The affinity matrix can bind specifically to mTOR from total cell lysate. The reaction showed better sensitivity with Rapamycin concentration of 0.1  $\mu\text{M}$ .

### 3.2.1.1.3.2 The effect of buffer

The environment surrounding the affinity matrix might affect the efficiency of the affinity purification. To test whether the buffer would affect the binding of the GST-FKBP12 to beads, a PBS buffer, pH 7.4 (no additives) was tested against the lysis buffer. There was no significant difference between the lysis buffer used and PBS buffer on binding GST-FKBP12 to Glutathione Sepharose beads (Figure 3.7).

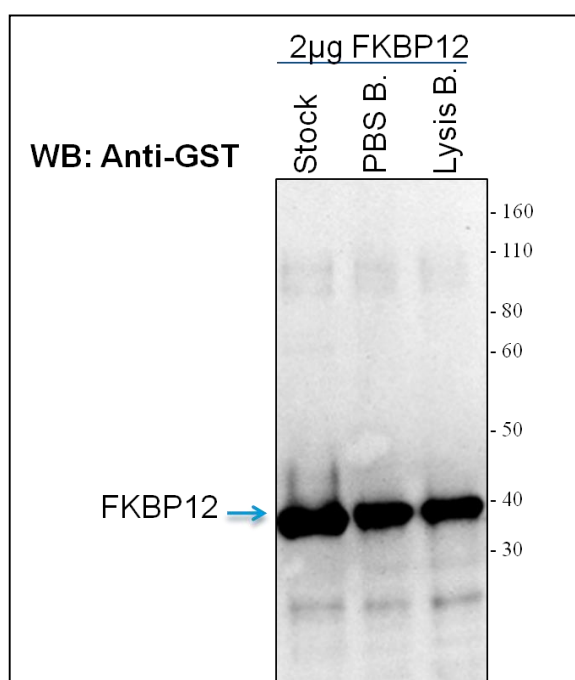


**Figure 3.7: Western blotting to study the effect of buffer on GST-FKBP12 binding efficiency to Glutathione Sepharose beads.**

There was no significant difference between the lysis buffer used in the study and PBS buffer on the binding of GST-FKBP12 to Glutathione Sepharose beads.

### 3.2.1.1.3.3 The effect of beads on protein binding

The quality and purity of Glutathione Sepharose beads, used to prepare the affinity matrix, might affect the efficiency of affinity purification. To elucidate

whether beads from different source would improve the binding efficiency, beads from different manufactures and different company, were tested. There was no significant difference between the amounts of GST-FKBP12 coupled to the new (Amersham Pharmacia Biotech) beads and those used previously (Thermo scientific) (Figure 3.8).

When the amount of beads was doubled, a higher amount of mTOR was purified. However, when the same amount of beads was used and the protein concentration was doubled there was no significant improvement on the amount of mTOR purified (Figure 3.9). These results demonstrated that the amount of beads is limiting the quantity of the protein purified and not the protein concentration or the source of beads.

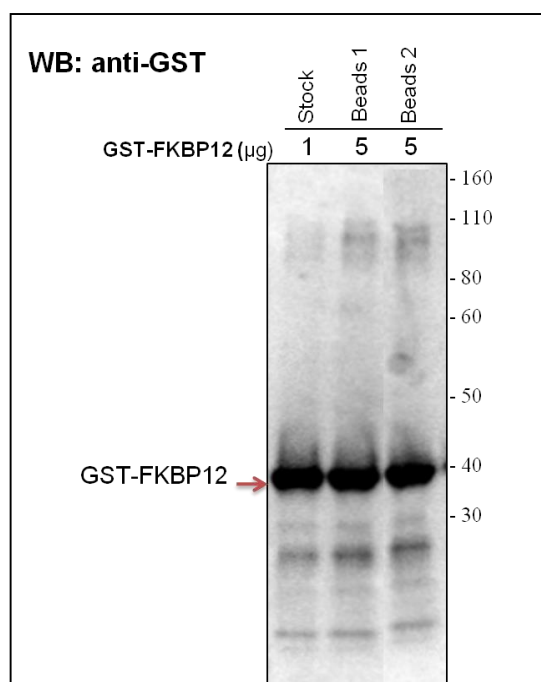


**Figure 3.8: Western blotting to study the effect of Beads on FKBP12 binding efficiency.**

GST-FKBP12 was incubated with beads from different manufacturers and there is no significant different between the amounts of GST-FKBP12 coupled to beads from different company.

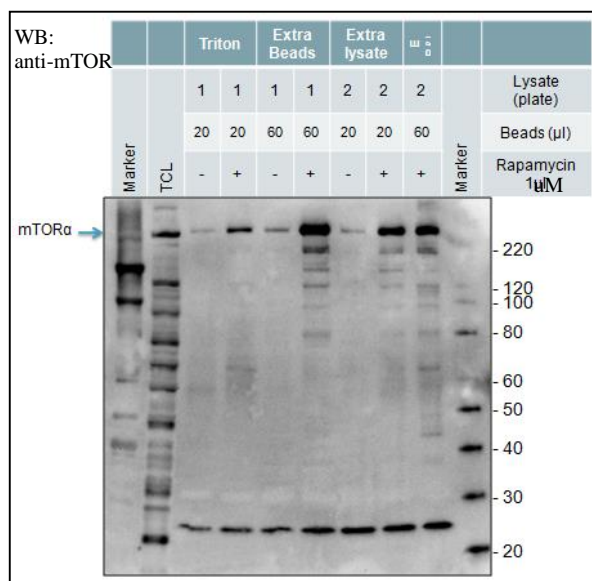


**Figure 3.9: Western blotting to study the effect of bead volume and protein concentration on the amount of mTOR purified using the affinity matrix.** There was no effect on the amount of mTOR purified when the protein concentration doubled. In contrast, a higher amount of mTOR was purified with more beads.

#### 3.2.1.1.3.4 The effect of GST-FKBP12

#### 3.2.1.1.3.5 Different purification isolates of the protein

GST-FKBP12 is part of the affinity matrix and its purity would be expected to affect the binding affinity to mTOR. During the expression and purification, the GST-FKBP12 was eluted from the beads using 30 mM glutathione. The eluted protein was dialysed two times against PBS and once against 50% glycerol in PBS to remove the excess glutathione. To prepare the affinity matrix, the GST-FKBP12 was re-coupled again to new beads. This process of elution and re-coupling might affect the efficiency of the affinity purification.

In addition, the presence of glutathione would possibly affect the binding of GST-FKBP12 to the beads.

Elution of the GST-FKBP12 from the purification beads and re-coupling to the affinity matrix could affect the sensitivity of the affinity matrix. To overcome this problem, GST-FKBP12 was again purified but the protein was left on the beads (no elution step was performed). Therefore, four independent expression and purifications conditions of the GST-FKBP12 were assessed to eliminate all factors expected to affect the affinity matrix.

The resulting mTOR indicated that the expression and purification process is very reproducible and higher concentrations of GST-FKBP12 resulted in no significant improvement in the amount of mTOR purified (Figure 3.6 the old GST-FKBP12, and Figure 3.10 the new FKBP12). The same expression methods with different purification approaches (with or without elution) were performed at different stages of the research project, thus it was not possible to directly compare the differences between purifications.

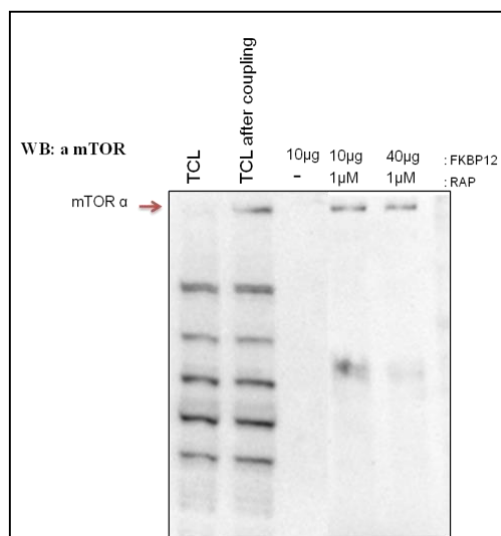


**Figure 3.10: Western blotting to study the effect of GST-FKBP12 concentration on the binding efficiency of mTOR to affinity matrix.**

There is no significant difference between the amounts of mTOR purified with different GST-FKBP12 concentrations.

### 3.2.1.1.3.6 The effect of different GST-FKBP12 concentrations

The concentration of GST – FKBP12 is believed to be crucial for the affinity of the matrix. Excess GST-FKBP12 concentration leads to the formation of free affinity matrix which will compete with the one bound to the beads for mTOR, consequently it will be washed out. Whereas using very few concentration might limit the amount of mTOR purified. Therefore, the concentration of GST-FKBP12 needs to be optimised and tested. A different concentration of GST-FKBP12 in the affinity matrix does not affect the yield of mTOR purified (Figure 3.10). These results suggest that there is another factor which limits the amount of mTOR purified.

After adjusting several factors affecting the efficiency of the affinity purification, the main goal was to examine the pattern of the immuno-reactive bands purified from different cell line and tissues by the use of the affinity matrix.

### **3.2.1.1 Patterns of mTOR immuno-reactive bands from different tissues and cell lines**

Different tissues and cell line extracts were tested using the affinity matrix. When the extracts of these cell line and tissues were immuno-blotted they generated different patterns of immuno-reactive bands against an mTOR specific antibody. Affinity purification of mTOR from rat hearts, starved and starved stimulated HEK 293 cells show different immuno-reactive bands representing potential mTOR splicing isoforms (Figure 3.11 and Figure 3.12).

The isolation process of a new isoform for mTOR consisted of five different stages. At this point of the protein analysis approach, stages one to four were successfully achieved; the first stage was purification of GST-FKBP12 from bacteria and testing the quality of purified protein; the second was preparing the affinity matrix; then the third was testing the affinity matrix and the fourth, examining the pattern of immuno-reactive mTOR splicing isoforms from cell lines and rats tissue.

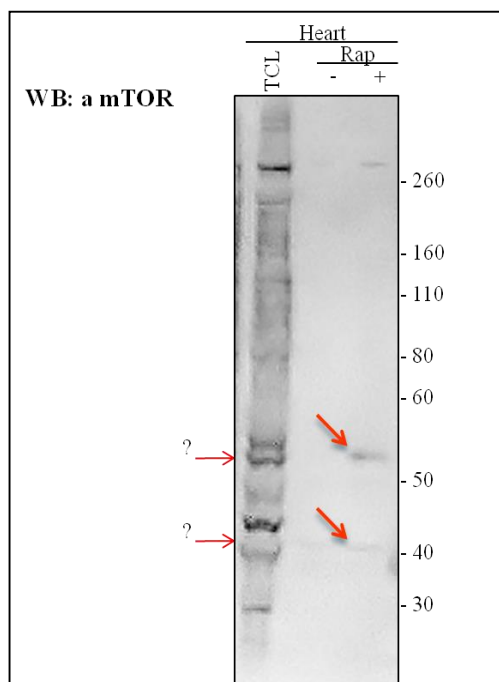


**Figure 3.11: Western blotting of affinity purified mTOR from Rats' Heart.** The arrow highlighted immune-reactive bands with anti mTOR C-terminal (Millipore), representing potential splicing isoform.

Ideally, the next stage would have been to examine specifically associated potential mTOR proteins with mass-spectrometry analysis. Initially, two potential mTOR isoforms have been purified and analysed by silver stain. However, it was not possible to purify sufficient amounts of these potential mTOR proteins for mass-spectrometric analysis. mTOR $\alpha$  was hardly visible by silver staining and increasing the stain intensity leads to a high background signals. Any potential alternative splicing isoforms were expected to be even less abundant and more difficult to observe.

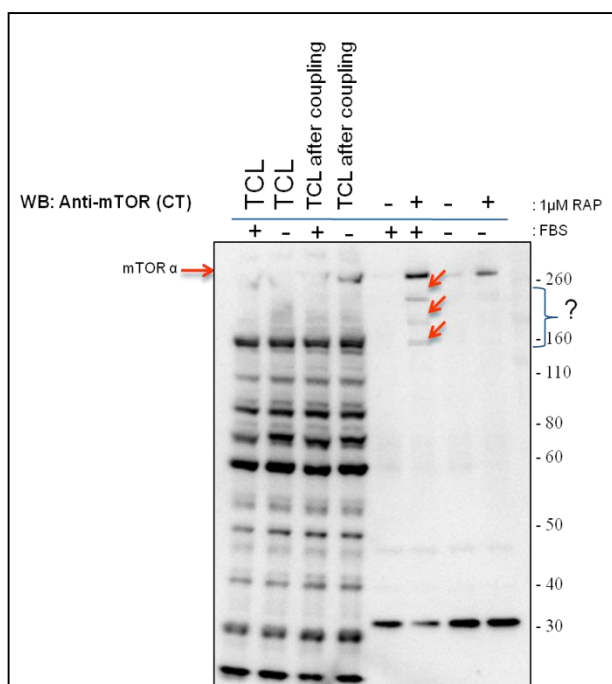


**Figure 3.12: Western blotting of affinity purified mTOR from Starved and starved stimulated HEK 293.**

The arrow highlighted immuno-reactive bands with anti mTOR C-terminal (Millipore), representing potential splicing isoform.

Recently, a three-dimensional (3D) structure of human mTORC1 was determined by cryo-electron microscopy (Yip et al.2010). Yip et al revealed that extended incubation of mTORC1 with rapamycin may induce disassembly of mTORC1, and may lead to conformational changes. This could potentially explain why the binding efficiency of mTOR to the affinity matrix was weak and did not purify sufficient amount of mTOR protein for mass-spectrometry analysis. Subsequently, adjustments in the purification protocol have been made by minimising the incubation time of mTOR with the affinity matrix, which contains rapamycin to 15 minutes rather than 1 hour as in all previous results demonstrated in this study. This modification resulted in two clear immuno-reactive bands with intensity similar to or

higher than mTOR $\alpha$ . These intense bands represent potential mTOR isoforms. These bands migrated on SDS-PAGE to a relative molecular weights of approximately 130 kDa and 135 kDa (Figure 3.13).

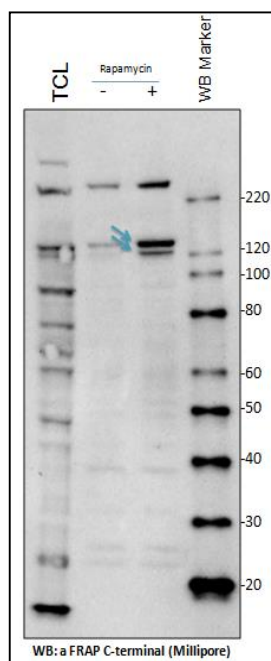


**Figure 3.13: Western blotting of affinity purified mTOR from HEK 293 using the modified procedure, after the 3D structure has been revealed (15 min incubation with rapamycin).**

The arrows highlight immuno-reactive bands with anti mTOR C-terminal (Millipore), representing potential splicing isoform.

To further examine the potential mTOR isoforms, the 130 and 135 kDa bands, the cell lysate were blotted with antibodies targeting different mTOR domains. Figure 3.14 summarises numerous mTOR-specific antibodies that are commercially available. Five antibodies which recognise different mTOR domains were selected.

These are listed below:

1. **anti FRAP C-terminal (Millipore)**

Peptide (C-DTNAKGNKRSRTRTDSYS) corresponding to amino acids  
2433-2450 of mTOR

2. **anti mTOR C-19 (Santa Cruz)**

Epitope mapping at the C-terminus of mTOR, blocking peptide the last 19  
amino acids at the C-terminal

3. **anti mTOR Phospho-specific C-terminal (Millipore) around 2448**

Recognizes mTOR when phosphorylated on Ser2448

4. **anti FRAP (N-19): (Santa Cruz)**

Epitope mapping at the N-terminus of FRAP of human origin. Blocking  
peptide, sc-1549 P

5. **anti mTOR F11: (Gnna Panasyuk)**

Epitope mapping corresponding at 1332-1504 amino acids of human origin

The presence of the 130 and 135 kDa bands was confirmed by Western blotting analysis. The two potential isoforms were present in the Western blot with three antibodies, anti- mTOR targeting the kinase domain (anti FRAP COOH-terminal generated by Millipore), FATC domains (anti mTOR C-19 Santa Cruz) and the NH<sub>2</sub>-terminus of the HEAT repeats domain (anti-mTOR N-19 target the first 19 amino acid at the NH<sub>2</sub>-terminus of the mTOR).

Since the two bands were reactive with antibodies targeting the FATC, kinase and HEAT repeats domains, we can hypothesise that kinase, FATC and the NH<sub>2</sub>-terminal of the HEAT repeats domains are present in both the 130 and 135 kDa proteins. In addition, the 130 and 135 kDa bands were purified using the affinity

matrix, and while FRB domain bind to the affinity complex, this indicate the presence of FRB in both bands.

Only one band was immune-reactive with each of anti-mTOR F11, and the phosphor-specific antibody. Anti-mTOR F11 target the C-terminus of the HEAT repeats domain and small part of the neighbouring FAT domain, which is missing in mTOR $\beta$ . The band which is non-reactive with anti-mTOR F11 is similar to mTOR $\beta$  isoform which lacks most of the HEAT and FAT domains. Furthermore, one of these potential isoforms can be phosphorylated (Figure 3.15).

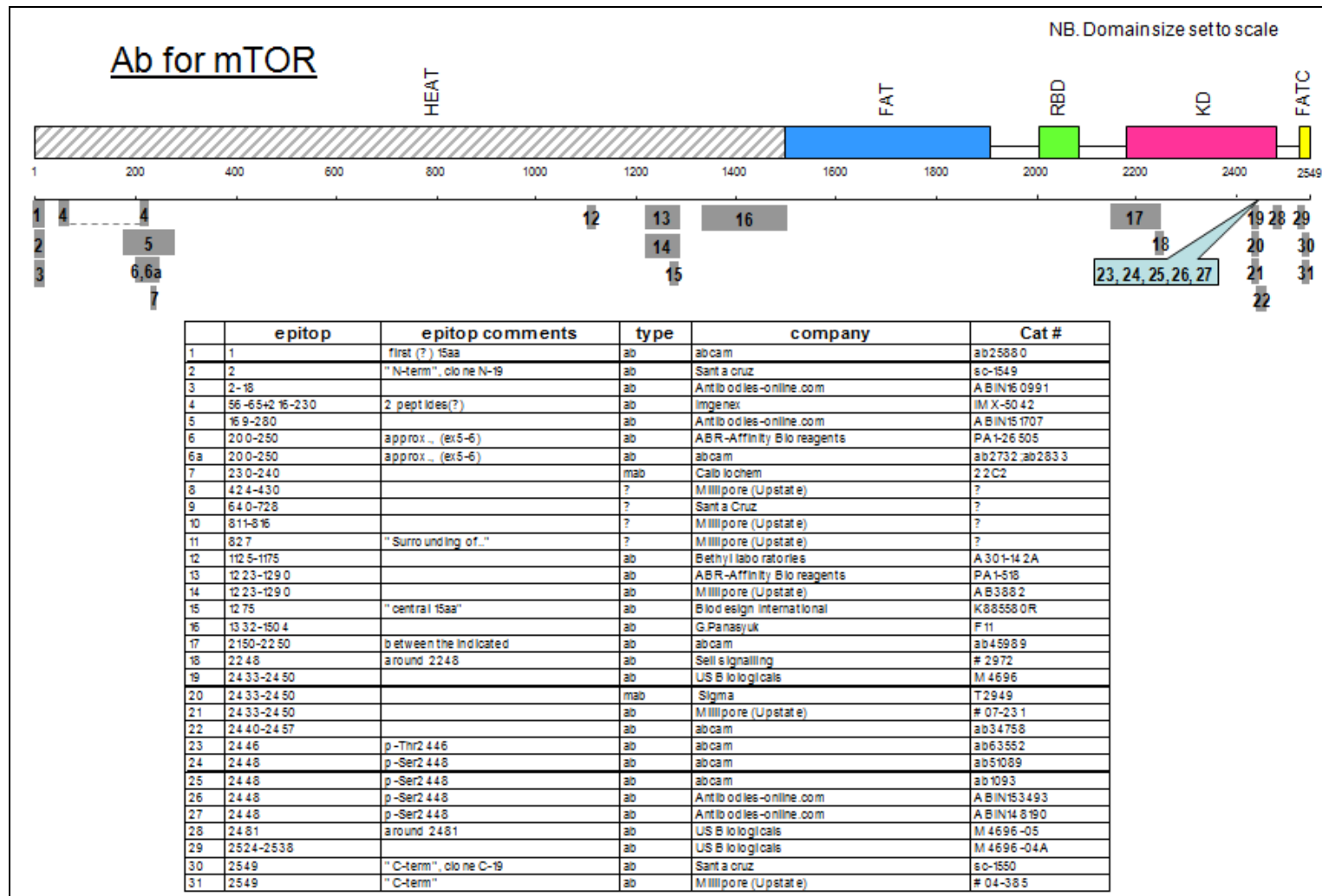


**Figure 3.14: Commercially available antibodies against different mTOR epitope.**

### 3.2.1.2 Summary of protein analysis approach

Although we have successfully identified potential splicing isoforms of mTOR, the quantity of endogenous proteins purified using the GST-FKBP12-Rapamycin affinity matrix was not sufficient for MS-MS analysis. Many optimisation steps to increase the sensitivity and specificity were applied, however, with limited success.

The majority of mTOR protein from total cell lysates did not bind to the GST-FKBP12-Rapamycin affinity matrix for unknown reason. It could be due to the low *in vitro* affinity of FKBP12-Rapamycin for endogenous mTOR complexes 1 and 2. This affinity was not good enough to pull-down a significant amount of the mTOR from the total cell lysate. This phenomenon is not uncommon since other groups used a much larger amount of total tissue or cell lysates to isolate mTOR $\alpha$ , about 100 times more than the number of cells we have used. Using this amount of cell lysate requires extended incubation and since the extended incubations of cells with Rapamycin leads to disassembly of mTORC1 (Yip et al. 2010b), it was impossible to use that amount in our protocol which requires a short exposure of mTOR to rapamycin. The success resulted from using less exposure time resulted in two intense new immune-reactive bands. However, no significant enrichment in the affinity purification of endogenous mTOR (enough for mass-spectrometry analysis) on the GST-FKBP12-Rapamycin matrix was observed. Since rapamycin is known to affect the integrity of mTORC1, therefore using rapamycin in this approach may lead to dissociation of mTOR from the affinity matrix.

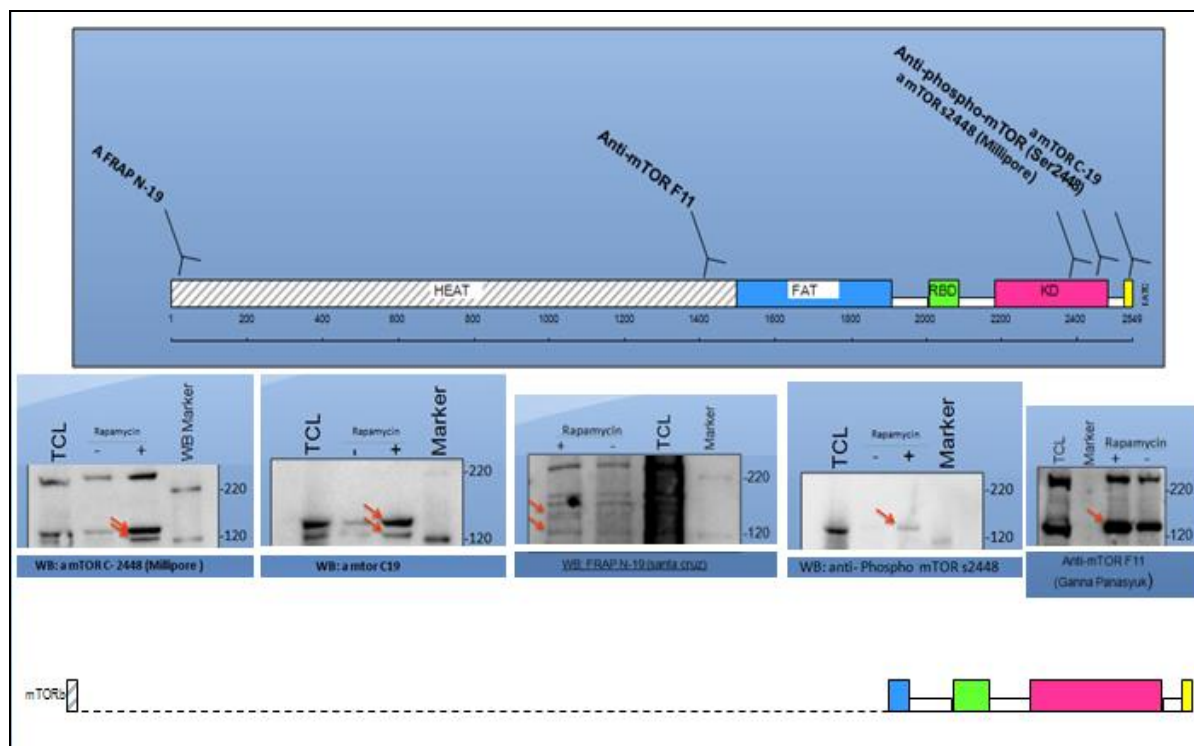


**Figure 3.15: Western blotting of affinity purified mTOR against different antibodies.** The two bands were immuno-reactive with three antibodies, anti mTOR targeting the kinase domain, FATC domains and the NH<sub>2</sub>-terminous of the HEAT repeats domain. Only one band was immune-reactive with each of anti-mTOR F11, and the phosphor-specific antibody.

### 3.2.2 Bioinformatics and molecular approaches

The exon-intron structure of the mTOR gene (156,973 nucleotides) were analysed for alternative starting codons and potential alternative splicing isoforms. The full length mTOR mRNA (cDNA of 7,554 nucleotides) does not start with or contain a Kozak sequence; consequently it is very difficult to predict the alternative translation initiation start codon.

Extensive bioinformatics analysis allowed us to identify several potential alternative start codons and potential novel splicing isoforms. One of these was revealed by searching the protein databases. This clone, [EAW71681.1](#), was reported by Celera

Genomics (WGS) human genome sequencing project, which was generated by the whole-genome shotgun sequencing method. This clone lacks exon 25 (amino acid 1219-1267). This exon is located in between HEAT repeats and FATC domains. The HEAT repeats act as a binding site for substrate presenting proteins, while the FATC is involved in the activation of the mTOR kinase activity. It is interesting to study the effect of this deletion on the kinase activity of mTOR and the ability of mTOR to form complexes with substrate presenting proteins.

Another extensive bioinformatics search of EST and RNA analysis resulted in the identification of two cDNA clones coding two potential mTOR splicing isoforms designated mTOR $\gamma$  and mTOR $\delta$  ([AK302863.1](#)). The mTOR $\delta$  results from a frame shift in the middle of the FATN domain and leads to a premature translation stop codon, while mTOR $\gamma$  possesses a 12 amino acid deletion which is located in the kinase domain (Figure 3.16).

The COOH-terminal of mTOR $\delta$  results from a frame shift in the middle of FAT domains and leads to a premature translation stop codon. This frame shift resulted in a new amino acid sequence. To further investigate the existence of mTOR $\delta$ , an antibody targeting the COOH-terminal of the mTOR $\delta$  was generated by collaborators. Further details about anti-mTOR $\delta$  presented in chapter four. The expression of mTOR $\delta$  was confirmed by Western blotting in different cell lines, including HEK 293, Hep-2G, MC7 and Hela (Figure 3.17).

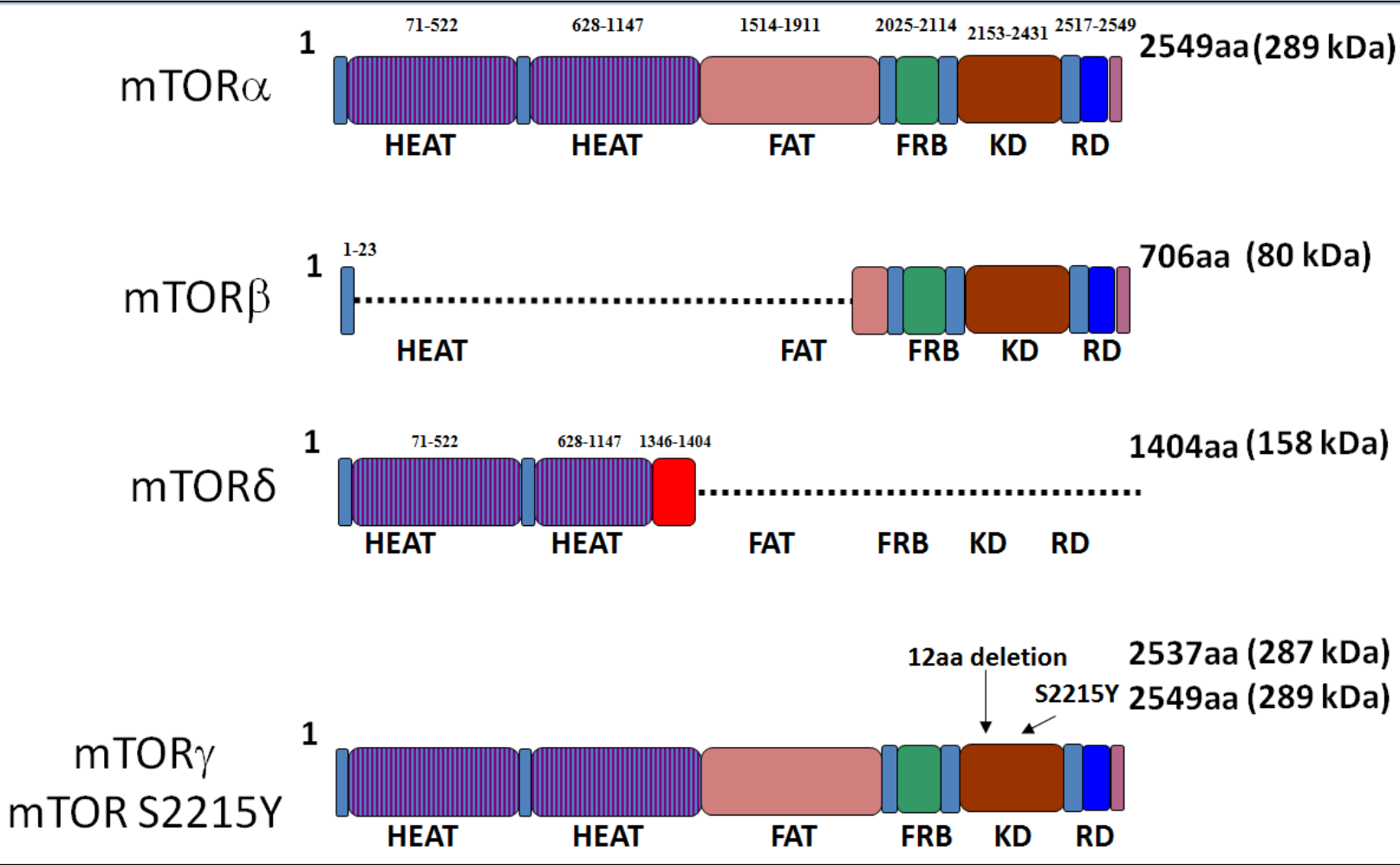
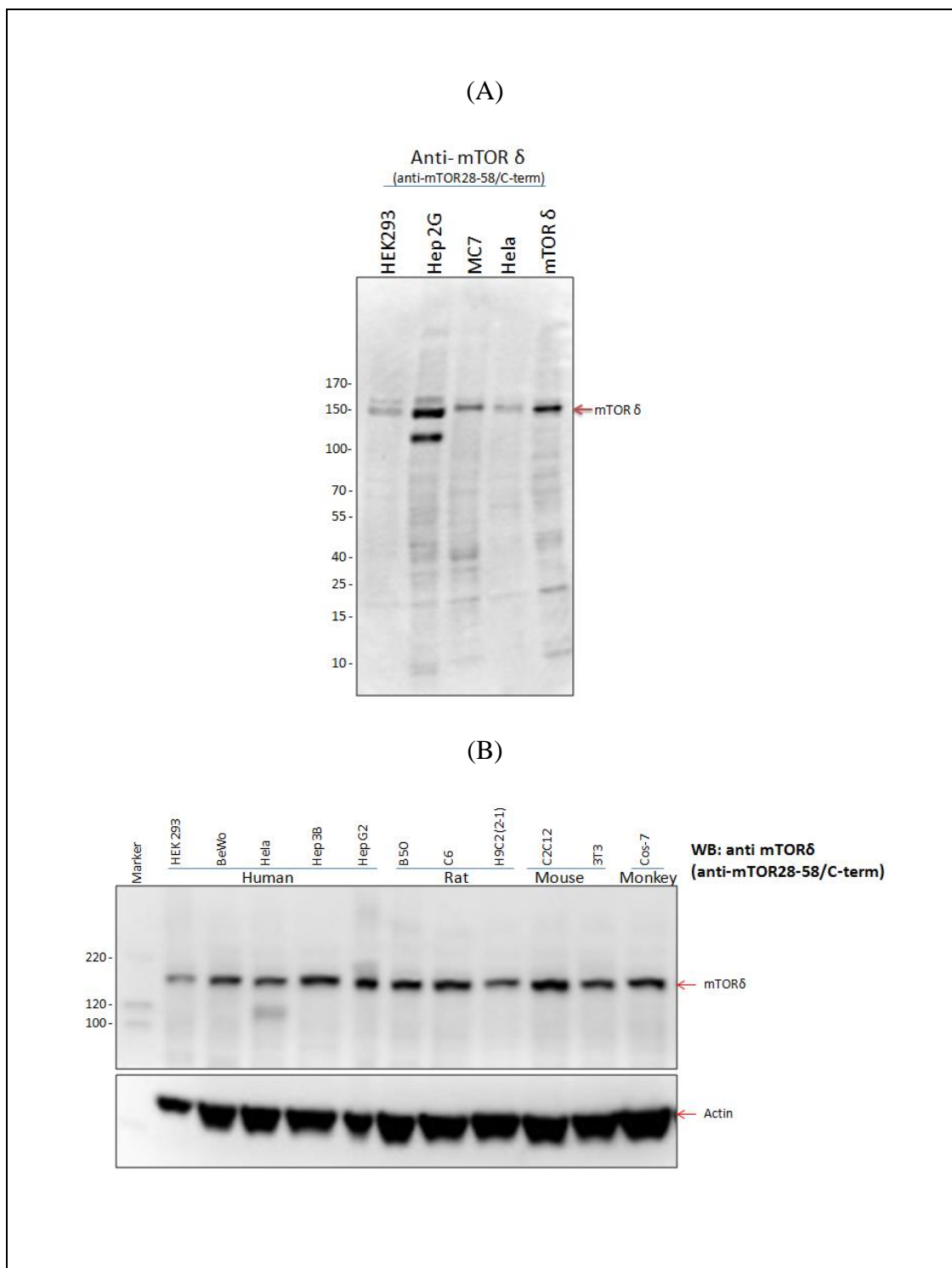


Figure 3.16: Schematic domain organization of mTOR splicing forms



**Figure 3.17: Western blotting analysis testing the expression of mTOR $\delta$  in different cell lines.**

(A) and (B) show clear immuno-reactive bands from different cell lines when blotted with an antibody targeting mTOR $\delta$ .

# **CHAPTER 4**

## **Molecular characterisation and functional analysis of mTOR $\delta$**

## Chapter 4: Molecular characterisation and functional analysis of mTOR $\delta$

---

### 4.1 Molecular characteristics of the mTOR $\delta$ isoform

#### 4.1.1 Introduction

As mentioned in Chapter three extensive bioinformatics analyses revealed a novel mTOR splicing isoform denoted mTOR $\delta$ . The identified alternatively spliced form, mTOR $\delta$ , was found in the cell lysates of different cell lines via western blotting analysis. In contrast to the full-length wild-type mTOR $\alpha$ , mTOR $\delta$  lacks the kinase domain. Thus, it would be interesting to study the effect of this isoform on the mTOR mediated cellular functions. In this study, we generated mammalian expression constructs for the mTOR $\delta$  and control proteins. Stable cell lines were created to study the relative importance of this isoform and its possible role in the regulation of mTOR activity.

In addition, mTOR $\delta$  is a novel spliced isoform of mTOR resulting from a frame-shift in the middle of the FAT domain leading to a premature stop codon. As a result of the frame shift, a novel amino acid sequence is generated at the COOH-terminus of this particular isoform. The predicted molecular weight of this spliced isoform is approximately 158 kDa. The isoform lacks the FRB, regulatory and kinase domains. Thus, it is thought that the mTOR $\delta$  protein acts as a dominant negative regulator of

mTOR signalling by sequestering substrate-presenting proteins such as raptor and rictor.

The main focus in studying the mTOR $\delta$  isoform was to investigate its effect on the regulation of the mTOR pathway and on the mTOR-mediated cellular processes, including cell proliferation, cell cycle regulation and tumourigenesis.

cDNA clones were constructed and sub-cloned into the pcDNA3 mammalian expression vector. The pcDNA3 plasmid is designed to provide high-level expression of recombinant proteins in a wide range of mammalian cells. In the pcDNA3 vector, the cDNA sequence is inserted at the COOH-terminus of the human cytomegalovirus (CMV) promoter. This permits high-level constitutive expression in mammalian hosts ([Invitrogen guide](#)). The bovine growth hormone (BGH) polyadenylation signal is located immediately after the multiple cloning site (MCS) at the COOH-terminus of the inserted cDNA. This BGH polyadenylation signal enhances the transcription termination and poly-adenylation of mRNA.

A laboratory in Japan reported that a point mutation in the kinase domain of mTOR $\alpha$  resulted in nutrient-independent activation of mTORC1 (Sato et al. 2010). This point mutant was denoted S2215Y. The wild-type form of mTOR (mTOR $\alpha$ ) and the activated mutant (mTOR S2215Y) were used as controls to assess the activity of mTOR $\delta$  (Figure 4.1). The full-length mTOR $\alpha$  cDNA consists of 7,647 nucleotides, whereas that of the mTOR $\delta$  isoform consists of 4,212 nucleotides.

An mTOR $\beta$  isoform mutant was generated in our laboratory by Christopher Fu (Figure 4.2). The S2215Y point mutation was introduced into the DNA sequence of mTOR $\beta$  using a set of primers for site-directed mutagenesis and was denoted

mTOR $\beta$  S2215Y. The mTOR $\beta$  plasmids were amplified and purified using the QIAGEN Miniprep Plasmid Purification kit. DNA sequence analysis was then performed to ensure that the correct mutation had been introduced into the cDNA sequence.

All of the mTOR isoform plasmids used in this study were cloned from the previously created mTOR $\beta$  S2215Y mutant in addition to mTOR $\alpha$  from Addgene and mTOR $\delta$  from the National Institute of Technology and Evaluation (NITE).

The mTOR $\alpha$ , mTOR $\delta$  and mTOR S2215Y cDNA sequences were cloned as Flag-tagged fusion proteins in the pcDNA3 mammalian expression vector. As a result, the generated recombinant fusion proteins can be purified and detected using a Flag expression system. The Flag expression system is useful for western blotting, immuno-histochemistry, immuno-precipitation, flow-cytometry and protein purification and for studying protein-protein interactions and protein localisation. This small hydrophilic (8-amino acid peptide) tag significantly improves the detection and purification of recombinant fusion proteins when used together with highly specific and sensitive anti-Flag antibodies. The 8-amino acid peptide (Asp-Tyr-Lys-Asp-Asp-Asp-Asp-Lys) is fused to the recombinant mTOR proteins when they are expressed. This Flag peptide sequence is likely to be positioned on the surface of the expressed protein due to its hydrophilic nature. As a result, it is likely to be detected by the anti-Flag antibody. In addition, due to the small size of the Flag tag, it is unlikely to obscure other epitopes, domains or alter the function or characteristics of the fusion protein. Another DNA sequence analysis was therefore performed to verify that the correct Flag-tagged DNA sequences had been introduced into the pcDNA3 expression vector.

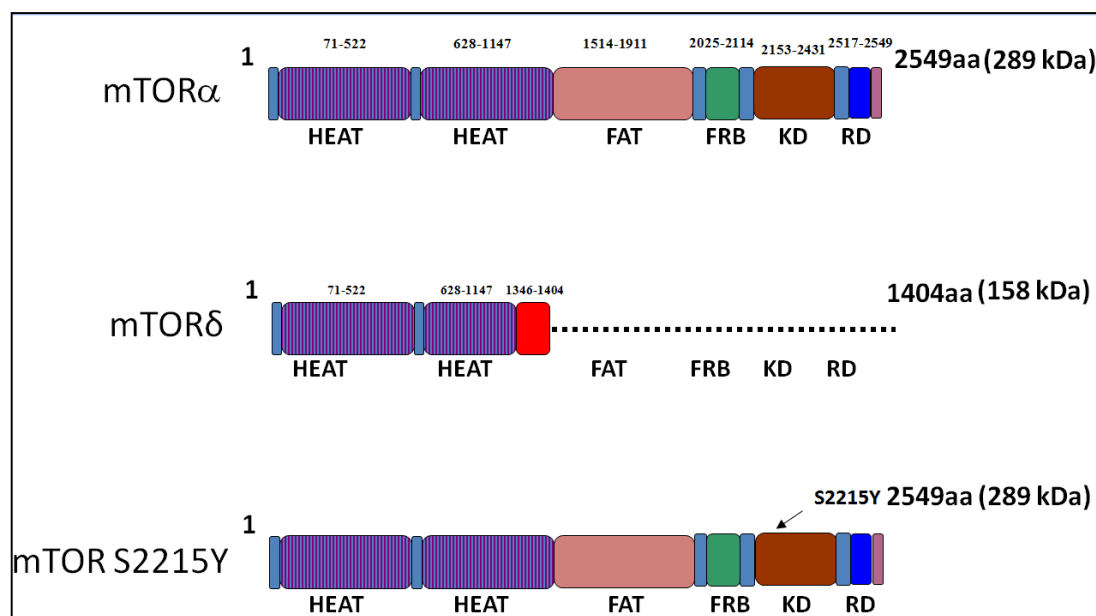


**Figure 4.1: Schematic representation of the domain organisation of the mTOR $\delta$  splice isoform.**

mTOR $\alpha$  is the full-length form of mTOR. mTOR $\delta$  is a novel mTOR splicing isoform resulting from a frame-shift in the middle of the FAT domain that leads to a stop codon, resulting in premature termination. The S2215Y point mutation in the mTOR kinase domain was identified by searching the COSMIC database of somatic mutations. This mutation has been shown to confer constitutive mTOR activation, even under conditions of nutrient deprivation.

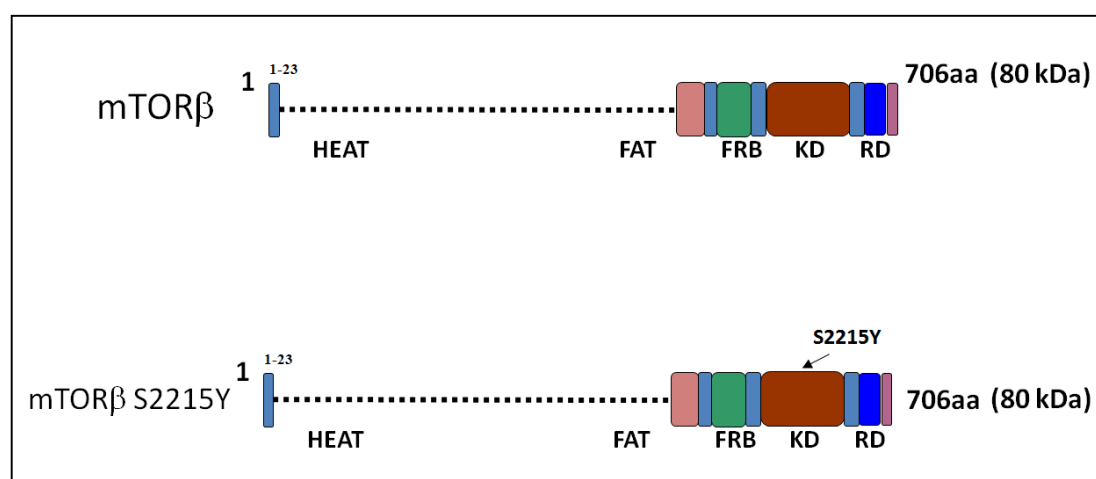


**Figure 4.2: Schematic representation of the domain organisation of the mTOR $\beta$  mutant.**

mTOR $\beta$  is a novel mTOR splicing isoform that lacks HEAT repeats and the majority of its FATN domains. In this study, the mTOR $\beta$  point mutant was denoted mTOR $\beta$  S2215Y. mTOR $\alpha$  exhibits the same COOH-terminal sequence as mTOR $\beta$  and the position of the S2215Y mutation will therefore be at the same place in mTOR $\alpha$ .

#### 4.1.2 Generation of Flag-tagged mTOR $\alpha$ and mTOR S2215Y plasmids

As mentioned previously, mTOR $\alpha$  and mTOR $\beta$  share the same COOH-terminus, which includes the kinase domain where the S2215Y mutation is located. In addition, mTOR $\beta$  lacks most of its HEAT repeats and FAT domains, which are located at the NH<sub>2</sub>-terminus of mTOR. Therefore, to generate mTOR $\alpha$  and mTOR S2215Y, the NH<sub>2</sub>-termini of the wild-type mTOR $\beta$  and the mTOR $\beta$  mutant which harbouring the S2215Y mutation were replaced with the full-length NH<sub>2</sub>-terminus of the wild-type mTOR $\alpha$ . The Flag tag sequence was introduced into the DNA at the NH<sub>2</sub>-terminus of the full-length mTOR $\alpha$ . This process resulted in the generation of pcDNA3-Flag-mTOR $\alpha$  and pcDNA3-Flag-mTOR S2215Y (Figure 4.3).

The pcDNA3-mTOR $\beta$  and pcDNA3-mTOR $\beta$  S2215Y plasmids were linearised with the HindIII restriction enzyme. The ends of the linearised plasmids were then blunted using T4 DNA ligase. The linearised and blunted plasmids were re-digested with the KpnI restriction enzyme. This resulted in a small fragment containing the NH<sub>2</sub>-terminal region of mTOR $\beta$ . This NH<sub>2</sub>-terminal fragment was then replaced with the full-length NH<sub>2</sub>-terminus of Flag-mTOR $\alpha$  from pcDNA-Flag-mTOR $\alpha$  (Figure 4.4). To prepare the full-length NH<sub>2</sub>-terminal fragment, pcDNA-Flag-mTOR $\alpha$  was linearised with the NotI restriction enzyme and blunted with T4 DNA ligase. The plasmid was then re-digested with the KpnI restriction enzyme. The resultant NH<sub>2</sub>-terminus of full-length Flag-mTOR was blunted from its NH<sub>2</sub>-terminal side, and the COOH-terminus consisted of KpnI restriction sequence. The pcDNA3 containing the COOH-terminus of mTOR and codes for either full-length or the S2215Y point

mutation was blunted from its COOH-terminal and exhibit KpnI restriction sequence from its NH2-terminal. These two fragments, the pcDNA3 containing the COOH-terminus of mTOR isoforms and the full-length NH2-terminus of mTOR, were then ligated together using T4 DNA ligase.

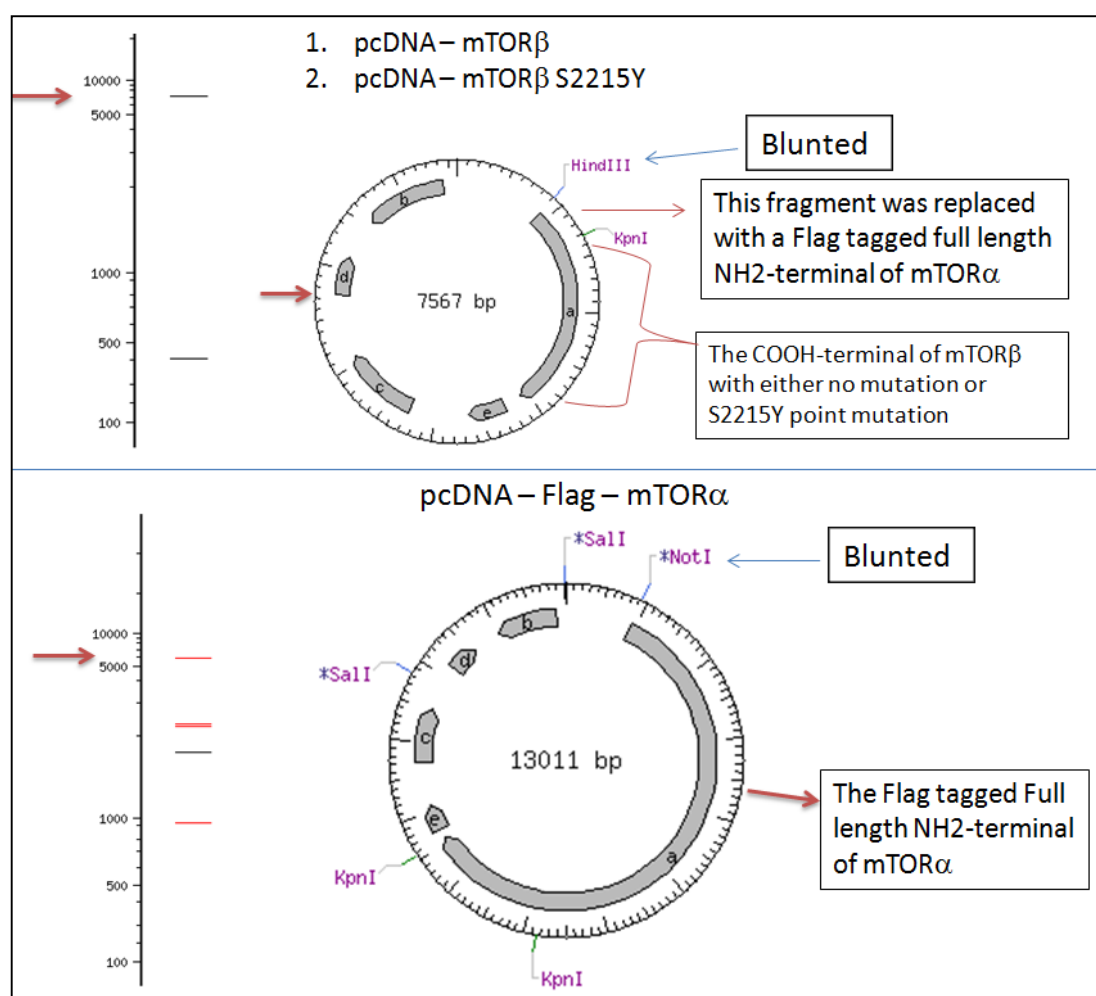


**Figure 4.3: Plan for the generation of the pcDNA3-Flag-mTOR $\alpha$  and pcDNA3-Flag-mTOR S2215Y isoforms.**

The pcDNA-mTOR $\beta$  isoforms (top) were linearised using the HindIII restriction enzyme, blunted using T4 DNA ligase and digested again with KpnI. This process resulted in two fragments: a large fragment containing the pcDNA3 plasmid and the COOH-terminal of mTOR and a small NH2-terminal fragment. pcDNA-Flag-mTOR $\alpha$  (bottom) was linearised using the NotI restriction enzyme, blunted using T4 DNA ligase and digested again with KpnI and SalI. This process resulted in a full-length NH2-terminal of mTOR $\alpha$  with a blunt end at its NH2-terminus and a KpnI

sequence at its COOH-terminal. This fragment was then ligated to the pcDNA3 containing the COOH-terminus of mTOR.

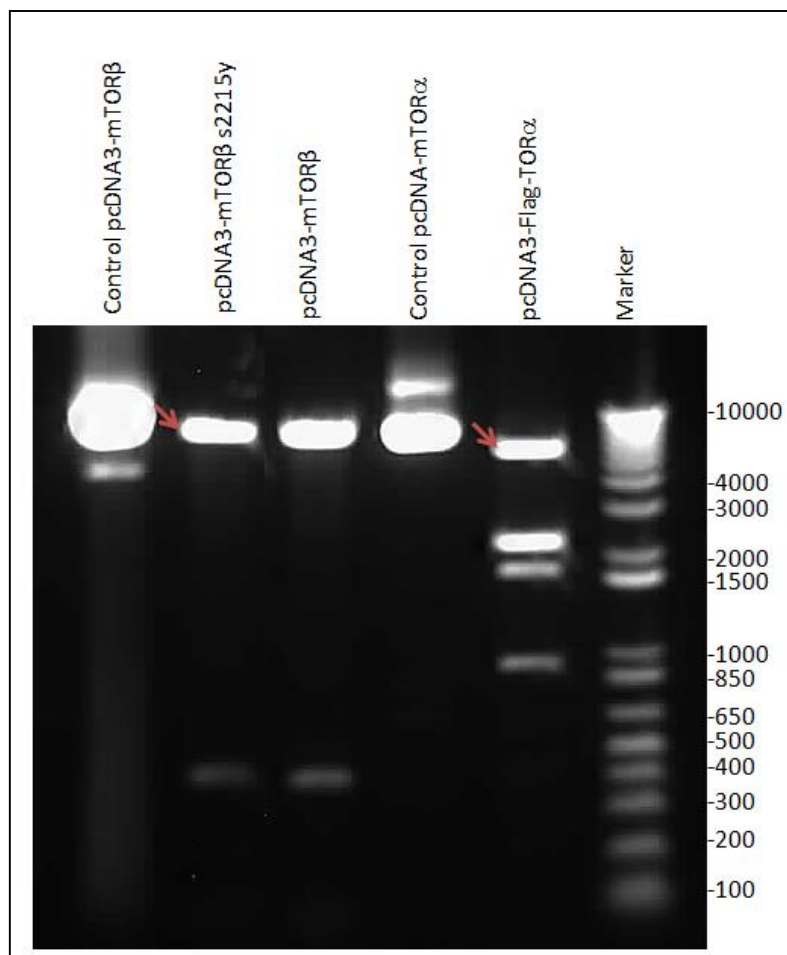


**Figure 4.4: Agarose gel image of the DNA fragments used for the construction of pcDNA3-Flag-mTOR $\alpha$  and pcDNA3-Flag-mTOR S2215Y.**

The pcDNA3-mTOR $\beta$  and pcDNA3-mTOR $\beta$  S2215Y plasmids were digested with HindIII and KpnI. In addition, the pcDNA3-Flag-mTOR $\alpha$  plasmids was digested with Sall, KpnI and NotI. These plasmids were electrophoresed in a 0.8% agarose gel. The NH<sub>2</sub>-terminus of the wild-type mTOR $\beta$  and mutated mTOR $\beta$  plasmids were digested and replaced with the Flag-tagged full-length NH<sub>2</sub>-terminus of mTOR $\alpha$ .

The mutant DNA molecules were transformed into bacteria, and 8 colonies from each mutant were amplified and analysed on an agarose gels to confirm the size and the quality of the purified plasmids (Figure 4.5). Digestion analysis of the DNA was then performed to verify that the DNA was inserted into the plasmid. The restriction analysis was carried out using the *Hin*II restriction enzyme, followed by analysis on 0.8% agarose gel. The digestion of plasmids with inserts results in a band of approximately 1,280 bp. This band was absent in all of the selected colonies in the lanes indicated with blue number in Figure 4.5. However, all of the colonies in the lanes indicated with red numbers were positive for the fragment representing the insert from the digested plasmid (Figure 4.6 and Figure 4.7). Therefore, these colonies contained the cDNA insert within the plasmid. DNA sequence analysis was then performed to verify that the mutations were present.

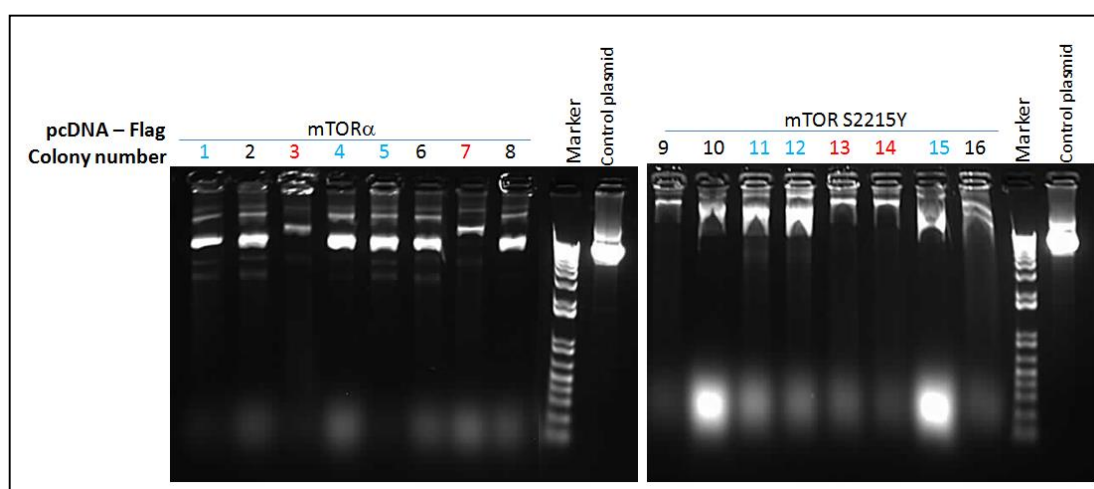


**Figure 4.5: Agarose gel image of colonies selected for digestion and sequencing analysis.** The constructed plasmids were transformed into bacteria and plated in selection media. Eight colonies from each mutant were selected for plasmid purification and tested on agarose gels to check the size and quality of the purified plasmids. The plasmids were then thoroughly tested through digestion and sequencing analysis. The results of the digestion analysis can be seen in Figure 4.6 and Figure 4.7.

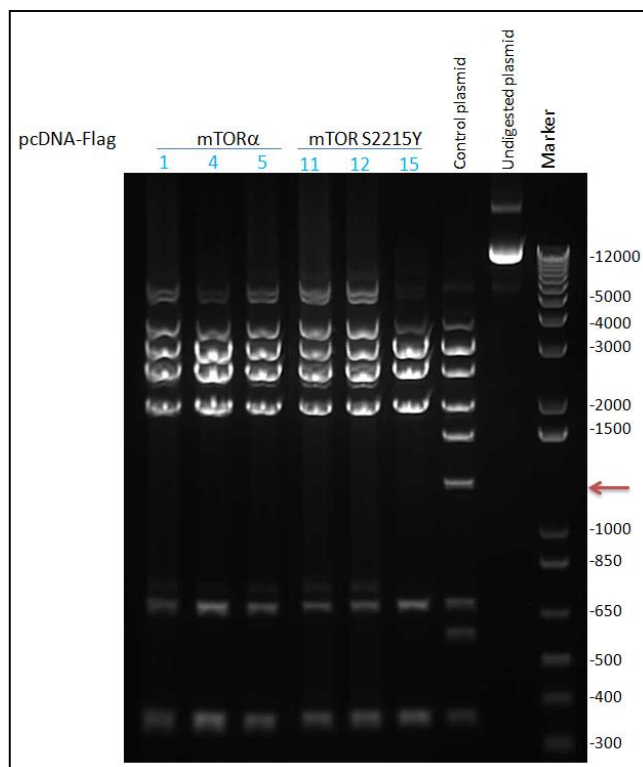


**Figure 4.6: Agarose gel image of the results of the digestion analysis of the pcDNA3–Flag–mTOR $\alpha$  and pcDNA3–Flag–mTOR S2215Y plasmids for the first selection which showed negative results.**

Digestion analysis was performed to verify that the DNA was inserted into the plasmid. The plasmids were digested using the *Hin*1I restriction enzyme and run on 0.8% agarose gel. The digestion of plasmids with inserts should result in a band of approximately 1,280 bp. This band was absent in all selected colonies indicated with blue numbers.

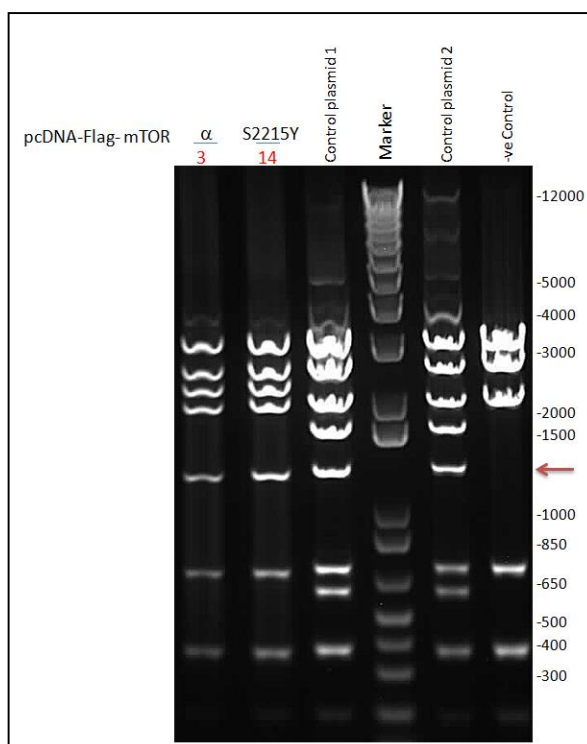


**Figure 4.7: Agarose gel image of the results of the digestion analysis of the pcDNA3–Flag–mTOR $\alpha$  and pcDNA3–Flag–mTOR S2215Y plasmids for the second selection which demonstrated positive results.**

Digestion analysis was performed to verify that the DNA was inserted into the plasmids. The plasmids were digested with the *Hin*1I restriction enzyme and run on 0.8% agarose gel. The obtained band with a size of approximately 1,280 bp confirms that the insert is present in all of the selected colonies (indicated with red numbers).

### 4.1.3 Generation of the pcDNA3–Flag–mTOR $\delta$ plasmid

mTOR $\delta$  shares the same NH<sub>2</sub>–terminus as of the wild–type mTOR $\alpha$ . Therefore, the pcDNA3–Flag–mTOR $\delta$  plasmid was constructed by replacing the COOH–terminus of pcDNA3–Flag–mTOR $\alpha$  with the COOH–terminus of mTOR $\delta$  (Figure 4.8). The pcDNA3–Flag–mTOR $\alpha$  and pME18S–FL3–mTOR $\delta$  plasmids were digested with the *Eco*RI and *Xba*I restriction enzymes. The COOH–terminus of mTOR $\delta$  and the pcDNA3 plasmid containing the NH<sub>2</sub>–terminal of Flag–mTOR were purified using a DNA gel extraction kit (QIAGEN) and ligated using T4 DNA ligase (Figure 4.9).

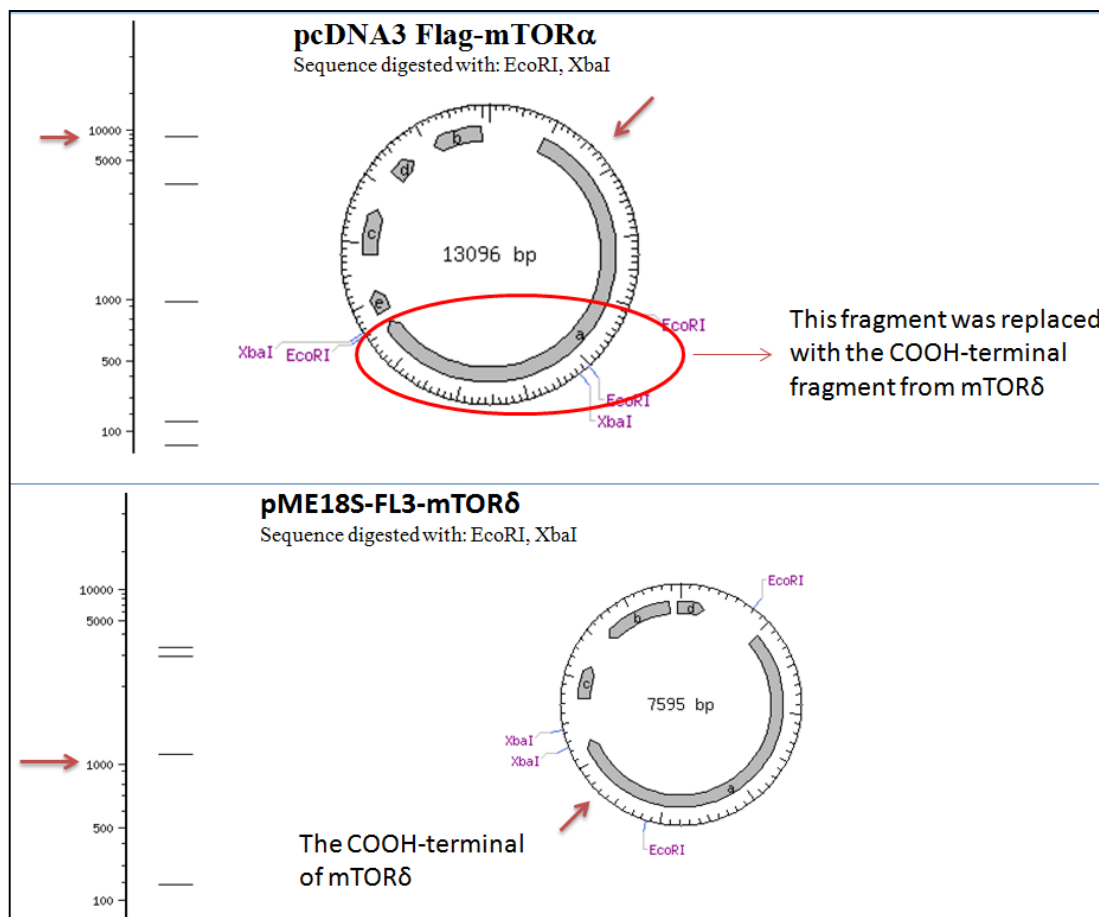


**Figure 4.8: Plan to generate pcDNA3-Flag-mTOR $\delta$ .**

The pcDNA3-Flag-mTOR $\alpha$  isoform was digested with EcoRI and XbaI (top). As a result, the COOH-terminus of mTOR $\alpha$  was removed from the plasmid, whereas the NH<sub>2</sub>-terminus remains attached to the plasmid. This NH<sub>2</sub>-terminus is shared with the NH<sub>2</sub>-terminus of mTOR $\delta$ . pME18S-FL3-mTOR $\delta$  was also digested with EcoRI and XbaI (bottom). This digestion resulted in the full-length COOH-terminus of mTOR $\delta$  containing the EcoRI sequence at its NH<sub>2</sub>-terminus and the XbaI sequence at its COOH-terminus. This fragment was then ligated to pcDNA3 containing the NH<sub>2</sub>-terminus of mTOR.

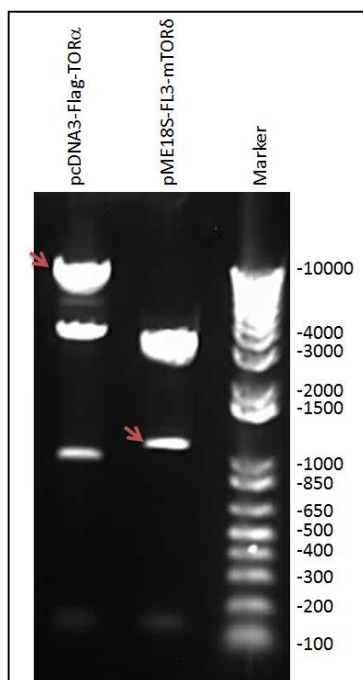


**Figure 4.9:** Agarose gel image of the DNA fragments used for the construction of pcDNA3–Flag–mTOR $\delta$ .

The pcDNA3–Flag–mTOR $\alpha$  and pME18S–FL3–mTOR $\delta$  plasmids were digested with EcoRI and XbaI. These plasmids were then electrophoresed in a 0.8% agarose gel, and the resulting COOH–terminus of mTOR $\alpha$  was replaced with the COOH–terminus of mTOR $\delta$ .

#### 4.1.4 DNA sequence analysis of the generated plasmids

Sequence analysis of the generated plasmids was performed to verify the presence of the DNA sequences and the mutation. Samples of the pcDNA3-Flag-mTOR $\alpha$  and pcDNA3-Flag-mTOR S2215Y plasmids were sent to GATC Biotech for DNA sequence analysis. The pcDNA3–Flag–mTOR $\delta$  plasmids were sequenced at the Wolfson Institute for Biomedical Research, UCL. The presence of the full–length Flag–mTOR $\alpha$  DNA inserts was confirmed by sequencing analysis and multiple sequence alignment.

The results indicate that the active mTOR S2215Y has a point mutation (TCT to TAT) in the kinase domain of mTOR $\alpha$ . The sequencing results of mTOR S2215Y aligned against the mTOR $\alpha$  sequence can be seen in Figure 4.10.



**Figure 4.10: Sequencing analysis of pcDNA3-Flag-mTOR S2215Y.**

The top of this figure presents the sequence alignment highlighting the point mutation. The lower part of the figure presents the sequence in the chromatogram, indicating that the mutation had been generated. Alignment of the resulting sequence against the mTOR $\alpha$  sequence indicated that the mTOR S2215Y point mutation (TCT to TAT) had been successfully generated and that the DNA was inserted in the pcDNA3-Flag-mTOR plasmid.

These plasmids were then used to generate a recombinant protein and stable cell lines over-expressing a Flag-tagged recombinant form of mTOR. The obtained recombinant proteins and stable cell lines were then used to study the mTOR $\delta$  isoform *in vitro* and in cells.

In Figure 4.11 the mTOR $\delta$  COOH-terminal sequence is highlighted in red, which is the sequence that was added to the pcDNA3 plasmid containing the Flag-tagged mTOR NH2-terminal.

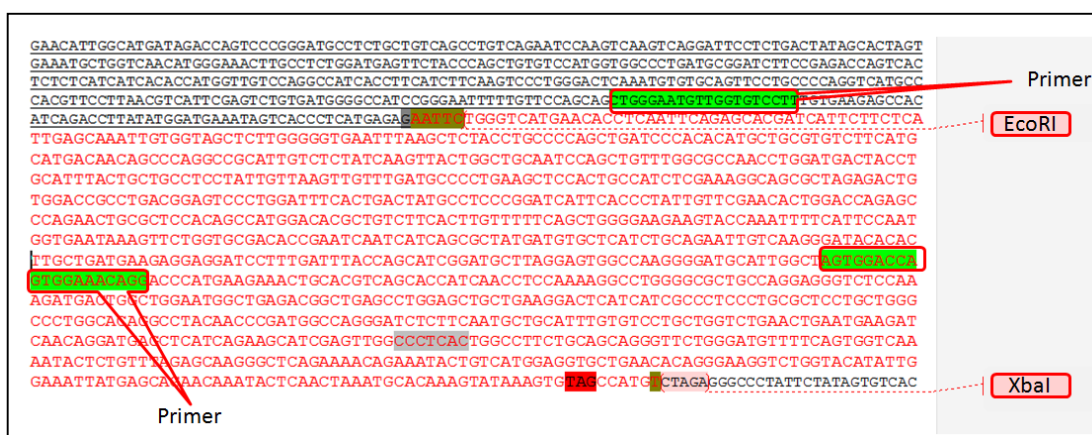


**Figure 4.11: mTOR $\delta$  COOH-terminal sequence highlighted in red.**

This sequence was added to the pcDNA3 plasmid containing the Flag-tagged mTOR NH2-terminus. The sequences highlighted in green demonstrate the primer sequences that were used for sequencing. The restriction/ligation sites for the EcoRI and XbaI restriction enzymes are highlighted between brackets.

The alignment of the obtained sequence of mTOR $\delta$  fragment against the predicted sequence of mTOR $\delta$  can be seen in Figure 4.12. This novel and unique amino acids sequence which resulted from a splicing-mediated frame shift in the middle of FAT

domain was cloned into pET expression plasmid and expressed in bacteria as His-tag fusion protein. Recombinant His-mTOR $\delta$ C was purified nearly to homogeneity using NTA affinity chromatography and used to generate mTOR $\delta$  specific polyclonal antibodies in mouse. We used recombinant His-mTOR $\delta$ C protein for affinity purification of mTOR $\delta$  specific antibodies from the sera of immunized animals.

➤ mTOR $\delta$  COOH-terminal sequence (28 – 59 amino acids)

CTCAGAAAACAGAAATACTGTCATGGAGGTGCTGAACACAGGGAAGGTCTGGTACATATTGGA AATT  
ATGAGCAGAACAATACTCAACTAAATGCACAAAGTATAAAGTGTAGCCATG

mTOR $\delta$ Sequencing-s-Tag	-----CTCAGAAAACAGAAATACTGTCATGGAGGTGCTGAACACAGGGAAGGTCT GATCCGAATTCTCAGAAAACAGAAATACTGTCATGGAGGTGCTGAACACAGGGAAGGTCT *****
mTOR $\delta$ Sequencing-s-Tag	GGTACATATTGGA AATTATGAGCAGAACAATACTCAACTAAATGCACAAAGTATAAAGT GGTACATATTGGA AATTATGAGCAGAACAATACTCAACTAAATGCACAAAGTATAAAGT *****
mTOR $\delta$ Sequencing-s-Tag	GTAGCCATGT----- GTAGCCATGTCTAGCTCGAGCACCACCACCACCACCACCACCACCTAATTGATTAATACCT *****

**Figure 4.12: Nucleotide sequence alignment of the mTOR $\delta$  fragment.**

The mTOR $\delta$  fragment, which encodes a novel amino acid sequence that was used to generate a specific antibody targeting mTOR $\delta$ , was aligned against the predicted sequence of mTOR $\delta$ .

#### 4.1.5 Generation of stable cell lines expressing mTOR $\delta$

To gain insight into the possible effects of the mTOR $\delta$  isoform, HEK 293T cell lines stably expressing the mTOR $\delta$ , mTOR $\alpha$  or mTOR S2215Y isoforms were used as a research model. The parental HEK 293T cells and HEK 293T cells expressing wild-

type mTOR $\alpha$  or the activated form mTOR S2215Y were used as controls in the following functional analysis. Cells transfected with Flag- mTOR S2215Y were employed as a positive control. Cells transfected with the empty vector, referred to as parental cells, were used as a negative control.

Mammalian expression vectors encoding the DNA sequence of Flag-mTOR were generated for all of the mTOR isoforms. The generated expression vectors were confirmed by restriction and sequencing analysis. These constructs contain the neomycin resistance gene, allowing the selection of transfected cells with Geneticin (G-418). Geneticin is an aminoglycoside analogue of Gentamicin sulphate. Geneticin is commonly used as a selective agent for eukaryotic cells. Geneticin interferes with the function of the 80S ribosomes and protein synthesis in eukaryotic cells. The Geneticin resistance gene (neomycin) is commonly used in mammalian expression vectors. Cells expressing these resistance markers can be selected when the culture is treated with a culture medium containing Geneticin. As a result, stable colonies of mammalian cells expressing these resistance markers can be generated in a period of 10 to 20 days.

HEK 293 cells were transfected with each vector separately, and transiently transfected cells exhibited adequate levels of expression for all of mTOR isoforms (Figure 4.13). This result demonstrated that the transfection was efficient and that the expression of the fusion protein in transiently transfected HEK 293 cells was abundant. To generate stable cell lines, prior to Geneticin treatment, HEK 293 cells were tested for Geneticin resistance, and the optimum concentration for selection was obtained.

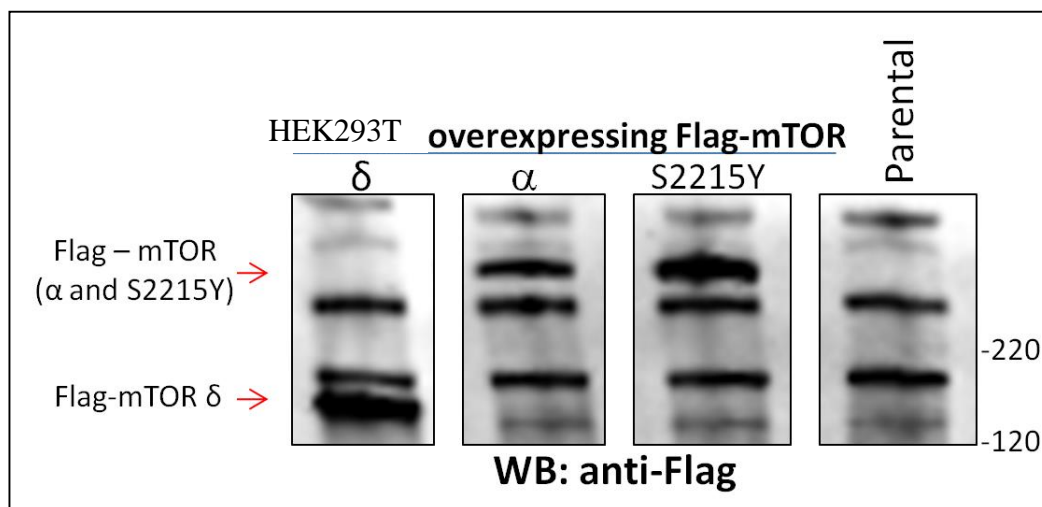


**Figure 4.13: Western blot confirming the expression of Flag-mTOR $\delta$ , Flag-mTOR $\alpha$  and Flag-mTOR S2215Y in transfected HEK 293T cells.**

HEK 293T cells transfected with the pcDNA3-Flag-mTOR $\alpha$ , pcDNA3-Flag-mTOR $\delta$  or pcDNA3-Flag-mTOR S2215Y isoforms were lysed, 24 hours post transfection cells, then resolved via SDS-PAGE and immuno-blotted with an anti-Flag antibody.

HEK 293 cells over-expressing the mTOR isoforms were then selected by G-418 treatment. The cell lines were treated with the optimum concentration (1,200  $\mu\text{g/ml}$ ) of G-418 for 2 weeks. Single colonies were visualised under microscopic examination. These cells were then collected and mixed together to generate polyclonal cell lines over-expressing each of the different mTOR isoforms separately. The cells were then maintained under a minimum G-418 concentration (200  $\mu\text{g/ml}$ ). Unfortunately, the selected cell lines lost the expression of the mTOR $\gamma$  and mTOR $\alpha$  isoforms within a week. The generation of stable cell lines was repeated with different selection conditions, including a wide range of Geneticin concentration and confluency, with no success. The concentration of G-418 used for the selection of HEK 293 cells generally does not exceed 800  $\mu\text{g/ml}$ . During the analysis of the

sensitivity of our HEK 293 cells to G-418, a concentration of 800  $\mu\text{g/ml}$  was found to be insufficient to kill the cells. The HEK 293 cells may have become resistant to Geneticin. It is well known that Geneticin is a slow killer of eukaryotic cells. For Geneticin to be effective, the compound must be of a high purity so that a smaller amount can be used to achieve greater selection with minimal toxicity from either Geneticin itself or contaminants. In addition, Geneticin has been considered the gold standard antibiotic for the selection of cells transfected with the neomycin resistant gene for approximately two decades. Therefore, this widespread use might have promoted a wide ranging resistance against Geneticin.

To overcome this problem, the HEK 293 cells were co-transfected with plasmids containing different mTOR isoforms and with the pcDNA 4/TO plasmid. pcDNA 4/TO contains the Zeocin resistance gene, which allows the selection of stable lines using Zeocin. After co-transfection, the transiently transfected cells exhibited an adequate level of expression, and Zeocin treatment was initiated for 12 days. Five single colonies for each isoform were isolated and tested for Flag-mTOR expression. For each isoform, one colony of HEK 293 cells stably expressing the Flag-mTOR isoform was used for all subsequent experiments. Therefore, the results indicated that this co-transfection was successful, and HEK 293 cells were capable of expressing the mTOR fusion proteins.

At a later stage in my PhD research, I found that the HEK 293 cell line used in this chapter and chapter 5 was actually HEK 293T cell line which already contains a neomycin resistance gene. This finding explains the poor selection achieved using G-418, even under treatment with high G-418 concentrations.

These recombinant proteins were then used to study the mTOR $\delta$  isoform *in vitro* and *in vivo*. The recombinant proteins were employed to perform an *in vitro* kinase assay using immuno-precipitated mTOR isoform complexes. In addition, these recombinant mTOR isoforms were also employed to analyse the effect of this isoform on cellular functions controlled by the mTOR signalling pathway.

Finally, HEK 293T cells over-expressing these mTOR isoforms were employed to elucidate whether mTOR $\delta$  over-expression is able to antagonise tumourigenesis mediated by the mTOR signalling pathway using colony formation assays and a xenograft model in nude mice (in progress).

## 4.2 Functional Analysis

Until present, the only recognised activity of mTOR is its kinase activity. mTOR phosphorylates S6K, 4EBP1 and PKB/Akt *in vivo* and *in vitro* (Harada et al. 2001; Ma & Blenis 2009; Vivanco & Sawyers 2002). The mTOR $\delta$  isoform is the result of a frame-shift leading to the absence of the kinase domain. It is thought that mTOR $\delta$  acts as a dominant negative regulator of mTOR signalling by sequestering the substrate-presenting proteins raptor and rictor.

In addition to the novel amino acid sequence at the COOH-terminal of the mTOR $\delta$  spliced isoform, mTOR $\delta$  retains HEAT repeats domain at the NH<sub>2</sub>-terminus. The HEAT repeat is thought to mediate the mTOR localization on the cell membrane (Liu & Zheng 2007).

The presence of mTOR isoforms is likely to affect the mTOR pathway and mTOR-mediated cellular processes such as cell growth, survival and cell cycle regulation. Hence, we are prompted to study the cellular localisation of mTOR $\delta$  and the effect of

mTOR $\delta$  on the cell proliferation, cell cycle, cell size, overall tumourigenicity and tumour progression.

To study the effect of mTOR $\delta$  on cellular proliferation, MTT proliferation assays were performed. To elucidate whether mTOR $\delta$  over-expression is able to antagonise tumorigenesis mediated by the mTOR signalling pathway, colony formation assays were performed, and a xenograft model in nude mice is in the process of development. To perform these experiments, mammalian expression vectors containing the coding sequences of the Flag-mTOR $\delta$ , Flag-mTOR $\alpha$  and Flag-mTOR S2215Y isoforms were generated, and stable HEK 293T cell lines were generated as discussed in section 4.1.24.1.3.

The MTT proliferation assay has been used to study the effect of over-expression of the mTOR $\delta$  isoform on cellular proliferation. A HEK 293T cell line over-expressing Flag-mTOR S2215Y was used as a positive control, and HEK 293T cells transfected with an empty vector were used as a negative control. In addition, a HEK 293T cell line over-expressing wild-type (mTOR $\alpha$ ) was included in the study to compare its cellular proliferation with that of mTOR $\delta$ .

#### **4.2.1 mTOR $\delta$ kinase activity**

The mTOR protein is defined as the functional subunit of two mTOR complexes. mTOR complex 1 phosphorylates S6K and 4E-BP1, whereas mTOR complex 2 phosphorylates Akt. In contrast to mTOR $\alpha$  and mTOR $\beta$ , mTOR $\delta$  lacks the kinase domain and possesses a new amino acid sequence at its COOH-terminus. Therefore, mTOR $\delta$  will be unable to phosphorylate the mTOR substrates S6K, 4E-BP1 and Akt.

#### 4.2.2 MTT assay – cell proliferation assay

mTOR functions at the intersecting of various signalling pathways that control multiple cellular functions. mTOR integrates intracellular and extracellular signals to regulate cell growth, proliferation and survival (Corradetti & Guan 2006; Hay & Sonenberg 2004). mTOR protein regulates these various cellular processes via the activation of Akt, 4EBP1 and S6K. Akt inactivates several pro-apoptotic factors and mediates the stabilisation of cell surface amino acid transporters, promoting cellular growth and survival (Edinger & Thompson 2002; Guertin, Stevens et al. 2006; Vivanco & Sawyers 2002). Together, 4E-BP1 and S6K1 promote mRNA translation, ribosome biogenesis and autophagy (Hara et al. 2002; Kim, Sarbassov et al. 2002; Kim, et al. 2003; Ruggero & Pandolfi 2003). In contrast, S6K1 generates a negative feedback loop to reduce survival signals and inhibit the pro-apoptotic protein BAD (Harada et al. 2001). Because wild-type mTOR plays a key role in the regulation of cell proliferation, mTOR $\delta$  is expected to be involved in the regulation of mTOR activities.

An MTT proliferation assay was performed to assess the differences in the levels of proliferation inhibition in response to the starvation of HEK 293T cells over-expressing the mTOR $\delta$  splicing isoform compared with parental HEK 293T cells. The MTT assay is a colorimetric assay for measuring the activity of live cells. In viable cells, cellular enzymes reduce the tetrazolium dye, MTT, to produce a strongly pigmented formazan product (Promega). The absorbance of the pigmented product was measured using a micro-plate absorbance plate reader (Tecan).

We used the created HEK 293T stable cell lines over-expressing mTOR $\delta$ , mTOR $\alpha$  and mTOR S2215Y isoforms and parental cells. About 5000 HEK 293T cells were

plated per well in 96 wells plate and nourished with DMEM containing 10% FBS. When the HEK 293T cell lines reached about 70% confluency, cells were starved of serum. Two days after starvation, MTT dye was added to wells and incubated for 3 hours, followed by the absorbance measurement. From day 2 to days 6 after starvation, measurement was taken daily. The optical density determined at 490 nm using a plate reader. Results are normalized to the blank which contains media MTT but no cells.

The HEK 293T cells over-expressing mTOR $\delta$  exhibited decreased cellular proliferation compared with the parental cells. The significant difference in the cell proliferation was observed after 72 hours ( $P < 0.05$ ) (Figure 4.14).

In conclusion, this demonstrated that the mTOR $\delta$  protein is a negative regulator of the proliferative activity of HEK 293T cells.

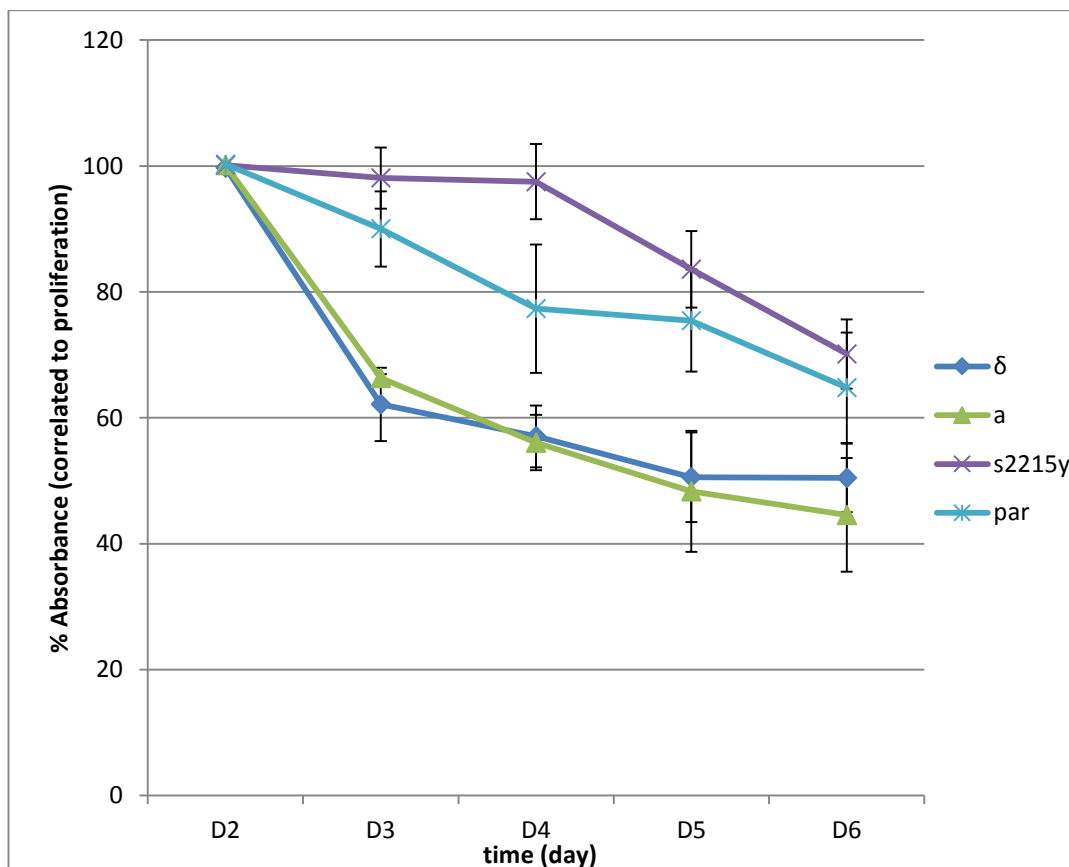


**Figure 4.14: Parental HEK 293T cells demonstrate a higher proliferation potential than HEK 293T cells over-expressing the mTOR $\delta$  isoform.**

The MTT proliferation assay was performed using HEK 293T cells over-expressing mTOR $\alpha$ , mTOR $\delta$ , mTOR S2215Y or parental cells under condition of starvation. The same number of cells was seeded for all cell lines. Once the cells had reached optimum confluence, they were placed under starvation conditions. After 48 hours of starvation, the CellTiter 96 one solution reagent (MTT) was added, followed by three hours incubation and then the absorptions were measured at 490nm. From day 2 to day 6 after starvation, measurements were performed daily. Each data point represents the mean  $\pm$  SEM from three independent experiments ( $P < 0.05$ ,  $n = 3$ , independent experiments).

### 4.2.3 Colony formation assay

The mTOR protein plays a critical role in the regulation of cellular processes, including cell growth, proliferation and survival and protein synthesis (Corradetti & Guan 2006; Hay & Sonenberg 2004). It is well known that extracellular signals and intracellular signals enhance the mTOR activity. The enhanced mTOR activity is implicated in tumourigenesis and promotes tumour progression. As noted previously, mTOR $\delta$  lacks the kinase domain. Thus, mTOR $\delta$  lacks catalytic activity and will not phosphorylate the mTOR $\alpha$  targets, including S6K, 4EBP1 and Akt. Using an MTT proliferation assay, we demonstrated that mTOR $\delta$  inhibits cellular proliferation. It would be interesting to elucidate whether over-expressed mTOR $\delta$  is able to antagonise tumourigenesis mediated by mTOR signalling pathway.

Colony formation assays, also known as clonogenic assays, are *in vitro* cell survival assays based on the ability of a single cell to grow into a colony in a compressed and unfavourable environment. The number of colonies derived from cells exhibiting oncogenic survival and proliferation properties will be significantly higher than the number of colonies derived from normal cells.

Our previous results indicated that, in cancer, the mTOR $\delta$  has the potential to promote reproductive cell death. To elucidate whether mTOR $\delta$  has an oncogenic or anti-oncogenic effect, colony formation assays were performed. These assays basically measured the number of cells that were able to undergo continuous division in the HEK 293T cell line over-expressing mTOR $\delta$  compared with the parental HEK 293T cell line.

Parental HEK 293T cells and HEK 293T cells over-expressing mTOR $\delta$ , mTOR $\alpha$  or mTOR S2215Y were seeded at appropriate dilutions using soft agar to form colonies over a period of 1 to 3 weeks. The colonies were then stained with 0.005% crystal violet for 3 hours at 37 °C and photographed. The fold increase or decrease in the number of colonies that were able to survive was measured. Five independent experiments, each were performed in triplicate.

Figure 4.15 indicates that very few spontaneous colonies were formed from 2,000 or 4,000 HEK 293T cells over-expressing mTOR $\delta$  compared with parental HEK 293T cells. The parental cells exhibited a four-fold increase in the number of colonies. In addition, consistent with MTT results the colony formation assay indicated that the number of colonies generated from HEK 293T cells over-expressing mTOR $\alpha$  was significantly lower ( $p < 0.05$ ) than the number of colonies generated from parental HEK 293T cells (Figure 4.15).

Therefore, the results suggest that when the mTOR $\delta$  protein is stably expressed in HEK 293T cells, mTOR $\delta$  causes either cell cycle arrest or cell death and, hence, a reduced number of colonies. This observation is in accord with the MTT data, which demonstrated that mTOR $\delta$  over-expression inhibited cell proliferation.

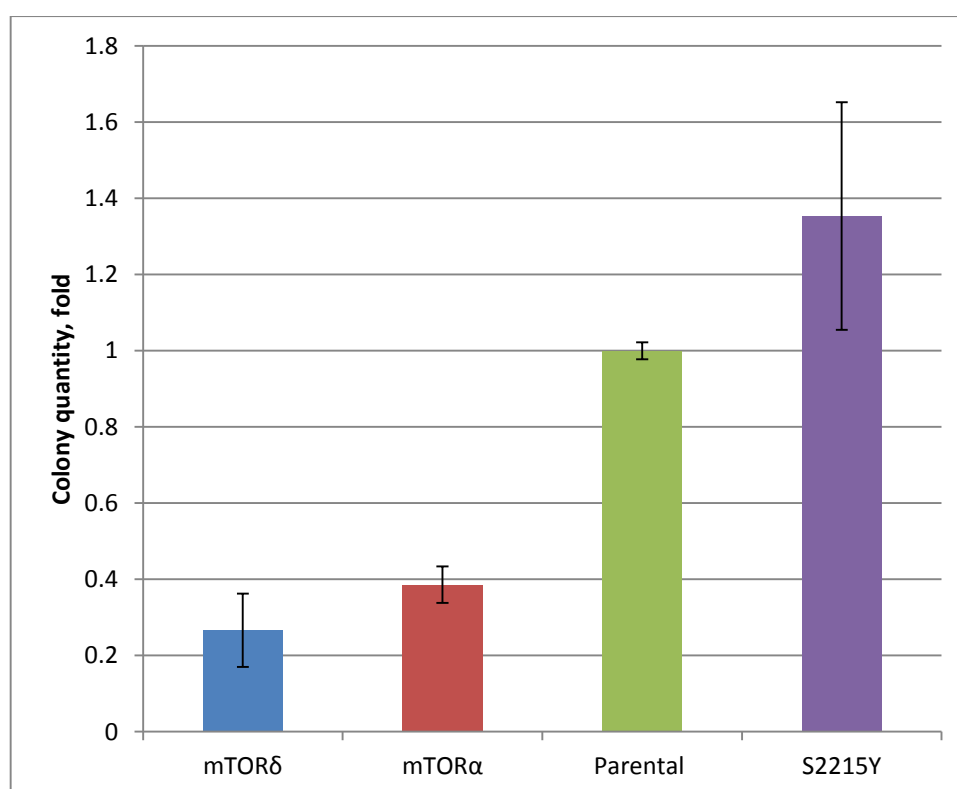
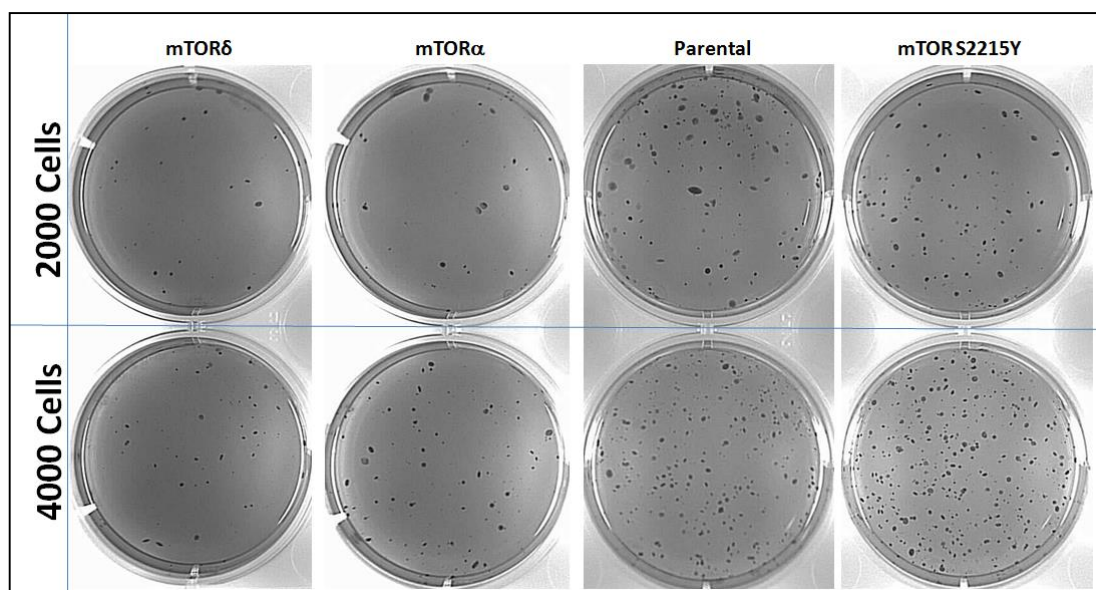


**Figure 4.15: The mTOR $\delta$  protein stably enhances either cell cycle arrest or cell death.**

Anchorage-independent growth of parental HEK 293T cells and HEK 293T cells over-expressing mTOR $\delta$ , S2215Y or mTOR $\alpha$  in soft agar. Cells were plated in a thin layer of agarose mixed with culture medium. Two weeks later, colonies were stained with 0.005% crystal violet, photographed and counted. The number of folds increase or decrease was plotted. Data are presented as the means  $\pm$ SEM of five independent experiments. Parental cells exhibited a four-fold increase in the number of colonies compared with cells over-expressing mTOR $\delta$ .

#### 4.2.4 Discussion and conclusions

The initial aim of this study was to identify novel mTOR isoforms to better understand the regulation of the mTOR signalling pathway and its contribution to cancer. This goal was achieved through protein, molecular and bioinformatics analytical approaches, leading to the isolation of a cDNA clone encoding a novel homologous protein, mTOR $\delta$ . The mTOR $\delta$  protein lacks the FRB and kinase domains which are crucial for mTOR kinase activity.

To study the molecular characteristics of the mTOR $\delta$  protein and elucidate its potential role in tumourigenesis, a mammalian expression vector was constructed, and stable cell lines over-expressing mTOR $\delta$  were generated. The full coding sequences of mTOR $\alpha$ , mTOR $\delta$  and mTOR S2215Y were successfully cloned into the pcDNA3 vector with a Flag-tag positioned at the NH<sub>2</sub>-terminus of the mTOR isoforms. The sequences of the constructs were verified by digestion and sequencing analysis. The expression of the fusion protein in HEK 293T cells that were either transiently transfected or stably expressing the mTOR isoforms was confirmed via Western blot analysis. Immuno-precipitation with Protein G beads coated with an anti-Flag antibody appeared to be efficient, based on the copious amounts of proteins that could be detected by Western blotting analysis. Subsequently, the recombinant proteins and stable cell lines were used to characterise mTOR $\delta$  *in vitro* and *in vivo*.

In contrast to mTOR $\alpha$ , the mTOR $\delta$  lacks the kinase domain. As a result, mTOR $\delta$  lacks catalytic activity and is unable to phosphorylate mTOR $\alpha$  targets. mTOR can only function in two distinct complexes, mTORC1 and mTORC2. The raptor, rictor and mLST8 proteins are critical for mTOR activity. Compared to the other partners in the complexes, they appear to make the most important contribution to the mTOR

activity (Guertin et al. 2006;Hara et al. 2002;Kim et al. 2002;Sancak et al. 2008;Sarbasov et al. 2004).

The component that binds to mTOR and also to the mTOR targets S6K and 4E-BP1 is represented by raptor. Researchers have demonstrated that raptor binds to mTOR as well as S6k and 4E-BP1 and facilitate their phosphorylation by mTOR. Therefore raptor can be defined as the substrate presenting protein of mTOR complex 1 (Nojima et al. 2003).

A common partner of mTOR complexes is mLST8, a 36-kDa polypeptide that has seven “WD40” repeats (Nakashima et al. 2013). The binding site for mLST8 is represented by the catalytic domain of mTOR and an exaggerated expression and a sudden decrease of mLST8 have been demonstrated to increase the function of mTORC1. Some studies used mice that lacked mLST8 and revealed that this protein is necessary for binding of mTOR and rictor but not for the mTOR-raptor connection, therefore mLST8 is more important for mTORC2 in comparison to mTORC1 (Guertin et al. 2006). The specific role of mLST8 in relation with mTORC1 is still unclear and remains to be discovered.

We hypothesised that mTOR $\delta$  would act as a negative regulator of mTOR $\alpha$  by sequestering mLST8 and the substrate-presenting proteins raptor and rictor. Raptor has been reported to bind to mTOR via a strong NH<sub>2</sub>-terminal interaction and a weaker COOH-terminal interaction (Hara et al. 2002;Kim et al. 2002;Sancak et al. 2008). Because the identified mTOR $\delta$  splicing isoform lacks most of its COOH-terminus, including FRB, kinase, FATC and part of the FAT, but retains domains responsible for the protein-protein interaction modules, including the HEAT repeats

at the NH<sub>2</sub>-terminal, it is assumed that the interaction of mTOR with raptor will not be affected.

The mTOR $\beta$  splicing isoform is missing many important protein domains required for interactions, such as the HEAT and FAT domains, but it retains the FRB, kinase, RD and FATC domains. Additionally, studies have demonstrated that mTOR $\beta$  has the ability to form complexes *in vivo* with known complements of the full-length mTOR, raptor and rictor (Panasyuk et al. 2009).

In addition, we have demonstrated that the proliferation of HEK 293T cells expressing mTOR $\delta$  is significantly inhibited compared with parental HEK 293T cells in response to 72 hours of starvation.

In a systematic review of the current and future directions of mTOR inhibitor development, expert opinion indicated that the preclinical results for mTOR inhibitors suggest a potent anti-proliferative activity against a broad panel of tumour cell lines (Fasolo and Sessa 2011). The mTOR $\alpha$  and mTOR $\beta$  proteins phosphorylate Akt, S6K1 and 4E-BP1, promoting cell survival and proliferation (Edinger & Thompson 2002;Guertin et al. 2006;Vivanco & Sawyers 2002). It is therefore hypothesised that, because mTOR $\delta$  lacks a kinase domain, it may compete with mTOR $\alpha$  and mTOR $\beta$  for crucial binding partners such as the substrate-presenting proteins raptor and rictor, thereby inhibiting mTOR-mediated regulation of cell proliferation.

Since our results demonstrating that mTOR $\delta$  possesses anti-oncogenic potential, this result suggesting that the mTOR $\delta$  protein expression causes either cell cycle arrest or cell death, consequently antagonise the oncogenic potentials. In clonogenic assays,

approximately four-fold more colonies were generated from parental HEK 293T cells compared with HEK 293T cells over-expressing mTOR $\delta$ .

Consistent with the previous study in which mTOR $\beta$  was identified and characterised, the number of colonies generated from HEK 293T cells over-expressing mTOR $\alpha$  was significantly lower than the number of colonies generated by parental HEK 293T cells. The study in which mTOR $\beta$  was isolated found that the HEK 293T cells over-expressing mTOR $\alpha$  did not exhibit any significant features associated with oncogenic transformation. Cells over-expressing mTOR $\alpha$  failed to generate a significant number of anchorage-independent colonies in soft agar culture and were incapable of forming tumours in immuno-suppressed mice *in vivo* (Panasyuk et al. 2009).

The inhibited mTOR $\alpha$  activity produce a strong feedback loop by S6K-IRS which may inhibit the whole process of cell growth and proliferation. mTORC1 can be reactivated by amino acids, energy and nutrient, however mTORC2 is insensitive to amino acids and nutrient. Therefore Akt will be inhibited and apoptosis will be activated.

Taken together, our results support the hypothesis that mTOR $\delta$  expression reduces cellular proliferation and inhibits tumour progression. However, the mechanism underling mTOR $\delta$ -mediated responses remain to be found. One possible mechanism is that mTOR $\delta$  may down-regulate mTOR function by sequestering the substrate-presenting proteins of mTOR complexes.

# **CHAPTER 5**

## **Molecular characterisation and functional analysis of mTOR $\gamma$**

## Chapter 5: Molecular characterisation and functional analysis of mTOR $\gamma$

---

### 5.1 Molecular characteristics of the mTOR $\gamma$ isoform

#### 5.1.1 Introduction

Dysregulation of the mTOR signalling pathway is implicated in various disorders. The mTOR protein has attracted great interest as a target for cancer treatment. In chapter 3, we identified two mTOR isoforms, termed mTOR $\delta$  and mTOR $\gamma$ . The extensive analysis of mTOR $\delta$  was discussed in chapter 4. Chapter 5 discusses the molecular characteristics and functional analysis of the mTOR $\gamma$  splicing isoform.

The mTOR $\gamma$  isoform was identified through extensive bioinformatics analysis of the EST database. mTOR $\gamma$  consists of 2,537 amino acids, and its molecular weight is 287 kDa. In comparison with the full-length wild-type mTOR $\alpha$ , 12 amino acids are absent in the kinase domain of the mTOR $\gamma$  splicing isoform. This deletion is located at the beginning of the kinase domain, which contains certain conserved residues that are critical for its kinase activity. This deletion removes the entire beta 5 strand from the catalytic domain, which includes the critical Lys2187 residue. The Lys2187 is thought to interact with the  $\alpha$ -phosphate of adenosine tri-phosphate (ATP) (Sturgill and Hall 2009). Therefore, mTOR $\gamma$  is an interesting protein with the potential to play a major role in the regulation of mTOR signalling and, thus, mTOR-mediated

cellular functions. We hypothesized that this 12–amino acid deletion in the kinase domain might disrupt the kinase activity of the mTOR $\gamma$  splicing isoform, thus, the main focus of this study was to investigate the potential effect of this deletion on the kinase activity of mTOR $\gamma$ , on mTOR signalling pathway regulation and the cellular processes mediated by mTOR.

To elucidate the possible role and function of this deletion, a mammalian expression construct expressing this splicing isoform was generated. Using the obtained construct, a stable HEK 293T cell line over-expressing mTOR $\gamma$  was generated. The stable cell line was used to study the catalytic activity and the role of mTOR $\gamma$  in the regulation of the mTOR pathway and cellular functions.

In addition to mTOR $\gamma$ , mTOR $\alpha$ , mTOR $\delta$  and mTOR S2215Y were also employed in this study. The wild–type mTOR $\alpha$  and the activated mutant mTOR S2215Y were used as positive controls to study the characteristics of mTOR $\gamma$ . Because, mTOR $\delta$  lacks the kinase domain, it was used as a negative control (Figure 5.1).

For *in vitro* experiments, wild–type mTOR $\alpha$ , the activated mTOR S2215Y mutant and mTOR $\delta$ , which lacks the kinase domain, were used. For *in vivo* investigations, a parental HEK 293T cells which was transfected with an empty vector, and cells individually expressing mTOR $\alpha$ , mTOR $\delta$ , mTOR $\gamma$  and mTOR S2215Y were used.

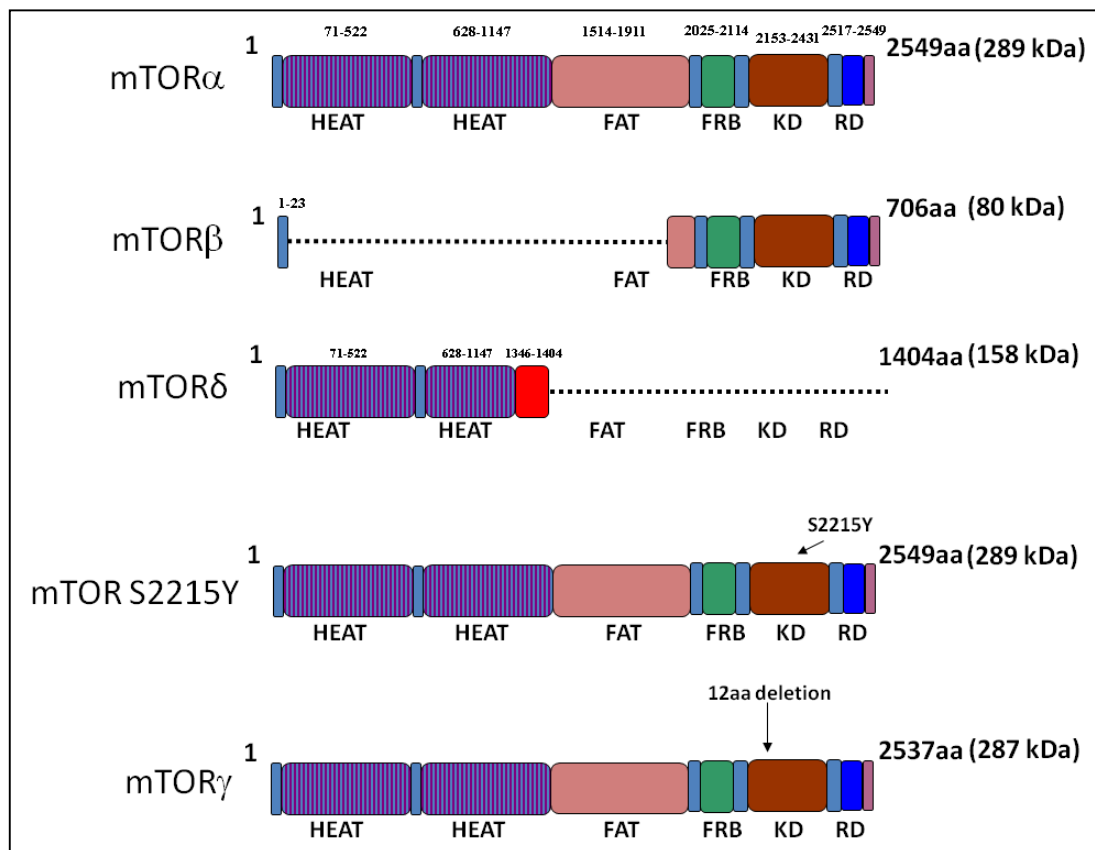


**Figure 5.1: A schematic representation of the domain organisation of the mTOR $\gamma$  splicing isoform.**

mTOR $\gamma$  possesses 12–amino acid deletion in the kinase domain. This deletion involves conserved residues that are critical for kinase activity. The mTOR $\beta$  isoform lacks most of the NH<sub>2</sub>-terminus and processes oncogenic potential. mTOR $\delta$  is a novel mTOR splicing isoform that lacks the kinase domain.

### 5.1.2 Generation of a Flag-tagged mTOR $\gamma$ plasmid

The mammalian expression vector pcDNA3 was used to generate constructs containing the sequences of mTOR $\alpha$ , mTOR $\delta$  and mTOR S2215Y, and stable HEK 293T cell lines were obtained as described in chapter 4. Thus, pcDNA3 and HEK 293T cells were the vector and cell line of choice, respectively, for cloning mTOR $\gamma$  and generating a stable cell line. Similar to the other vectors in the research model, the cDNA sequence was cloned as a Flag-tagged fusion protein in the pcDNA3 mammalian expression vector. Thus, the generated recombinant Flag-tagged fusion protein can be purified and detected using an anti-Flag antibody. Another DNA sequencing analysis was performed to verify that the correct DNA sequence was introduced into the pcDNA3 expression vector.

The 12-amino acid deletion was introduced into the nucleotide sequence of pcDNA3-mTOR $\beta$  in our laboratory by Christopher Fu (Figure 5.2). The generated protein was denoted mTOR $\beta$   $\Delta$ 12. This deletion was introduced into the cDNA sequence of mTOR $\beta$  using a set of primers for the 12-amino acid deletion.

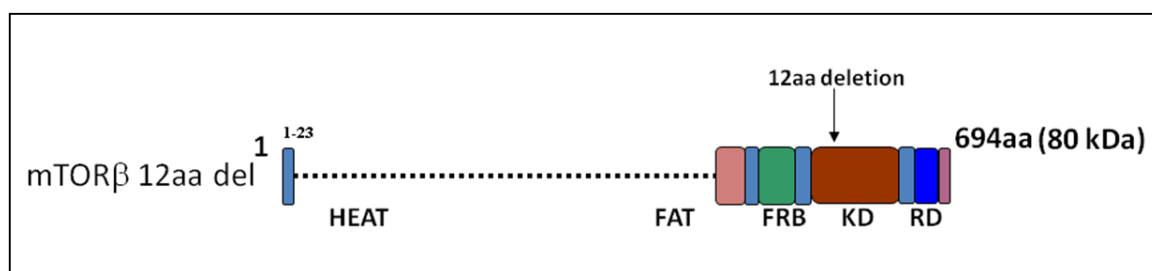


**Figure 5.2:** A schematic diagram demonstrating the location of the 12-amino acid deletion in mTOR $\beta$ .

mTOR $\alpha$  exhibits the same COOH-terminal region as mTOR $\beta$ . Thus, the position of the 12-amino acid deletion is at the same position in mTOR $\alpha$ . The COOH-terminus of mTOR $\beta$   $\Delta$ 12 was used for the generation of mTOR S2215Y.

The pcDNA3-mTOR $\beta$   $\Delta$ 12 plasmid was amplified and purified using the QIAGEN Miniprep Plasmid Purification kit. DNA sequence analysis was then performed to ensure that the correct mutations were introduced into the mTOR $\beta$  DNA sequence. The mTOR $\gamma$  isoform was constructed from mTOR $\beta$  with a 12-amino acid deletion, in addition to pcDNA3-Flag-mTOR $\alpha$ , which was discussed in chapter 4.

The 12-amino acid deletion in mTOR $\gamma$  lies in the kinase domain, which is located at the COOH-terminus of the DNA sequence of mTOR. mTOR $\beta$  shares the same COOH-terminal as mTOR $\alpha$  and lacks most of the NH<sub>2</sub>-terminus of mTOR. Therefore, the NH<sub>2</sub>-terminus of mTOR $\beta$ , which was cloned as pcDNA3-mTOR $\beta$   $\Delta$ 12, was replaced with the full-length NH<sub>2</sub>-terminal of the wild-type mTOR $\alpha$ . The DNA sequence of the Flag-tag was inserted into the mTOR $\gamma$  DNA sequence at the NH<sub>2</sub>-terminal. This insertion resulted in pcDNA3-Flag-mTOR $\gamma$  plasmid (Figure 5.3).

The pcDNA3-mTOR $\beta$   $\Delta$ 12 plasmid was linearised using the HindIII restriction enzyme. The ends of the linearised plasmid were then blunted using T4 DNA ligase. This linearised and blunted plasmid was subsequently re-digested with the KpnI restriction enzyme to produce two DNA fragments. The small fragment consists of the NH<sub>2</sub>-terminal DNA sequence of mTOR $\beta$   $\Delta$ 12. This fragment was then replaced with the full-length NH<sub>2</sub>-terminus of mTOR $\alpha$  (Figure 5.4). The large fragment consisted of the pcDNA3 nucleotide sequence attached to the nucleotide sequence of COOH-terminus of mTOR with the 12-amino acid deletion. The large fragment was

blunted from its COOH-terminal and possessed the KpnI restriction sequence at its NH<sub>2</sub>-terminal.

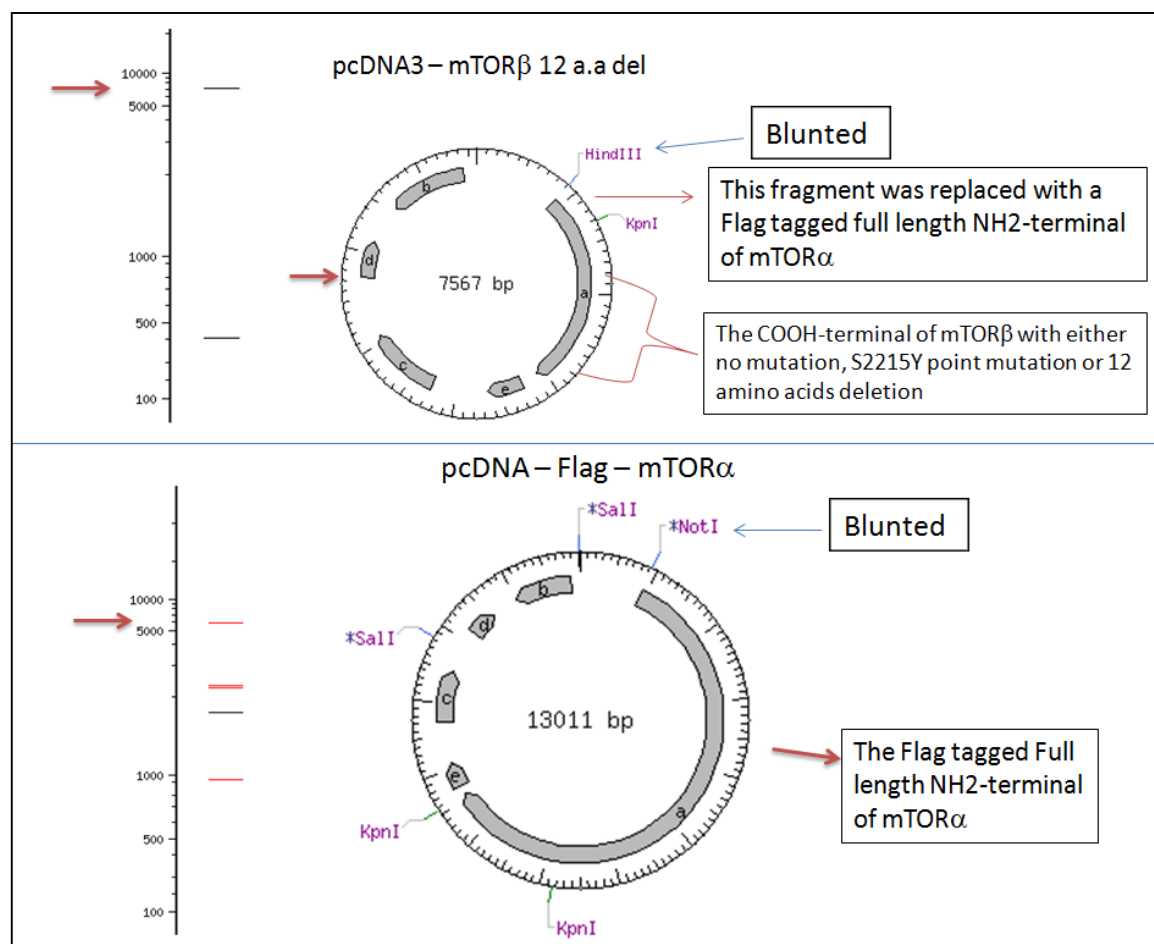


**Figure 5.3: The plan for the construction of the pcDNA3–Flag–mTOR $\gamma$  isoform.**

pcDNA3–mTOR $\beta$   $\Delta$ 12 (top) was linearised using the HindIII restriction enzyme, blunted using T4 DNA ligase and re-digested with KpnI. These digestions resulted in two fragments, a large fragment containing the pcDNA3 plasmid and the COOH-terminus of mTOR (including the 12-amino acid deletion) and a small NH<sub>2</sub>-terminal fragment. pcDNA–Flag–mTOR $\alpha$  (bottom) was linearised using the NotI restriction enzyme, blunted using T4 DNA ligase and re-digested with KpnI and SalI, resulting in the full length NH<sub>2</sub>-terminal fragment of mTOR $\alpha$  blunted from its NH<sub>2</sub>-terminal site and containing the KpnI restriction sequence at its COOH-terminus. This fragment was then ligated to the compatible ends of the pcDNA3 fragment containing the COOH-terminus of mTOR $\gamma$ .

The pcDNA–Flag–mTOR $\alpha$  plasmid was linearised with the NotI restriction enzyme and blunted with T4 DNA ligase. The plasmid was then re–digested with the KpnI restriction enzyme. The resultant NH<sub>2</sub>–terminus of the full–length Flag–mTOR was blunted at its NH<sub>2</sub>-terminus and possessed a KpnI restriction sequence at its COOH–terminal. The pcDNA3 plasmid containing the COOH–terminus of mTOR $\beta$   $\Delta$ 12 was then ligated to the full–length NH<sub>2</sub>–terminus of mTOR $\alpha$  using T4 DNA ligase to generate pcDNA3–Flag–mTOR $\gamma$ .

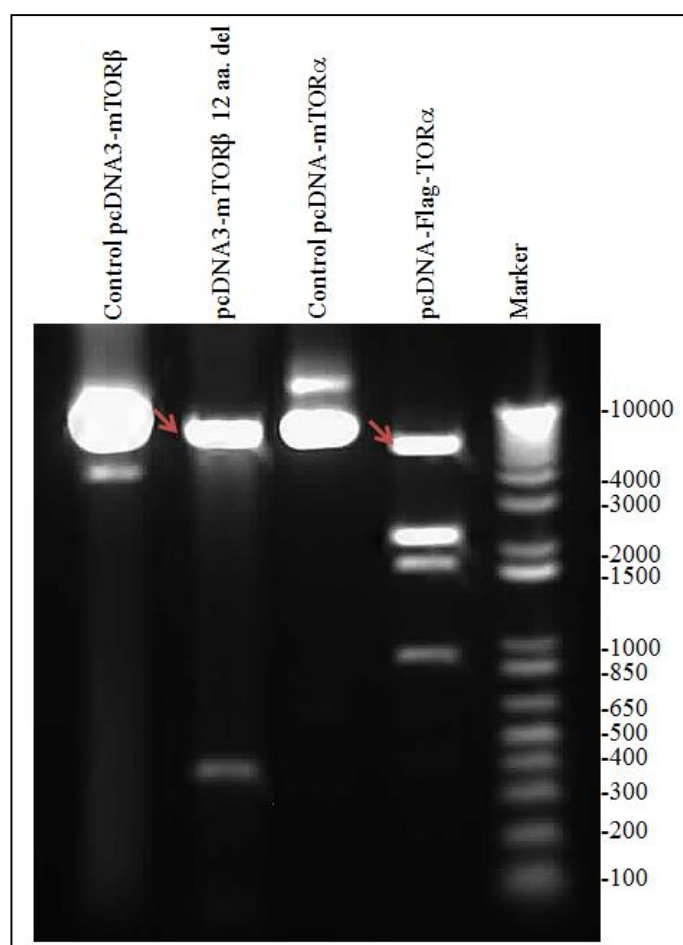


**Figure 5.4:** Agarose gel image of the DNA fragments used for the construction of pcDNA3–Flag–mTOR $\gamma$ .

The pcDNA3–mTOR $\beta$  and pcDNA3–mTOR $\beta$   $\Delta$ 12 plasmids were digested with HindIII and KpnI, and the pcDNA3–Flag–mTOR $\alpha$  plasmid was digested with Sall, KpnI and NotI. The digested plasmids were then electrophoresed on a 0.8% agarose gel, and the NH<sub>2</sub>–terminus of the mutated mTOR $\beta$  plasmids were digested and replaced with the Flag–tagged full–length NH<sub>2</sub>–terminus of mTOR $\alpha$ .

The generated plasmid was transformed into *E.coli*, and 8 colonies were amplified. The amplified colonies were subjected to agarose gel electrophoresis to confirm the size and the quality of the purified plasmids (Figure 5.5).

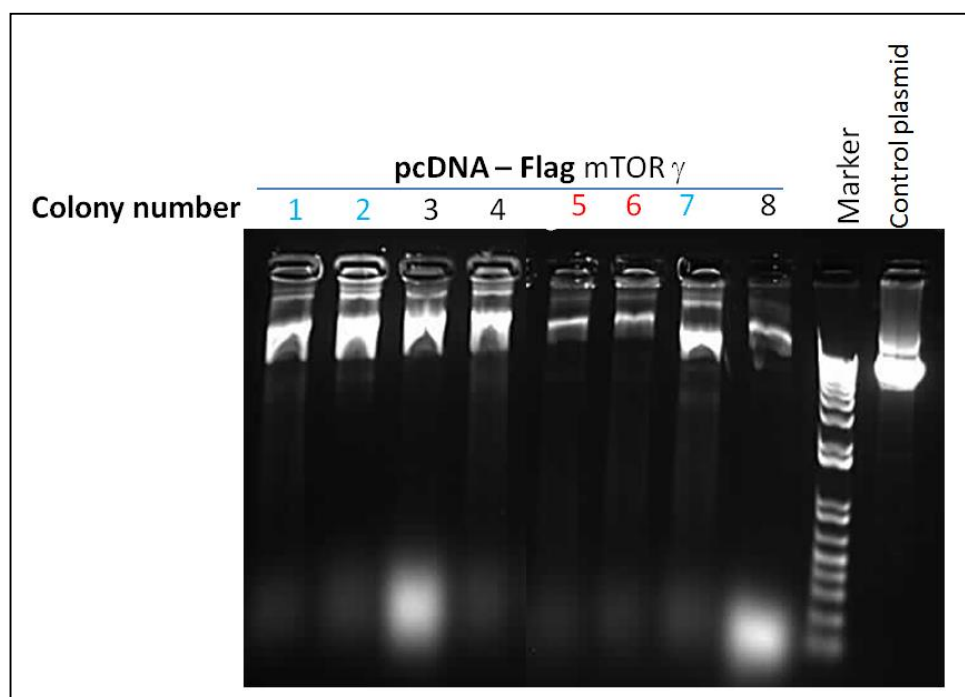


**Figure 5.5: Agarose gel image of the pcDNA3–Flag–mTOR $\gamma$  colonies selected for digestion analysis.**

The generated plasmids were transformed into bacteria and plated in selection media. Eight colonies of each mutant were selected for plasmid purification and tested on 0.8% agarose gel to confirm the size and quality of the purified plasmids. The plasmids were then thoroughly tested by digestion and sequencing analysis.

To verify that the correct DNA sequence was inserted into the plasmid, the generated plasmid was analysed via restriction digestion analysis. The plasmid was digested using the *Hin*1I restriction enzyme and run on 0.8% agarose gel. Digestion of the plasmid containing the insert was expected to produce a band at approximately 1280

bp. The results clearly demonstrated that the colonies in the lanes labelled with blue numbers lacked the desired band (Figure 5.6), whereas all of the colonies in the lanes labelled with red numbers were positive for the desired fragment (Figure 5.7). Therefore, the colonies in the lanes labelled with red numbers were collected and the DNA sequence was verified by sequencing analysis.

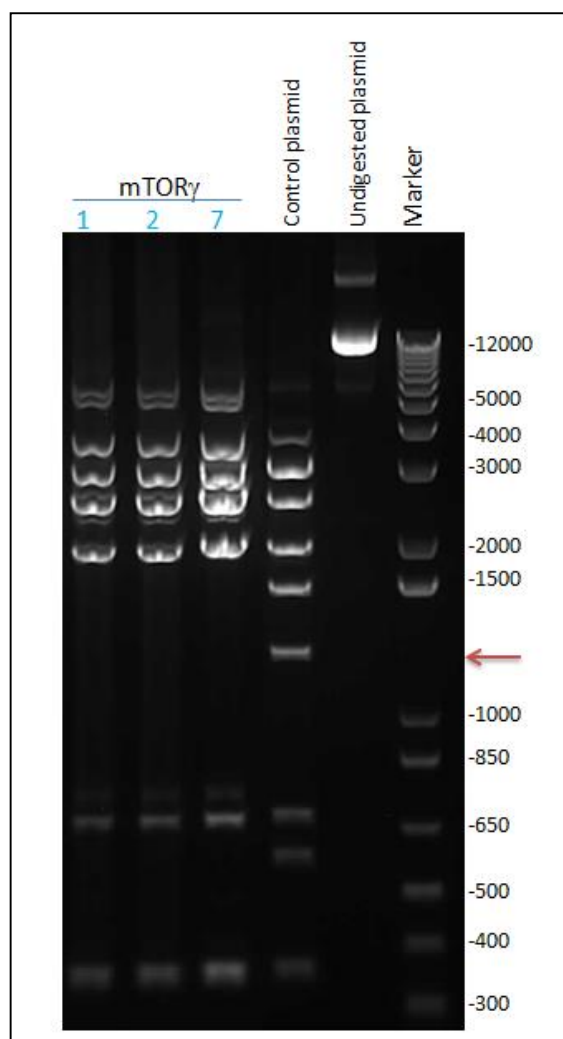


**Figure 5.6: Agarose gel image of the results of the digestion analysis of the constructed pcDNA3–Flag–mTOR $\gamma$  plasmid showing the absence of the insert band (negative result).**

Digestion analysis was performed to verify that the DNA was inserted into the plasmid. The pcDNA3–Flag–mTOR $\gamma$  plasmid was digested using the *Hin*II restriction enzyme and subjected to electrophoresis in 0.8% agarose gel. The absence of a band at approximately 1280 bp indicated that the DNA sequence was not inserted in colony numbers 1, 2 and 7 (labelled with blue numbers).

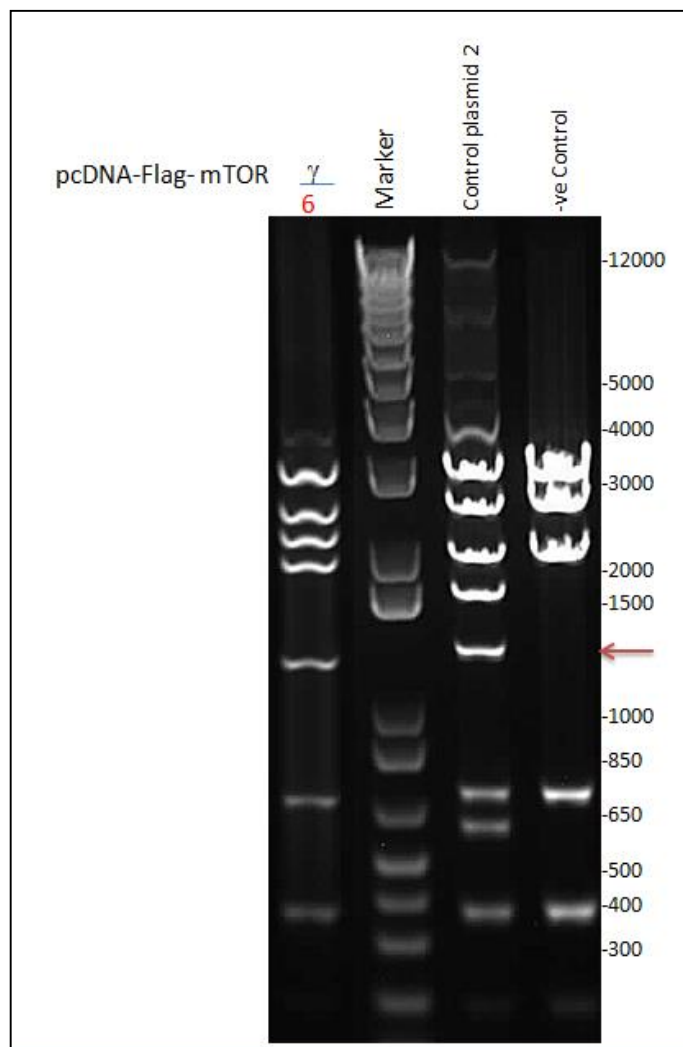


**Figure 5.7:** Agarose gel image of the resultant of the digestion analysis of the constructed pcDNA3-Flag-mTORy plasmid confirming the presence of the insert band. To verify that the DNA sequence was inserted into the plasmid, the plasmids were digested using the Hin1I restriction enzyme and subjected to electrophoresis on 0.8% agarose gel. The presence of a band approximately 1280 bp in size confirmed that the DNA sequence was inserted into the plasmid from the selected colony (indicated with red numbers).

### 5.1.3 DNA sequence analysis of the constructed pcDNA3 – Flag – mTOR $\gamma$ plasmid

Sequence analysis of the constructed plasmid was then performed to verify that the DNA sequence of the NH<sub>2</sub>-terminus had been inserted and that the 12-amino acid DNA sequence was deleted. A sample of the pcDNA3-Flag-mTOR $\gamma$  plasmid was sent to GATC Biotech for DNA sequence analysis. The sequencing results revealed that the DNA sequence was indeed inserted and that the 12-amino acids were deleted. A sequence alignment was performed between the generated mTOR $\gamma$  and mTOR $\alpha$ , and the location of the 12-amino acid deletion is highlighted below (Figure 5.8). This plasmid was then used to generate a stable cell line over-expressing Flag-tagged recombinant mTOR $\gamma$  to further study the mTOR $\gamma$  isoform *in vitro* and *in vivo*.

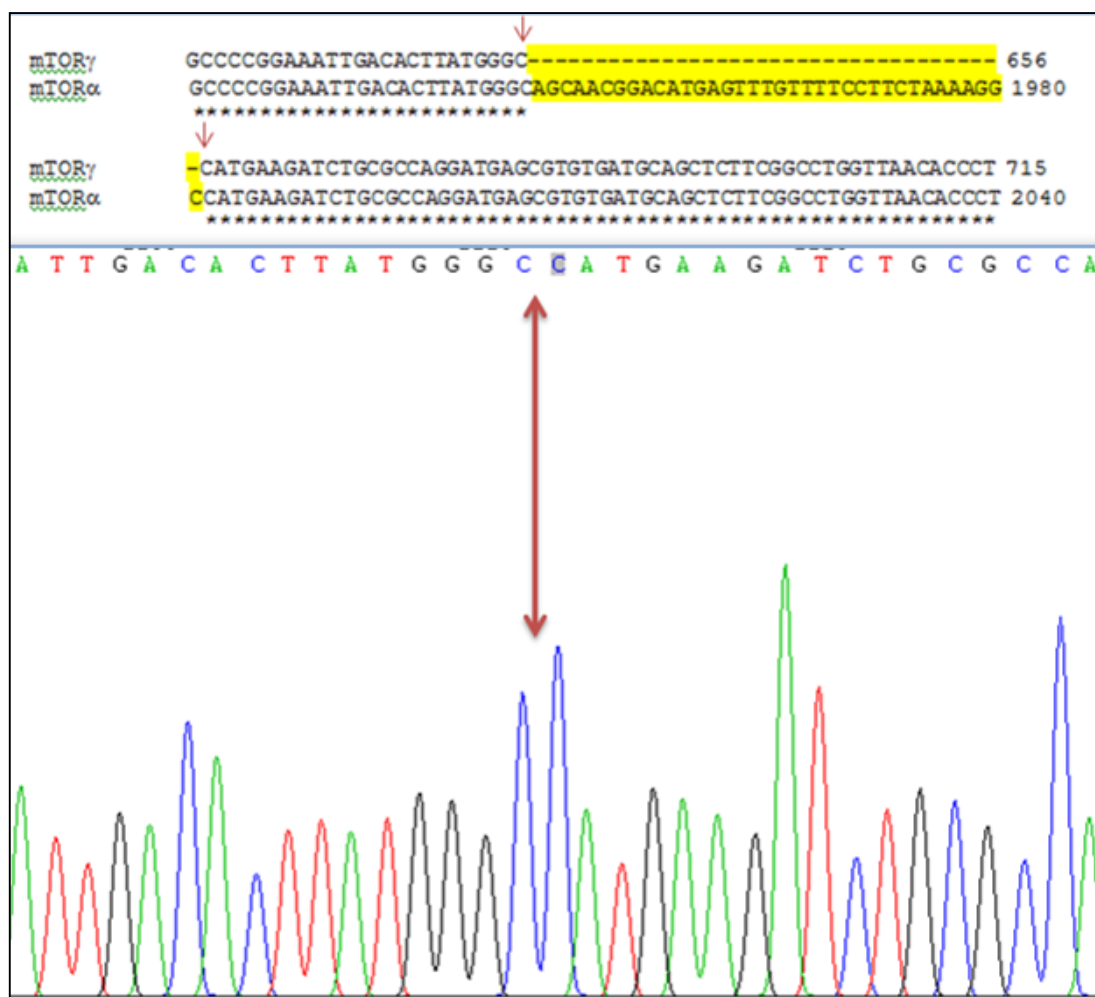


**Figure 5.8: Sequencing analysis of pcDNA3-Flag-mTOR $\gamma$ .**

The obtained sequence is aligned against the mTOR $\alpha$  sequence with the 12 amino acids highlighted (top). The chromatogram shows the sequence indicating the site of the 12-amino acid deletion (Bottom).

#### 5.1.4 Generation of HEK 293T cells stably expressing the mTOR $\gamma$ isoform

To investigate the potential of mTOR $\gamma$  to play a major role in mTOR pathway regulation and mTOR-mediated cellular processes, HEK 293T cells stably expressing the mTOR $\gamma$  isoform were generated. HEK 293T cell lines over-expressing mTOR $\alpha$ , mTOR $\delta$  and mTOR S2215Y, generated in Chapter 4, were used as controls in this study.

As described in section 5.1.2, the mammalian expression vector pcDNA3 was used to generate a construct encoding the Flag-mTOR $\gamma$  isoform. The pcDNA3 construct contains the neomycin resistance gene for the selection of transfected cells using G-418. As noted in chapter four, G-418 was not the best antibiotic for selecting our stock of HEK 293 cells which found to be HEK 293T not HEK 293.

To address the issue of the poor selection achieved using G-418, a new strategy was followed that involved co-transfection with two plasmids with different selection markers: pcDNA3-Flag-mTOR $\gamma$  (G-418) and pcDNA 4/TO (Zeocin). To generate a stable cell line similar to the control cell lines, HEK 293T cells were co-transfected with the pcDNA3-Flag-mTOR $\gamma$  and pcDNA 4/TO plasmids. Due to the presence of the Zeocin resistance gene in pcDNA 4/TO, stable cell lines were selected using Zeocin. The optimum concentration of Zeocin for selection was predetermined (200  $\mu\text{g}/\text{mL}$ ). Cells were treated with the optimum concentration of Zeocin to select co-transfected cells and generate a stable cell line. Twelve days later, single colonies were visible. Five single colonies were isolated and tested for Flag-mTOR $\gamma$  expression. Two colonies demonstrated a sufficient level of recombinant mTOR $\gamma$  expression. One of the single colonies of HEK 293T cells stably expressing the mTOR $\gamma$  isoform was used to study the potential role of mTOR $\gamma$  in the mTOR pathway. Thus, HEK 293T cells stably expressing sufficient levels of mTOR $\gamma$  were successfully generated. To precisely study the effects of the mTOR $\gamma$  isoform, we employed several controls, including HEK 293T cell lines stably expressing Flag-mTOR $\alpha$ , Flag-mTOR $\delta$  and Flag-mTOR S2215Y isoforms. The expression of the mTOR isoforms is shown in Figure 5.9.

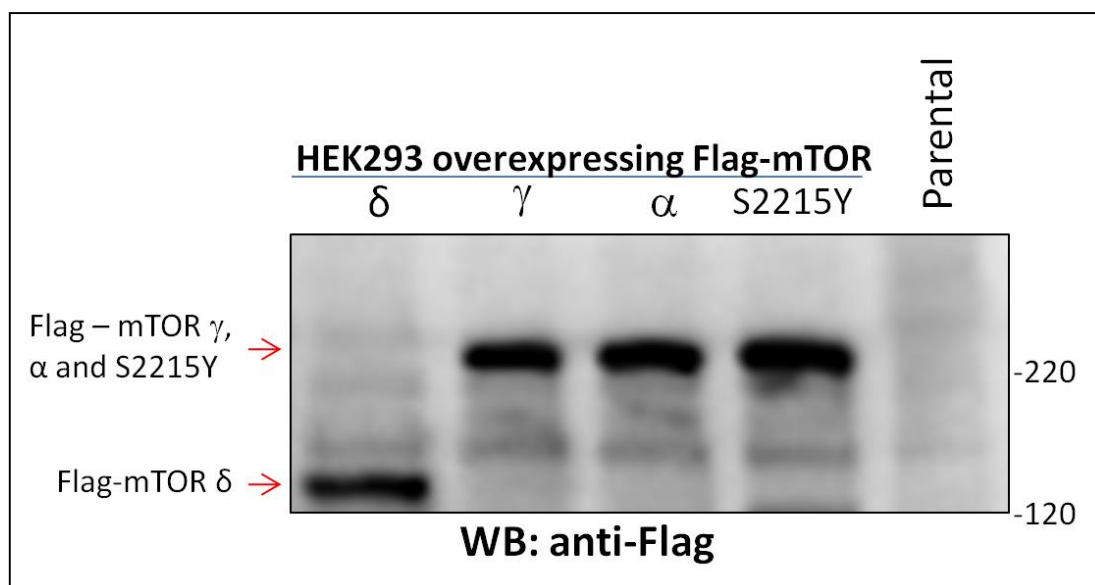


**Figure 5.9: Western blot confirming the high expression of Flag-mTOR $\gamma$  in parallel with the other mTOR isoforms in HEK 293T cell lines.**

HEK 293T cells were transfected with the pcDNA3-Flag-mTOR $\alpha$ ,  $\delta$ ,  $\gamma$  or S2215Y isoform. These cells were then lysed, and the lysates were resolved by SDS-PAGE and subjected to immuno-blotting with an anti-Flag antibody.

The HEK 293T cells over-expressing the mTOR $\gamma$  isoform were then used to investigate the effect of the 12-amino acid deletion on kinase activity using an *in vitro* kinase assay, in addition to the effect of mTOR $\gamma$  in the regulation of the mTOR pathway and the role of the mTOR $\gamma$  splicing isoform in mTOR-mediated cellular processes. Finally, the stable cell lines were used to elucidate whether mTOR $\gamma$  over-expression induces oncogenic effects or antagonises the oncogenic characteristics of the mTOR signalling pathway. A tumorigenicity analysis was performed based on a colony formation assay and the results will be further validated using a xenograft model in nude mice (still in progress).

## 5.2 Functional Analysis

It is well known that mTOR regulates cellular growth, proliferation and survival through its catalytic activity and the phosphorylation of Akt, S6K and 4EBP1 (Edinger & Thompson 2002;Guertin et al. 2006;Vivanco & Sawyers 2002). As the 12-amino acid deletion in the mTOR $\gamma$  splice isoform is located within the kinase domain, this deletion may affect the kinase activity and, consequently, mTOR-mediated cell growth, survival and proliferation.

The main focus about mTOR $\gamma$  was to determine whether this deletion affects the regulation of mTOR and to determine its ability to phosphorylate known physiological substrates of mTOR. In addition, we were interested in elucidating whether mTOR $\gamma$  over-expression would affect tumorigenesis mediated by the mTOR signalling pathway. We explored these questions by examining *in vitro* mTOR $\gamma$  kinase activity and by studying the effect of the over-expression of mTOR $\gamma$  on cellular proliferation using an MTT proliferation assay. The overall oncogenic potential was assessed via colony formation assays and xenograft model in nude mice (in progress).

To perform the mentioned experiments and analyses, mammalian expression vectors containing Flag-mTOR sequences for different isoforms, including mTOR $\alpha$ , mTOR $\delta$ , mTOR $\gamma$  and mTOR S2215Y were generated and confirmed through restriction and sequencing analysis. HEK 293T cells were transfected with each of the constructs individually. HEK 293T cells stably expressing mTOR $\delta$ , mTOR $\alpha$ , mTOR $\gamma$  and mTOR S2215Y were generated. A sufficient level of expression of these mTOR isoforms was confirmed through Western blot analysis.

### 5.2.1 mTOR kinase assay

The mTOR protein is a serine/threonine protein kinase that can only function in two intact complexes. mTORC1 is activated by growth factors and nutrients such as amino acids, glucose and energy. Activated mTORC1 phosphorylates S6K1 and 4E-BP1 and thereby, modulates protein synthesis and cellular growth directly (Hay & Sonenberg 2004; Ma & Blenis 2009; Richter & Sonenberg 2005). In response to growth factors, mTORC2 phosphorylates and activates Akt/PKB, SGK1 and PKC, thereby regulating cellular survival and proliferation. Akt plays a critical role in multiple cellular processes, including glucose metabolism, apoptosis, cell proliferation, transcription and cell migration (Frias et al. 2006; Guertin & Sabatini 2007; Hresko & Mueckler 2005; Lee et al. 2005; Yang et al. 2006).

To investigate the kinase activity of mTOR $\gamma$ , an *in vitro* kinase assay was performed. In this experiment, the main goal was to assess the catalytic activity of the immunopurified mTOR complex from HEK 293T cells overexpressing mTOR $\gamma$  relative to the control group. As mentioned previously, for the *in vitro* experiments, the control group consisted of HEK 293T cells overexpressing Flag-mTOR S2215Y and HEK 293T cells overexpressing Flag-mTOR $\alpha$  as positive controls, whereas cells overexpressing Flag-mTOR $\delta$  were used as a negative control. HEK 293T cells were plated in two 100 mm plates. Once a suitable confluency was reached (approximately 70-80%), the cells were lysed, and the Flag-mTOR complexes for each isoform were immunoprecipitated using anti-Flag antibodies. Each immunoprecipitation product was mixed with the mTORC1 substrate 4E-BP1, and the kinase reaction was

performed. The kinase activity in the reaction mixture was then assessed according to the phosphorylation of specific sites on 4E-BP1 via western blotting with a phospho-specific (Thr)37/p(Thr)46 antibody. A clear immuno-reactive band was observed for mTOR $\alpha$  and mTOR S2215Y. In contrast, the mTOR $\gamma$  reaction, similar to mTOR $\delta$ , did not exhibit any band for phospho-4E-BP1.

These results clearly indicate that in contrast to the full-length mTOR $\alpha$  and mTOR S2215Y, the mTOR $\gamma$  splicing isoform was unable to phosphorylate the mTOR target 4E-BP1 (Figure 5.10). The phosphorylation level of Thr 37/Thr 46 in 4E-BP1 was increased in the activated mTOR S2215Y mutant compared with mTOR $\alpha$ , whereas mTOR $\delta$  and mTOR $\gamma$  were unable to phosphorylate 4E-BP1. In conclusion, these results suggest that the mTOR $\gamma$  isoform does not function through mTORC1.

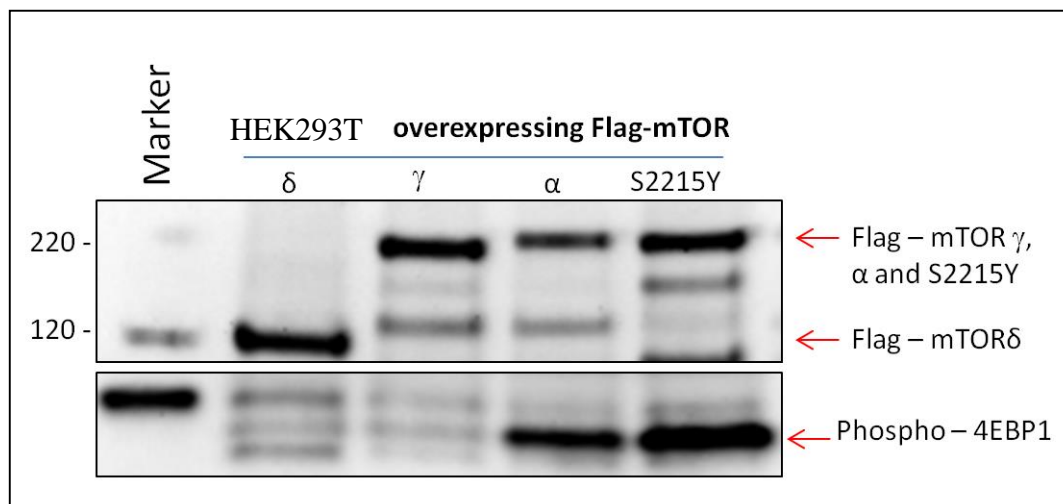


**Figure 5.10: *In vitro* kinase assay for mTOR $\gamma$ .**

Western blot analysis of the *in vitro* kinase activity of immuno-precipitated Flag-mTOR from the lysates of HEK 293T cells over-expressing different isoforms of Flag-mTOR. 4E-BP1, an mTOR complex 1 substrate, was added together with ATP to the IP mTOR complexes, followed by probing with anti-p-4E-BP1 (n=5, independent experiments).

### 5.2.2 MTT assay – cell proliferation assay

The catalytic activity of mTOR controls cellular proliferation via the phosphorylation of S6K1, 4E-BP1 and Akt. Akt plays a major role in cellular growth and survival (Edinger & Thompson 2002;Guertin et al. 2002). 4E-BP1 and S6K1 promote protein synthesis, ribosome biogenesis and autophagy (Hara et al. 2002;Kim et al. 2002;Kim et al. 2003;Ruggero & Pandolfi 2003). S6K1 generates a negative feedback loop to suppress PI3K activity, which leads to reduced survival signals and inhibits the pro-apoptotic protein BAD (Harada et al. 2001). Thus, the mTOR signalling pathway is one of the main regulators of cellular growth, survival and proliferation.

To assess the effect of mTOR $\gamma$  on cell proliferation, the MTT cell proliferation assay was performed. The MTT cell proliferation assay can be used to detect and measure the cytostatic properties of various substances that could change the cellular status from proliferation to quiescence. Because mTOR is a central regulator of cell proliferation, this method provides remarkable results. The absorbance of a pigmented product resulting from the reduction of MTT upon incubation with viable cells is correlated with decreases in cell viability due to destructive processes such as necrosis or apoptosis. The MTT proliferation assay was used to assess the cell viability of HEK 293T cell lines stably expressing mTOR $\gamma$  in comparison with the parental HEK 293T cell line (control) under starvation conditions. Starvation conditions were also utilised to minimise the effect of endogenous mTOR.

For the MTT assay, 5000 HEK 293T cells stably expressing the mTOR $\gamma$ , mTOR $\alpha$  and mTOR S2215Y isoforms were seeded into each well in 96-well plates. Once the cells reached 70% confluence, they were subjected to starvation conditions. Proliferation was assessed 2 days after starvation and these assessments were repeated daily for the following 4 days. MTT dye was added to the wells and the plates were incubated at 37 °C for 3 hours in the dark. The optical density was then measured at 490 nm. The obtained absorbance was normalised to the blank, which contained medium and MTT, but no cells.

The MTT assay produced a survival curve demonstrating the higher proliferation potential of parental cells compared with cells over-expressing mTOR $\gamma$ . After 72 hours, the proliferation of cells over-expressing the mTOR $\gamma$  isoform was significantly inhibited relative to the parental HEK 293T cells ( $P < 0.05$ ) (Figure 5.11).

As mentioned previously, the mTOR pathway plays an important role in cellular proliferation. The results presented here suggest that mTOR $\gamma$  is a negative regulator of cellular proliferation.

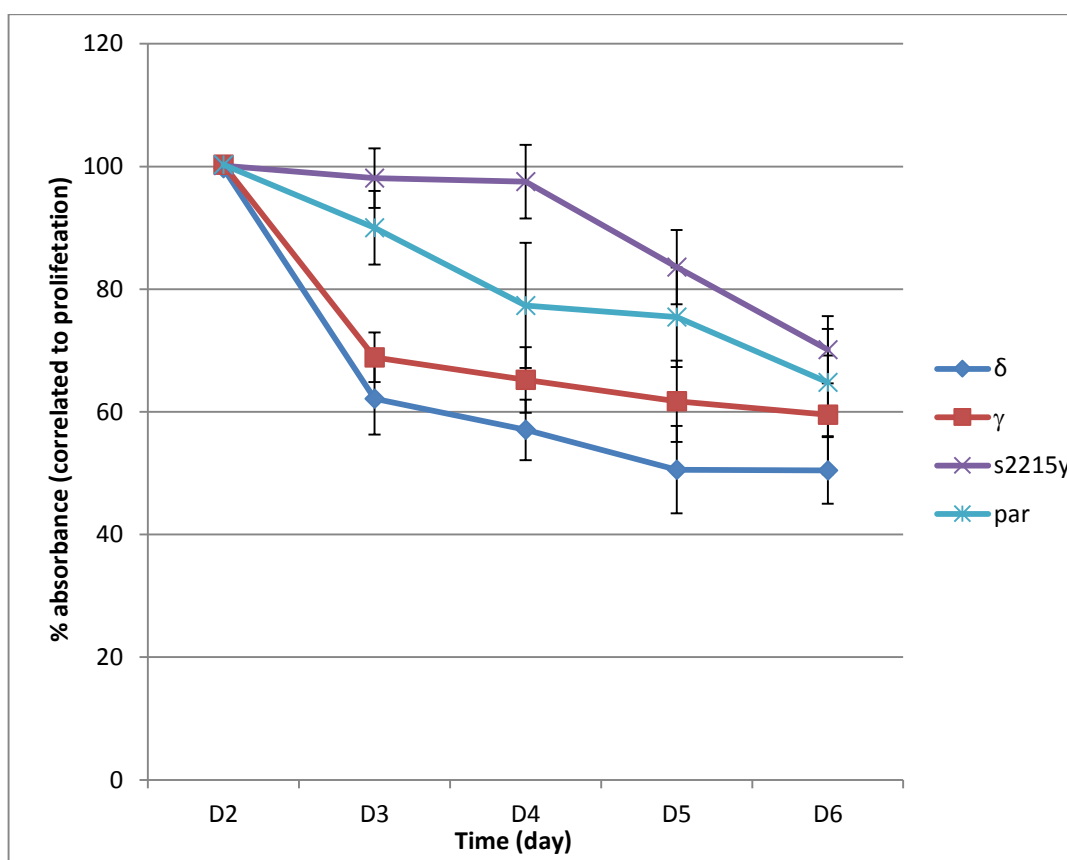


**Figure 5.11: mTOR $\gamma$  negatively regulates cellular proliferation.**

The parental HEK 293T cells and cells over-expressing mTOR $\gamma$ , TOR $\alpha$ , mTOR S2215Y were seeded into 96-well plates. The same number of cells was seeded per well, and once the cells reached approximately 70% confluence, they were subjected to serum starvation. After 48 hours of starvation, the CellTiter 96 One Solution reagent was added, followed by incubation for 3 hours, and after which the absorption was measured. Measurements of cell activity were performed two days after starvation and repeated daily for the following 4 days (MTT proliferation assay). Each point represents the mean  $\pm$  SEM from three individual experiments. The results are normalised to the blank which contained medium and MTT, but no cells. (n=3, independent experiments).

### 5.2.3 Colony formation assay

Cancerous transformation is the result of various alterations of genetic and epigenetic mechanisms. These oncogenic processes lead to a cell population that has the capacity to grow and proliferate in an individualised manner. These new cell properties lead to the phenomenon of cell immortality. Cancerous cells are able to grow under harsh conditions. A common method used to detect, monitor and measure cell proliferation under the harsh conditions associated with cancer is the assay based on colony development in soft agar.

The mTOR protein is implicated in tumour progression (Graff & Zimmer 2003). Previous results have demonstrated that the 12–amino acid deletion in mTOR $\gamma$  removes the kinase activity of this particular isoform *in vitro*. The MTT proliferation assay also demonstrated mTOR $\gamma$  in HEK 293T cells negative regulates cellular proliferation. These finding suggested that the mTOR $\gamma$  would have a negative effect on tumour progression. In this study, we used colony formation assays to elucidate the overall effect of the mTOR $\gamma$  protein expression on cellular tumourigenicity.

In this study, an *in vitro* model was employed, including parental HEK 293T cells and HEK 293T cells over-expressing mTOR $\gamma$ , mTOR $\alpha$  or mTOR S2215Y. Using 6-well plates, 2,000 or 4,000 cells were seeded in 3 ml of 0.3% soft agar. To allow the agar to solidify, the plates were left in the hood for approximately 15 minutes, followed by incubation at 37 °C. After two weeks, colonies were stained with 0.005% crystal violet for 3 hours at 37 °C and photographed. The number of colonies that were able to proliferate was counted. Here, we provide the results as the fold

increase or decrease in comparison with the colonies generated by parental HEK 293T cells. Figure 5.12 shows that there was a four-fold increase in the number of colonies generated by parental HEK 293T cells compared with cells over-expressing mTOR $\gamma$ . The number of colonies generated from HEK 293T cells over-expressing mTOR $\alpha$  was significantly lower than the number of colonies generated by the parental HEK 293T cells ( $p < 0.05$ ).

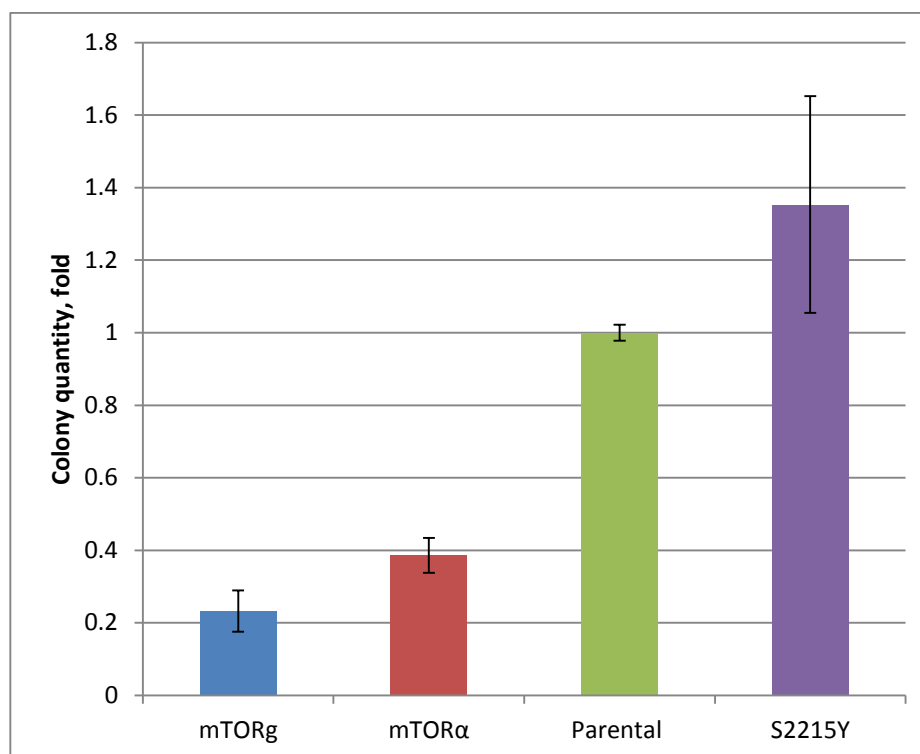
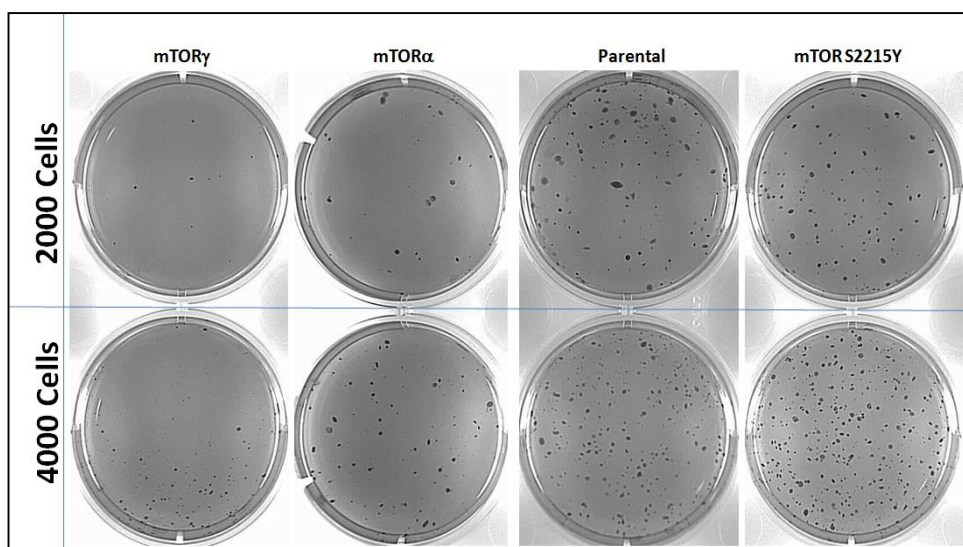


**Figure 5.12: mTOR $\gamma$  down-regulates the anchorage-independent growth of HEK 293T in soft agar.**

Parental HEK 293T cells or HEK 293T cells stably expressing mTOR $\gamma$ , mTOR $\alpha$  or mTOR S2215Y were plated in a thin layer of agarose in culture medium. Two weeks later, colonies were stained with 0.005% crystal violet, photographed and counted. Data are presented as the means  $\pm$ SEM of five experiments (n=5). The results were converted to the fold increase or decrease in relative to the number of colonies generated by the parental HEK 293T cells. The parental HEK 293T cells displayed a four-fold increase in the number of colonies produced relative to mTOR $\gamma$ .

#### 5.2.4 Discussion and conclusions

The initial aim of this study was to identify novel mTOR splicing isoforms. Protein, molecular and bioinformatics approaches led to the isolation of cDNA clones encoding the novel mTOR isoforms, mTOR $\delta$  and mTOR $\gamma$ . mTOR $\delta$  lacks the FRB and kinase domains, whereas mTOR $\gamma$  exhibits a 12–amino acid deletion in the kinase domain. The results presented in this chapter demonstrate the molecular characteristics of mTOR $\gamma$  and revealed some of its potential in cellular functions.

The full coding sequence of mTOR $\gamma$  was successfully cloned into the pcDNA3 vector, with a Flag–tag positioned at the N-terminus of this isoform. The construct was confirmed by digestion and sequencing analysis. Using the generated constructs, HEK 293T stable cell lines were generated. The expression of the fusion proteins in HEK 293T cells was also confirmed by Western blotting analysis. Immuno–precipitation with Protein G beads coated with the anti–Flag antibody resulted in copious amounts of protein that could be detected by western blotting.

The 12–amino acid deletion in mTOR $\gamma$  is located in the kinase domain. Therefore, the catalytic activity of this isoform was predicted to be affected by this deletion. This result prompted us to test whether mTOR $\gamma$  is able to phosphorylate a known substrate of mTOR $\alpha$ , 4E-BP1, *in vitro*. The *in vitro* kinase assay demonstrated that, in contrast to mTOR $\alpha$  and mTOR $\beta$ , mTOR $\gamma$  is incapable of phosphorylating the mTORC1 target 4E-BP1.

Many groups have reported that mTOR is a major player in the regulation of cellular growth, survival and proliferation (Corradetti & Guan 2006; Hay & Sonenberg 2004). Because mTOR $\gamma$  lacks the catalytic activity, we hypothesised that the level of

mTOR $\gamma$  protein expression could affect the proliferative activity of the HEK 293T cell line. The MTT assay indicated that, after 72 hours of starvation the proliferation of HEK 293T cells was significantly different between the cells over-expressing mTOR $\gamma$  and the control group, consisting of parental HEK 293T cells. In contrast, Panasyuk et al. (2009) found that the proliferation of HEK 293T cells over-expressing mTOR $\beta$  was significantly higher compared with parental cells.

The fact that the enhanced proliferative potential of HEK 293T cells over-expressing mTOR $\beta$  was associated with an enhanced oncogenic potentials led us to ask whether the reduced proliferative potential of HEK 293T over-expressing mTOR $\gamma$  will associate with less oncogenic potentials. A colony formation assay revealed about 4-fold increase in the number of colonies generated from parental HEK 293T cells compared to HEK 293T cells over-expressing mTOR $\gamma$ . These results suggested that over-expression of mTOR $\gamma$  in HEK 293T cells leads to anti-oncogenic potential.

A possible explanation for the effect of mTOR $\gamma$  is that, the deletion present in this isoform inhibits its catalytic activity by either removing an essential part of the kinase domain or leading to conformational changes that affect the formation of both mTOR complexes. The future directions of studies on mTOR $\gamma$  will be discussed in Chapter 6.

# **CHAPTER 6**

## **Discussion, Conclusion and future direction**

## Chapter 6: Discussion

---

### 6.1 mTOR protein

The mammalian Target of Rapamycin, recently given an official name of mechanistic target of rapamycin is an evolutionarily conserved serine/threonine protein kinase. mTOR is a large protein consisting of 2,549 amino acids, composed of multiple highly conserved domains, including the HEAT repeats, FATN, FRB, RD, kinase and FATC domains. The mTOR protein localised on the mitochondria, nucleus, Golgi, endoplasmic reticulum and predominantly, the cytosol (Desai et al. 2002;Drenan et al. 2004;Liu and Zheng 2007;Sabatini et al. 1999;Tirado et al. 2003;Withers et al. 1997).

The mTOR protein plays a critical role in the regulation of cellular processes, such as cellular growth, proliferation, cytoskeletal organisation, survival, RNA transcription and protein synthesis (Corradetti and Guan 2006;Hay and Sonenberg 2004). Dysregulation of the mTOR pathway is implicated in many disorders, including cancer, diabetes and cardiac hypertrophy (Beevers et al. 2006;Schaeffer and Abrass 2010;Young and Nickerson-Nutter 2005).

Extracellular and intracellular effectors including insulin, growth factors, and amino acids activate mTOR and enhance its activity (Hay & Sonenberg 2004). This enhanced mTOR activity is implicated in multiple disorders including, tumour progression. mTOR phosphorylates S6K1, Akt and 4E-BP1, thereby promoting cell growth, survival and proliferation (Edinger and Thompson 2002;Guertin et al.

2006;Hara et al. 2002;Kim et al. 2002;Kim et al. 2003;Ruggero and Pandolfi 2003;Vivanco and Sawyers 2002). The enhanced mTOR activity significantly shortens the cell cycle and stimulates cellular growth (Corradetti & Guan 2006;Hay & Sonenberg 2004;Obaya et al. 1999). Activated mTOR also increases protein synthesis, which is required for tumour growth and development (Hay & Sonenberg 2004). These features make mTOR an attractive target for cancer therapy. mTOR inhibitors exhibit a potent anti-proliferative activity against a broad panel of tumour cell lines (Fasolo and Sessa 2011). mTOR inhibitors are currently being evaluated in clinical trials for the treatment of various cancers (Barnett 2012).

In cells, mTOR can only function in two distinct complexes known as mTORC1 and mTORC2 (Hay & Sonenberg 2004;Ma and Blenis 2009;Richter and Sonenberg 2005). Some of the partners involved in the mTOR complexes, such as raptor and rictor, are essential for mTOR activity, whereas the absence of other partners has no effect on the mTOR function (Hara et al. 2002;Kim et al. 2002;Sancak et al. 2007).

In humans, the mTOR gene encodes two mTOR isoforms, the full-length mTOR $\alpha$  form and the short mTOR $\beta$  form. mTOR $\beta$  was identified in the Gouts' laboratory. mTOR $\beta$  lacks the majority of the HEAT repeat and FATN domains. In vivo, mTOR $\beta$  forms complexes with the substrate-presenting proteins raptor and rictor. In vitro, mTOR $\beta$  has been shown to phosphorylate the same substrates as originally reported for the full length mTOR $\alpha$ , including S6K1, PKB/AKT and 4EBP1. Over-expression of mTOR $\beta$  accelerates cell cycle progression and stimulates cellular proliferation. In addition, mTOR $\beta$  over-expression transforms immortal cells and causes tumour formation in nude mice. It is thought that modulation of cell proliferation via the mTOR signalling pathway could be achieved through mTOR $\beta$ . Because mTOR $\beta$  is a

proto-oncogene, it can be considered a potential target for anti-cancer therapies (Panasyuk et al. 2009).

Early studies in the field of cancer research focussed on genetic changes, including mutations, translocations, and over-expression etc. that are associated with malignancy and contribute to cancer development. Recent studies have revealed an increasing role of epigenetic changes in cancer development. These epigenetic changes include alterations that lead to the regulated production of different splicing isoforms of RNA. These changes in gene activity that are not caused by changes in the DNA sequence result in a single gene encoding for multiple proteins. These discoveries have added a new direction for future researches in the field of cancer research and drug development.(Bonnal et al. 2012;Kim et al. 2008;Singh and Cooper 2012;Warzecha and Carstens 2012).

Recent studies have revealed that alternative splicing and splicing regulators can regulate the tumorigenesis. Dysregulation of splicing regulators, including SF3B1 and SRSF6 is implicated in several types of cancer (Cohen-Eliav et al. 2013a;Golan-Gerstl et al. 2011a;Harbour et al. 2013;Kulis et al. 2012;Papaemmanuil et al. 2011;Quesada et al. 2012). In addition, many studies have reported that a number of tumour suppressors and oncogenes are modulated by alternative splicing (Cohen-Eliav et al. 2013b;Golan-Gerstl et al. 2011b;Jia et al. 2010;Venables 2006;Venables et al. 2009).

Additionally, it has recently been shown that splicing factors can play an oncogenic role in cells (Golan-Gerstl et al. 2011a;Lefave et al. 2011;Siegfried et al. 2013). The splicing factor SF2/ASF controls the alternative splicing of several onco-proteins including the oncogenic form of the mTOR target, S6K1. In addition, cells

transfected with the splicing factor SF2/ASF demonstrated high mTOR activity. Inhibition of mTOR activity blocks cellular transformation by SF2/ASF *in vitro* and *in vivo*. These results suggest that mTOR is a splicing target of SF2/ASF (Karni et al. 2007;Karni et al. 2008).

In a recent study, Huot et al. demonstrated that the splicing factor Sam68 regulates the alternative splicing of mTOR, and cells from Sam68<sup>-/-</sup> mice exhibit reduced levels of mTOR mRNA and reduced activity of the mTOR pathway. Within the mTOR gene, Sam68 binds specifically to intron splicing elements (ISEs) which is located at exon 5/intron 5 boundary leading to alternative termination. This binding results in the production of two mTOR isoforms of approximately 8 kb and 1 kb in various mouse tissues including white adipose tissue, the brain, and testis (Huot et al. 2012).

The most common barriers to the approval of an efficient drug by pharmaceutical companies and making it available in the market are poor response rate, poor sensitivity, high toxicity and side effects (Gomez-Martin et al. 2012). In the case of targeting a specific protein for the treatment of a disease, alternative splicing isoforms can contribute to the sensitivity, resistance and toxicity. In a splicing isoform, skipping exons or frame-shifts in a nucleotide sequence may lead to deletion of the drug-binding site which may give rise to the development of drug resistance. Moreover, a better understanding of the regulation of signalling pathways involved in tumour progression through the alternative splicing of components of these pathways may enhance the therapeutic potential and aid in the selection of drugs or combinations of drugs for cancer treatment in the clinic.

Within the mTOR pathway, the identification of alternative splicing isoforms of mTOR or mTOR substrates improves our understanding of mTOR pathway regulation and the sensitivity to mTOR inhibitors and further directs the selection of drugs for the treatment of cancer in the clinical setting. Selecting a common target sequence to inhibit all of the active isoforms enhances the sensitivity of an inhibitor, consequently permitting the usage of lower concentration with better efficacy and eventually less toxicity and fewer side effects.

In this study, we provide evidence of the existence of two novel mTOR splicing isoforms termed mTOR $\delta$  and mTOR $\gamma$  and their potential role in the regulation of the mTOR pathway.

## 6.2 Discussion

mTOR $\alpha$  consists of 2,549 amino acids, whereas mTOR $\gamma$  and mTOR $\delta$  isoforms, consists of 2,537 and 1,404 amino acids. The predicted molecular weights of the mTOR isoforms are 289, 287 and 158 kDa respectively. In contrast to wild-type mTOR $\alpha$ , mTOR $\gamma$  exhibits 12–amino acid deletion that removes the entire beta 5 strand from the catalytic domain. The beta 5 strand contains the Lys2187 residue which is critical for the catalytic activity of mTOR (Sturgill and Hall 2009).

mTOR $\delta$  is a novel mTOR splicing isoform generated by a frame–shift in the middle of the FAT domain, resulting in a novel amino acid sequence at its COOH–terminus and termination at a premature stop codon. The mTOR $\delta$  protein lacks a part of the FAT, FRB, kinase and FAT at the COOH–terminal domains, but retains the HEAT repeats. Therefore the mTOR $\delta$  isoform lacks the catalytic activity and cannot bind to the inhibitory FKBP12/Rapamycin complex. An antibody targeting the new sequence

at the COOH-terminus of mTOR $\delta$  was generated and the existence of the mTOR $\delta$  isoform *in vivo* was confirmed in the cell lysates of several cell lines by Western blot analysis.

The cDNA sequences of mTOR $\delta$  and mTOR $\gamma$  were cloned into the pcDNA3 mammalian expression vector. These constructs were used to produce Flag-tagged recombinant proteins and for the generation of HEK 293T cell lines stably expressing either the mTOR $\delta$  or mTOR $\gamma$ . The stable cell lines were then used to characterise the role of mTOR $\delta$  and mTOR $\gamma$  *in vitro* and *in vivo*.

The mTOR protein is the catalytic member of two mTOR complexes and this catalytic activity is the only activity of mTOR identified to date (Hay & Sonenberg 2004; Ma & Blenis 2009). mTOR phosphorylates several substrate proteins and among the best characterised mTOR substrates is the 4E-BP1, which regulates the protein synthesis by controlling the translation initiation process (Hay & Sonenberg 2004). This prompted us to investigate the catalytic activity of the mTOR $\gamma$ . *In vitro* kinase assay was performed to assess the phosphorylation status of 4E-BP1 protein when exposed to the mTOR $\gamma$  in the presence of ATP. The results indicated that, in contrast to mTOR $\alpha$  and mTOR $\beta$ , the mTOR $\gamma$  does not phosphorylate the 4E-BP1.

The defective catalytic activity of mTOR $\gamma$  caused by the 12-amino acid deletion can be explained by two hypotheses. First, it is possible that the 12 amino acid deletion removes an essential part for the kinase domain. This hypothesis is consistent with the finding of (Sturgill & Hall 2009) which indicates that the Lys2187 residue located within the deleted fragment is critical for the kinase activity of mTOR.

The second hypothesis is that the 12 amino acid deletion leads to significant conformational changes, resulting in an isoform that is incapable of forming intact

complexes with the essential mTOR regulators, raptor and rictor. The first hypothesis appears to be more realistic and is supported by the finding of Sturgill and Hall. The second hypothesis is weaker since the mTOR $\delta$  splicing isoform lack the majority of its COOH-terminal and retains the NH<sub>2</sub>-terminal and mTOR $\gamma$  shares the same NH<sub>2</sub>-terminal as mTOR $\alpha$ . Therefore the second hypothesis is contradicts the fact that raptor protein binds preferentially to the NH<sub>2</sub>-terminal region of mTOR and with a weaker affinity to the COOH-terminal of mTOR (Hara et al. 2002;Kim et al. 2002;Sancak et al. 2008). However, mTOR $\beta$  lacks the majority of its NH<sub>2</sub>-terminal sequence and still can form intact complexes with raptor, rictor and mLST8 *in vitro* and *in vivo* (Panasyuk et al. 2009).

mTOR integrates multiple intracellular and extracellular signals to regulate cell growth, survival, proliferation and the cell cycle via the phosphorylation of S6K1, Akt and 4E-BP1 (Harada et al. 2001;Hay & Sonenberg 2004;Ma & Blenis 2009). Over-activation of mTOR significantly shortens the cell cycle and stimulates cellular growth (Corradetti & Guan 2006;Obaya et al. 1999). mTOR inhibitors have shown a potent anti-proliferative activity against a broad panel of tumour cell lines (Fasolo & Sessa 2011). Because both the mTOR $\delta$  and mTOR $\gamma$  isoforms lack the catalytic activity, we hypothesise that the mTOR $\delta$  and mTOR $\gamma$  act as negative regulators of mTOR by sequestering the mTOR-associated proteins of mTORC1 and mTORC2. This prompted us to assess the effect of the over-expression of mTOR $\delta$  and the mTOR $\gamma$  on the proliferation of HEK 293T cell lines in comparison with parental HEK 293T cells. The parental HEK 293T cells exhibited a higher proliferative potential compared with HEK 293T cells over-expressing mTOR $\delta$  or mTOR $\gamma$ . Thus, these results suggest that the mTOR $\delta$  and mTOR $\gamma$  function as dominant negative regulators of cell proliferation. In contrast, Panasyuk et al. (2009) reported that the

mTOR $\beta$  is an active protein kinase and the proliferation of cells over-expressing the mTOR $\beta$  was found to be significantly higher compared with parental cells.

The ability of over-expressed mTOR $\delta$  and mTOR $\gamma$  to significantly inhibit cell proliferation led us to assess the oncogenic potential of these isoforms. Colony formation assays revealed a significant increase in the number of colonies generated from parental HEK 293T cells in comparison with HEK 293T cells over-expressing mTOR $\delta$  or mTOR $\gamma$ . These results strongly suggested that the mTOR $\delta$  and mTOR $\gamma$  inhibit the oncogenic potential of transformed cells.

In contrast to mTOR $\beta$ , which is an active protein kinase that triggers downstream signalling and is associated with the enhanced proliferation and proto-oncogenic transformation, mTOR $\delta$  and mTOR $\gamma$  lack the catalytic activity and act as dominant negative regulators of proliferation and possess anti-oncogenic characteristics (Panasyuk et al. 2009). Consistent with the finding of Panasyuk et.al, the number of colonies generated by parental HEK 293T cells was significantly greater compared to the number generated by HEK 293T cells over-expressing mTOR $\alpha$ .

Panasyuk et.al also reported that HEK 293T cells over-expressing mTOR $\alpha$  did not display any significant characteristics associated with oncogenic transformation. Cells over-expressing mTOR $\alpha$  failed to generate either significant anchorage-independent colonies in soft agar culture and were incapable of forming tumours in immuno-suppressed mice *in vivo* (Panasyuk et al. 2009).

Our results support the hypothesis which says that the identification of epigenetic changes and in particular the identification of new alternative splicing isoforms is

essential to better understand the regulation of the mTOR pathway and to make better choices of drugs which exhibit a greater activity and the best therapeutic window.

Furthermore, the diagnostic and therapeutic potentials by the regulation of signaling pathways using alternative splicing of components of the pathway is immense.

### 6.3 Conclusion

The aim of this study was to identify new mTOR splicing isoforms, the molecular characterization of the identified isoform and to study the role of their in the mTOR-mediated cellular processes, such as cell proliferation, cell survival and oncogenic transformation.

In this study we provide evidence for the existence of two novel mTOR splicing isoforms, termed mTOR $\delta$  and mTOR $\gamma$ . Bioinformatics and sequencing analysis revealed that mTOR $\delta$  retains only the N-terminal HEAT repeats and a unique protein sequence, originated from a splicing-mediated frame shift. On the other hand, mTOR $\gamma$  possesses a 12-amino acids deletion, located at the beginning of the kinase domain, which contains conserved residues that are critical for ATP binding and the kinase activity. The existence of both mTOR $\delta$  and mTOR $\gamma$  splicing variants was verified at the mRNA level through the identification of EST clones with corresponding exon-exon junctions. In addition, a specific immune-reactive band of approximately 150kDa was readily detected in a panel of cell lines when examined by Western blotting with specific anti-mTOR $\delta$  antibodies. Using transient and stable overexpression systems, we demonstrated that mTOR $\delta$  and mTOR $\gamma$  lack the kinase activity *in vitro*. We also found that stable overexpression of mTOR $\delta$  and mTOR $\gamma$  splicing forms in HEK293 cells results in the inhibition of cell proliferation and

colony formation in soft agar. Taken together, these novel findings suggest that identified mTOR $\delta$  and mTOR $\gamma$  have the potential to regulate the mTOR signalling pathway in a dominant-negative manner. However, the underlying mechanisms of uncovered regulation remain to be identified.

## 6.4 Future directions for mTOR $\delta$ and mTOR $\gamma$

A major effort is needed to exploit the full potential of these isoforms. It is important to elucidate the molecular mechanism by which mTOR $\delta$  and mTOR $\gamma$  regulate signalling pathways and cellular functions. It would be interesting to investigate the role of mTOR $\delta$  and mTOR $\gamma$  isoforms in the regulation of mTOR-mediated cellular functions such as cell growth, survival, and cell cycle regulation. Since the mTOR $\beta$  protein significantly shortens the G1 phase of the cell cycle and stimulate cellular proliferation, therefore it is important to test whether the mTOR $\delta$  and the mTOR $\gamma$  isoforms affect cell cycle regulation and cell size (Panasyuk et al. 2009).

The future work has been prioritised according to the relevance and importance of the information to better understand the role and regulation of mTOR $\delta$  and mTOR $\gamma$ . I have initiated the work on examining cellular localization of mTOR $\delta$  and mTOR $\gamma$  splicing variants, as well as the effect of the mTOR $\delta$  on cell cycle control, cell size and the progression of cancer in nude mice.

### 6.4.1 The effect of the mTOR $\delta$ and the mTOR $\gamma$ on the cell cycle and cell size

The treatment of cells with the mTOR inhibitor, rapamycin, leads to delayed cell cycle, reduced cell growth and cell size (Fingar et al. 2002). In addition it is proven that the mTOR $\beta$  protein significantly shortens the G1 phase of the cell cycle and stimulates the cellular proliferation (Panasyuk et al 2009).

In addition, in this study, the MTT proliferation assay and the colony formation assay have revealed that the mTOR $\delta$  and the mTOR $\gamma$  are dominant negative regulators of the cellular proliferation. It is important to elucidate whether the mTOR $\delta$  isoform arrest the cell cycle or take the cells into a programmed cell death.

This study can be performed using HEK 293T cells over-expressing the mTOR $\delta$  and cells over-expressing the mTOR $\gamma$  isoforms. The cellular DNA will be labelled with propidium iodide and scanned by FACScan flow-cytometer and forward scatter analysis.

#### **6.4.2 Cellular localization of the mTOR $\delta$ and the mTOR $\gamma$**

In cells, mTOR is localized predominantly in endoplasmic reticulum, Golgi, and mitochondria membranes, as well as the nucleus (Desai et al. 2002;Liu & Zheng 2007;Zhang et al. 2002). Liu and Zheng reported that a sequences located within the HEAT domains is implicated in mediating mTOR membrane localization (Liu & Zheng 2007). To create a better understanding about the regulation and the role of the mTOR $\delta$  and the mTOR $\gamma$  in cellular functions, it would be interesting to study the nuclear localization of these isoforms.

This can be performed by subcellular fractionation followed by immune-blotting and immune-florescence analysis to identify the subcellular localization of the mTOR $\delta$  and the mTOR $\gamma$ .

#### **6.4.3 The effect of the mTOR $\delta$ and the mTOR $\gamma$ on the progression of tumour in a xenograft model in nude mice**

It is hypothesized that the expression of the mTOR $\delta$  and the mTOR $\gamma$  would negatively affect the tumour progression. There is compelling evidence supporting

this hypothesis. The first evidence relies on the ability of mTOR protein to regulate multiple cellular processes including cellular growth, survival, development, metabolism, and angiogenic pathways. Dysregulation of these processes represent characteristic hallmarks of cancer (Hanahan and Weinberg 2011). Secondly, since the dysregulation of mTOR activities and mTOR signalling pathway is implicated in a wide variety of malignancies, the identified proteins are mTOR isoforms which may affect the mTOR pathway regulation. The third relies on the fact that the alternative splicing significantly regulates many oncogenes and tumour-suppressors.

In addition, the MTT proliferation assay has shown that the mTOR $\delta$  and the mTOR $\gamma$  are dominant negative regulators of the cellular proliferation. Moreover, series of colony formation assays have shown that the expression of the mTOR $\delta$  and the mTOR $\gamma$  in HEK 293T cells resulted in significantly less number of colonies compared to parental HEK 293T cells.

It would be interesting to elucidate whether the over-expression of the mTOR $\delta$  and the mTOR $\gamma$  splicing isoforms in a tumour can provide a significant anti-proliferative activity and obtain disease stabilization or even tumour regression, or enhance the efficacy of other anticancer drugs. This can be achieved by injecting nude mice with the HEK 293T cells over-expressing the mTOR $\delta$  and the mTOR $\gamma$  isoforms independently, and then the appearance and growth of tumours generated will be assessed over a period of 2 to 3 months. The tissue from the xenograft of nude mice will then be removed for microscopic and molecular studies.

#### **6.4.4 Binding partners of the mTOR $\delta$ and the mTOR $\gamma$**

In human cells, mTOR protein comes in two distinct multi-protein complexes, mTORC1 and mTORC2. In addition to mTOR protein, the mTORC1 is composed of

raptor, mLST8/GβL, PRAS40 and the recently reported IPMK (Hara et al. 2002;Kim et al. 2002;Kim et al. 2003;Kim et al. 2011;Vander et al. 2007). The second complex is mTORC2 which contains mTOR and mLST8/GβL, rictor, mSin1 and protor (Frias et al. 2006;Jacinto et al. 2004;Pearce et al. 2007;Sarbasov et al. 2004;Yang et al. 2006). As described in chapter 1, phosphorylation of different substrates depends on the association of mTOR with different partners, and some of these partners are critical, while lacking the others does not show any effect on the mTOR activities.

In yeast, TOR participates in a variety of cellular processes and some of these roles have not yet been identified in mammals (Crespo and Hall 2002;Rohde et al. 2001). It is important to identify the binding partners for the mTOR $\delta$  and mTOR $\gamma$  which will help to better understand which pathway and feedback loops and cross-talks they could participate in and its potential role on cellular functions. The novel amino acids sequence at the COOH-terminus of mTOR $\delta$  increase the chances of identifying new binding partners.

## Appendices

### Appendix A: Buffers and solutions

Solution/buffer	Ingredients
<b>EB Buffer</b> <b>(Extraction buffer) (Lysis buffer)</b>	20 mM Tris HCl pH 7.5, 1 % Triton X-100, 150 mM NaCl, 5 mM EDTA, 50 mM NaF, EDTAfree protease inhibitor cocktail (Roche)
<b>ECL reagent 1</b>	50 mM Tris-HCl pH 8.5, luminol, $\alpha$ -coumaric acid
<b>ECL reagent 2</b>	50 mM Tris-HCl pH 8.5, 0.02 % H <sub>2</sub> O <sub>2</sub>
<b>Hypotonic Buffer</b>	20 mM HEPES pH 7.9, 0.5 mM dithiotreitol (DTT), EDTA-free protease inhibitor cocktail (Roche)
<b>Kinase assay buffer</b>	50 mM Hepes, pH 7.5, 10 mM MgCl <sub>2</sub> , 1 mM DTT, 10 mM 3-glycerophosphate, 1 $\mu$ M PKA inhibitor
<b>Laemmli sample buffer (5X)</b>	250 mM Tris pH 6.8, 5 0% glycerol, 0.5 % bromophenol blue, 500 mM DTT, 10 % SDS
<b>LB Agar</b>	1 % (w/v) bactotryptone, 0.5 % (w/v) yeast extract, 0.5 % NaCl, 1.5 % (w/v) bacto-agar
<b>LB Broth</b>	1 % (w/v) tryptone, 0.5 % yeast extract, 0.5 %

Solution/buffer	Ingredients
	NaCl
<b>Loading Buffer (6X) (Laemmli sample buffer)</b>	0.25% (w/v) bromophenol blue, 0.25% (w/v) xylene cyanol FF, 30% (w/v) glycerol in water
<b>Phosphate-buffered saline (PBS)</b>	137 mM NaCl, 2.7 mM KCl, 4.3 mM Na <sub>2</sub> HPO <sub>4</sub> , 1.4 mM KH <sub>2</sub> PO <sub>4</sub> , pH 7.4
<b>Primary antibody buffer</b>	TBS, 2 % BSA, 0.1% TWEEN-20, 0.02 % Sodium azide
<b>Stripping buffer</b>	62.5 mM Tris-HCl, pH 6.7; 2 % SDS; 100 mM 2-mercaptoethanol
<b>TAE Buffer</b>	40 mM Tris-Acetate, 1 mM EDTA
<b>TBST buffer</b>	10 mM Tris, 150 mM NaCl, 0.1 % TWEEN-20
<b>Transfer Buffer</b>	25 mM Tris, 200 mM Glycine, 20% methanol (v/v))
<b>Tris-Glycine Running Buffer</b>	0.25 mM Tris, 250 mM glycine, 0.1 % SDS
<b>Tris-HEPEs Running Buffer</b>	100 mM Tris, 100 mM HEPES, 1 % SDS, pH 8.0
<b>Western Blocking Buffer</b>	1. TBS, 5 % non-fat dry milk, 0.1 % TWEEN-20 2. TBS, 2% BSA, 0.1% TWEEN-20

## References

- Avruch, J., Lin, Y., Long, X., Murthy, S., & Ortiz-Vega, S. 2005. Recent advances in the regulation of the TOR pathway by insulin and nutrients. *Curr.Opin.Clin.Nutr.Metab Care*, 8, (1) 67-72 available from: PM:15586002
- Beck, T. & Hall, M.N. 1999. The TOR signalling pathway controls nuclear localization of nutrient-regulated transcription factors. *Nature*, 402, (6762) 689-692 available from: PM:10604478
- Beevers, C.S., Li, F., Liu, L., & Huang, S. 2006. Curcumin inhibits the mammalian target of rapamycin-mediated signaling pathways in cancer cells. *Int.J.Cancer*, 119, (4) 757-764 available from: PM:16550606
- Blommaart, E.F., Luiken, J.J., Blommaart, P.J., van Woerkom, G.M., & Meijer, A.J. 1995. Phosphorylation of ribosomal protein S6 is inhibitory for autophagy in isolated rat hepatocytes. *J.Biol.Chem.*, 270, (5) 2320-2326 available from: PM:7836465
- Brown, E.J., Albers, M.W., Shin, T.B., Ichikawa, K., Keith, C.T., Lane, W.S., & Schreiber, S.L. 1994. A mammalian protein targeted by G1-arresting rapamycin-receptor complex. *Nature*, 369, (6483) 756-758 available from: PM:8008069
- Brown, E.J., Beal, P.A., Keith, C.T., Chen, J., Shin, T.B., & Schreiber, S.L. 1995. Control of p70 s6 kinase by kinase activity of FRAP in vivo. *Nature*, 377, (6548) 441-446 available from: PM:7566123

Brunn, G.J., Hudson, C.C., Sekulic, A., Williams, J.M., Hosoi, H., Houghton, P.J., Lawrence, J.C., Jr., & Abraham, R.T. 1997. Phosphorylation of the translational repressor PHAS-I by the mammalian target of rapamycin. *Science*, 277, (5322) 99-101 available from: PM:9204908

Brunn, G.J., Williams, J., Sabers, C., Wiederrecht, G., Lawrence, J.C., Jr., & Abraham, R.T. 1996. Direct inhibition of the signaling functions of the mammalian target of rapamycin by the phosphoinositide 3-kinase inhibitors, wortmannin and LY294002. *EMBO J.*, 15, (19) 5256-5267 available from: PM:8895571

Burnett, P.E., Barrow, R.K., Cohen, N.A., Snyder, S.H., & Sabatini, D.M. 1998. RAFT1 phosphorylation of the translational regulators p70 S6 kinase and 4E-BP1. *Proc.Natl.Acad.Sci.U.S.A.*, 95, (4) 1432-1437 available from: PM:9465032

Chen, J., Zheng, X.F., Brown, E.J., & Schreiber, S.L. 1995. Identification of an 11-kDa FKBP12-rapamycin-binding domain within the 289-kDa FKBP12-rapamycin-associated protein and characterization of a critical serine residue. *Proc.Natl.Acad.Sci.U.S.A.*, 92, (11) 4947-4951 available from: PM:7539137

Chen, S., Atkins, C.M., Liu, C.L., Alonso, O.F., Dietrich, W.D., & Hu, B.R. 2007. Alterations in mammalian target of rapamycin signaling pathways after traumatic brain injury. *J.Cereb.Blood Flow Metab*, 27, (5) 939-949 available from: PM:16955078

Chen, Y., Chen, H., Rhoad, A.E., Warner, L., Caggiano, T.J., Failli, A., Zhang, H., Hsiao, C.L., Nakanishi, K., & Molnar-Kimber, K.L. 1994. A putative sirolimus (rapamycin) effector protein. *Biochem.Biophys.Res.Commun.*, 203, (1) 1-7 available

from: PM:7521160

Chiang, G.G. & Abraham, R.T. 2005. Phosphorylation of mammalian target of rapamycin (mTOR) at Ser-2448 is mediated by p70S6 kinase. *J.Biol.Chem.*, 280, (27) 25485-25490 available from: PM:15899889

Chiu, M.I., Katz, H., & Berlin, V. 1994. RAPT1, a mammalian homolog of yeast Tor, interacts with the FKBP12/rapamycin complex. *Proc.Natl.Acad.Sci.U.S.A*, 91, (26) 12574-12578 available from: PM:7809080

Choi, J., Chen, J., Schreiber, S.L., & Clardy, J. 1996. Structure of the FKBP12-rapamycin complex interacting with the binding domain of human FRAP. *Science*, 273, (5272) 239-242 available from: PM:8662507

Choo, A.Y., Roux, P.P., & Blenis, J. 2006. Mind the GAP: Wnt steps onto the mTORC1 train. *Cell*, 126, (5) 834-836 available from: PM:16959561

Choo, A.Y., Yoon, S.O., Kim, S.G., Roux, P.P., & Blenis, J. 2008. Rapamycin differentially inhibits S6Ks and 4E-BP1 to mediate cell-type-specific repression of mRNA translation. *Proc.Natl.Acad.Sci.U.S.A*, 105, (45) 17414-17419 available from: PM:18955708

Corradetti, M.N. & Guan, K.L. 2006. Upstream of the mammalian target of rapamycin: do all roads pass through mTOR? *Oncogene*, 25, (48) 6347-6360 available from: PM:17041621

Crespo, J.L. & Hall, M.N. 2002. Elucidating TOR signaling and rapamycin action: lessons from *Saccharomyces cerevisiae*. *Microbiol.Mol.Biol.Rev.*, 66, (4) 579-91,

table available from: PM:12456783

Cunningham, J.T., Rodgers, J.T., Arlow, D.H., Vazquez, F., Mootha, V.K., & Puigserver, P. 2007. mTOR controls mitochondrial oxidative function through a YY1-PGC-1alpha transcriptional complex. *Nature*, 450, (7170) 736-740 available from: PM:18046414

Dancey, J.E. 2005. Inhibitors of the mammalian target of rapamycin. *Expert.Opin.Investig.Drugs*, 14, (3) 313-328 available from: PM:15833062

Dazert, E. & Hall, M.N. 2011. mTOR signaling in disease. *Curr.Opin.Cell Biol.*, 23, (6) 744-755 available from: PM:21963299

de Groot, R.P., Delmas, V., & Sassone-Corsi, P. 1994. DNA bending by transcription factors CREM and CREB. *Oncogene*, 9, (2) 463-468 available from: PM:8290258

Desai, B.N., Myers, B.R., & Schreiber, S.L. 2002. FKBP12-rapamycin-associated protein associates with mitochondria and senses osmotic stress via mitochondrial dysfunction. *Proc.Natl.Acad.Sci.U.S.A.*, 99, (7) 4319-4324 available from: PM:11930000

Di Como, C.J. & Arndt, K.T. 1996. Nutrients, via the Tor proteins, stimulate the association of Tap42 with type 2A phosphatases. *Genes Dev.*, 10, (15) 1904-1916 available from: PM:8756348

Dowling, R.J., Topisirovic, I., Fonseca, B.D., & Sonenberg, N. 2010. Dissecting the role of mTOR: lessons from mTOR inhibitors. *Biochim.Biophys.Acta*, 1804, (3) 433-439 available from: PM:20005306

Drenan, R.M., Liu, X., Bertram, P.G., & Zheng, X.F. 2004. FKBP12-rapamycin-associated protein or mammalian target of rapamycin (FRAP/mTOR) localization in the endoplasmic reticulum and the Golgi apparatus. *J.Biol.Chem.*, 279, (1) 772-778 available from: PM:14578359

Dunlop, E.A. & Tee, A.R. 2009. Mammalian target of rapamycin complex 1: signalling inputs, substrates and feedback mechanisms. *Cell Signal.*, 21, (6) 827-835 available from: PM:19166929

Edinger, A.L. & Thompson, C.B. 2002. Akt maintains cell size and survival by increasing mTOR-dependent nutrient uptake. *Mol.Biol.Cell*, 13, (7) 2276-2288 available from: PM:12134068

Fang, Y., Vilella-Bach, M., Bachmann, R., Flanigan, A., & Chen, J. 2001. Phosphatidic acid-mediated mitogenic activation of mTOR signaling. *Science*, 294, (5548) 1942-1945 available from: PM:11729323

Fasolo, A. & Sessa, C. 2011. Current and future directions in mammalian target of rapamycin inhibitors development. *Expert.Opin.Investig.Drugs*, 20, (3) 381-394 available from: PM:21299441

Feldman, M.E., Apsel, B., Uotila, A., Loewith, R., Knight, Z.A., Ruggero, D., & Shokat, K.M. 2009. Active-site inhibitors of mTOR target rapamycin-resistant outputs of mTORC1 and mTORC2. *PLoS.Biol.*, 7, (2) e38 available from: PM:19209957

Fingar, D.C. & Blenis, J. 2004. Target of rapamycin (TOR): an integrator of nutrient and growth factor signals and coordinator of cell growth and cell cycle progression.

*Oncogene*, 23, (18) 3151-3171 available from: PM:15094765

Fingar, D.C., Salama, S., Tsou, C., Harlow, E., & Blenis, J. 2002. Mammalian cell size is controlled by mTOR and its downstream targets S6K1 and 4EBP1/eIF4E. *Genes Dev.*, 16, (12) 1472-1487 available from: PM:12080086

Foster, D.A. 2004. Targeting mTOR-mediated survival signals in anticancer therapeutic strategies. *Expert.Rev.Anticancer Ther.*, 4, (4) 691-701 available from: PM:15270672

Frias, M.A., Thoreen, C.C., Jaffe, J.D., Schroder, W., Sculley, T., Carr, S.A., & Sabatini, D.M. 2006. mSin1 is necessary for Akt/PKB phosphorylation, and its isoforms define three distinct mTORC2s. *Curr.Biol.*, 16, (18) 1865-1870 available from: PM:16919458

Ganley, I.G., Lam, d.H., Wang, J., Ding, X., Chen, S., & Jiang, X. 2009. ULK1.ATG13.FIP200 complex mediates mTOR signaling and is essential for autophagy. *J.Biol.Chem.*, 284, (18) 12297-12305 available from: PM:19258318

Garcia-Martinez, J.M., Moran, J., Clarke, R.G., Gray, A., Cosulich, S.C., Chresta, C.M., & Alessi, D.R. 2009. Ku-0063794 is a specific inhibitor of the mammalian target of rapamycin (mTOR). *Biochem.J.*, 421, (1) 29-42 available from: PM:19402821

Gingras, A.C., Gygi, S.P., Raught, B., Polakiewicz, R.D., Abraham, R.T., Hoekstra, M.F., Aebersold, R., & Sonenberg, N. 1999. Regulation of 4E-BP1 phosphorylation: a novel two-step mechanism. *Genes Dev.*, 13, (11) 1422-1437 available from: PM:10364159

Gingras, A.C., Raught, B., Gygi, S.P., Niedzwiecka, A., Miron, M., Burley, S.K., Polakiewicz, R.D., Wyslouch-Cieszynska, A., Aebersold, R., & Sonenberg, N. 2001a. Hierarchical phosphorylation of the translation inhibitor 4E-BP1. *Genes Dev.*, 15, (21) 2852-2864 available from: PM:11691836

Gingras, A.C., Raught, B., & Sonenberg, N. 2001b. Regulation of translation initiation by FRAP/mTOR. *Genes Dev.*, 15, (7) 807-826 available from: PM:11297505

Gingras, A.C., Raught, B., & Sonenberg, N. 2004. mTOR signaling to translation. *Curr.Top.Microbiol.Immunol.*, 279, 169-197 available from: PM:14560958

Graff, J.R. & Zimmer, S.G. 2003. Translational control and metastatic progression: enhanced activity of the mRNA cap-binding protein eIF-4E selectively enhances translation of metastasis-related mRNAs. *Clin.Exp.Metastasis*, 20, (3) 265-273 available from: PM:12741684

Guertin, D.A. & Sabatini, D.M. 2005. An expanding role for mTOR in cancer. *Trends Mol.Med.*, 11, (8) 353-361 available from: PM:16002336

Guertin, D.A. & Sabatini, D.M. 2007. Defining the role of mTOR in cancer. *Cancer Cell*, 12, (1) 9-22 available from: PM:17613433

Guertin, D.A., Stevens, D.M., Thoreen, C.C., Burds, A.A., Kalaany, N.Y., Moffat, J., Brown, M., Fitzgerald, K.J., & Sabatini, D.M. 2006. Ablation in mice of the mTORC components raptor, rictor, or mLST8 reveals that mTORC2 is required for signaling to Akt-FOXO and PKCalpha, but not S6K1. *Dev.Cell*, 11, (6) 859-871 available from: PM:17141160

Hannan, K.M., Brandenburger, Y., Jenkins, A., Sharkey, K., Cavanaugh, A., Rothblum, L., Moss, T., Poortinga, G., McArthur, G.A., Pearson, R.B., & Hannan, R.D. 2003. mTOR-dependent regulation of ribosomal gene transcription requires S6K1 and is mediated by phosphorylation of the carboxy-terminal activation domain of the nucleolar transcription factor UBF. *Mol.Cell Biol.*, 23, (23) 8862-8877 available from: PM:14612424

Hara, K., Maruki, Y., Long, X., Yoshino, K., Oshiro, N., Hidayat, S., Tokunaga, C., Avruch, J., & Yonezawa, K. 2002. Raptor, a binding partner of target of rapamycin (TOR), mediates TOR action. *Cell*, 110, (2) 177-189 available from: PM:12150926

Harada, H., Andersen, J.S., Mann, M., Terada, N., & Korsmeyer, S.J. 2001. p70S6 kinase signals cell survival as well as growth, inactivating the pro-apoptotic molecule BAD. *Proc.Natl.Acad.Sci.U.S.A*, 98, (17) 9666-9670 available from: PM:11493700

Hardie, D.G. 2008. AMPK and Raptor: matching cell growth to energy supply. *Mol.Cell*, 30, (3) 263-265 available from: PM:18471972

Harris, T.E. & Lawrence, J.C., Jr. 2003. TOR signaling. *Sci.STKE.*, 2003, (212) re15 available from: PM:14668532

Hay, N. & Sonenberg, N. 2004. Upstream and downstream of mTOR. *Genes Dev.*, 18, (16) 1926-1945 available from: PM:15314020

Heesom, K.J. & Denton, R.M. 1999. Dissociation of the eukaryotic initiation factor-4E/4E-BP1 complex involves phosphorylation of 4E-BP1 by an mTOR-associated kinase. *FEBS Lett.*, 457, (3) 489-493 available from: PM:10471835

Heitman, J., Movva, N.R., Hiestand, P.C., & Hall, M.N. 1991. FK 506-binding

protein proline rotamase is a target for the immunosuppressive agent FK 506 in *Saccharomyces cerevisiae*. *Proc.Natl.Acad.Sci.U.S.A*, 88, (5) 1948-1952 available from: PM:1705713

Holz, M.K. & Blenis, J. 2005. Identification of S6 kinase 1 as a novel mammalian target of rapamycin (mTOR)-phosphorylating kinase. *J.Biol.Chem.*, 280, (28) 26089-26093 available from: PM:15905173

Horton, J.D., Goldstein, J.L., & Brown, M.S. 2002. SREBPs: activators of the complete program of cholesterol and fatty acid synthesis in the liver. *J.Clin.Invest*, 109, (9) 1125-1131 available from: PM:11994399

Hosokawa, N., Hara, T., Kaizuka, T., Kishi, C., Takamura, A., Miura, Y., Iemura, S., Natsume, T., Takehana, K., Yamada, N., Guan, J.L., Oshiro, N., & Mizushima, N. 2009a. Nutrient-dependent mTORC1 association with the ULK1-Atg13-FIP200 complex required for autophagy. *Mol.Biol.Cell*, 20, (7) 1981-1991 available from: PM:19211835

Hosokawa, N., Sasaki, T., Iemura, S., Natsume, T., Hara, T., & Mizushima, N. 2009b. Atg101, a novel mammalian autophagy protein interacting with Atg13. *Autophagy*, 5, (7) 973-979 available from: PM:19597335

Hresko, R.C. & Mueckler, M. 2005. mTOR.RICTOR is the Ser473 kinase for Akt/protein kinase B in 3T3-L1 adipocytes. *J.Biol.Chem.*, 280, (49) 40406-40416 available from: PM:16221682

Huang, S. & Houghton, P.J. 2001. Mechanisms of resistance to rapamycins. *Drug Resist.Updat.*, 4, (6) 378-391 available from: PM:12030785

Iiboshi, Y., Papst, P.J., Kawasome, H., Hosoi, H., Abraham, R.T., Houghton, P.J., & Terada, N. 1999. Amino acid-dependent control of p70(s6k). Involvement of tRNA aminoacylation in the regulation. *J.Biol.Chem.*, 274, (2) 1092-1099 available from: PM:9873056

Inoki, K., Zhu, T., & Guan, K.L. 2003. TSC2 mediates cellular energy response to control cell growth and survival. *Cell*, 115, (5) 577-590 available from: PM:14651849

Jacinto, E., Guo, B., Arndt, K.T., Schmelzle, T., & Hall, M.N. 2001. TIP41 interacts with TAP42 and negatively regulates the TOR signaling pathway. *Mol.Cell*, 8, (5) 1017-1026 available from: PM:11741537

Jacinto, E., Loewith, R., Schmidt, A., Lin, S., Rugg, M.A., Hall, A., & Hall, M.N. 2004. Mammalian TOR complex 2 controls the actin cytoskeleton and is rapamycin insensitive. *Nat.Cell Biol.*, 6, (11) 1122-1128 available from: PM:15467718

Jastrzebski, K., Hannan, K.M., Tchoubrieva, E.B., Hannan, R.D., & Pearson, R.B. 2007. Coordinate regulation of ribosome biogenesis and function by the ribosomal protein S6 kinase, a key mediator of mTOR function. *Growth Factors*, 25, (4) 209-226 available from: PM:18092230

Jiang, Y. & Broach, J.R. 1999. Tor proteins and protein phosphatase 2A reciprocally regulate Tap42 in controlling cell growth in yeast. *EMBO J.*, 18, (10) 2782-2792 available from: PM:10329624

Jung, C.H., Ro, S.H., Cao, J., Otto, N.M., & Kim, D.H. 2010. mTOR regulation of autophagy. *FEBS Lett.*, 584, (7) 1287-1295 available from: PM:20083114

Kim, D.H., Sarbassov, D.D., Ali, S.M., King, J.E., Latek, R.R., Erdjument-Bromage, H., Tempst, P., & Sabatini, D.M. 2002. mTOR interacts with raptor to form a nutrient-sensitive complex that signals to the cell growth machinery. *Cell*, 110, (2) 163-175 available from: PM:12150925

Kim, D.H., Sarbassov, D.D., Ali, S.M., Latek, R.R., Guntur, K.V., Erdjument-Bromage, H., Tempst, P., & Sabatini, D.M. 2003. GbetaL, a positive regulator of the rapamycin-sensitive pathway required for the nutrient-sensitive interaction between raptor and mTOR. *Mol.Cell*, 11, (4) 895-904 available from: PM:12718876

Kim, J.E. & Chen, J. 2000. Cytoplasmic-nuclear shuttling of FKBP12-rapamycin-associated protein is involved in rapamycin-sensitive signaling and translation initiation. *Proc.Natl.Acad.Sci.U.S.A*, 97, (26) 14340-14345 available from: PM:11114166

Kim, S., Kim, S.F., Maag, D., Maxwell, M.J., Resnick, A.C., Juluri, K.R., Chakraborty, A., Koldobskiy, M.A., Cha, S.H., Barrow, R., Snowman, A.M., & Snyder, S.H. 2011. Amino Acid Signaling to mTOR Mediated by Inositol Polyphosphate Multikinase. *Cell Metab*, 13, (2) 215-221 available from: PM:21284988

Kimball, S.R., Orellana, R.A., O'Connor, P.M., Suryawan, A., Bush, J.A., Nguyen, H.V., Thivierge, M.C., Jefferson, L.S., & Davis, T.A. 2003. Endotoxin induces differential regulation of mTOR-dependent signaling in skeletal muscle and liver of neonatal pigs. *Am.J.Physiol Endocrinol.Metab*, 285, (3) E637-E644 available from: PM:12773308

Koh, Y.K., Lee, M.Y., Kim, J.W., Kim, M., Moon, J.S., Lee, Y.J., Ahn, Y.H., &

Kim, K.S. 2008. Lipin1 is a key factor for the maturation and maintenance of adipocytes in the regulatory network with CCAAT/enhancer-binding protein alpha and peroxisome proliferator-activated receptor gamma 2. *J.Biol.Chem.*, 283, (50) 34896-34906 available from: PM:18930917

Koltin, Y., Faucette, L., Bergsma, D.J., Levy, M.A., Cafferkey, R., Koser, P.L., Johnson, R.K., & Livi, G.P. 1991. Rapamycin sensitivity in *Saccharomyces cerevisiae* is mediated by a peptidyl-prolyl cis-trans isomerase related to human FK506-binding protein. *Mol.Cell Biol.*, 11, (3) 1718-1723 available from: PM:1996117

Lang, C.H. & Frost, R.A. 2007. Sepsis-induced suppression of skeletal muscle translation initiation mediated by tumor necrosis factor alpha. *Metabolism*, 56, (1) 49-57 available from: PM:17161226

Laplante, M. & Sabatini, D.M. 2009a. An emerging role of mTOR in lipid biosynthesis. *Curr.Biol.*, 19, (22) R1046-R1052 available from: PM:19948145

Laplante, M. & Sabatini, D.M. 2009b. mTOR signaling at a glance. *J.Cell Sci.*, 122, (Pt 20) 3589-3594 available from: PM:19812304

Laplante, M. & Sabatini, D.M. 2012. mTOR signaling in growth control and disease. *Cell*, 149, (2) 274-293 available from: PM:22500797

Lee, C.C., Huang, C.C., Wu, M.Y., & Hsu, K.S. 2005. Insulin stimulates postsynaptic density-95 protein translation via the phosphoinositide 3-kinase-Akt-mammalian target of rapamycin signaling pathway. *J.Biol.Chem.*, 280, (18) 18543-18550 available from: PM:15755733

Liu, X. & Zheng, X.F. 2007. Endoplasmic reticulum and Golgi localization sequences for mammalian target of rapamycin. *Mol.Biol.Cell*, 18, (3) 1073-1082 available from: PM:17215520

Loewith, R., Jacinto, E., Wullschleger, S., Lorberg, A., Crespo, J.L., Bonenfant, D., Oppliger, W., Jenoe, P., & Hall, M.N. 2002. Two TOR complexes, only one of which is rapamycin sensitive, have distinct roles in cell growth control. *Mol.Cell*, 10, (3) 457-468 available from: PM:12408816

Long, X., Lin, Y., Ortiz-Vega, S., Yonezawa, K., & Avruch, J. 2005a. Rheb binds and regulates the mTOR kinase. *Curr.Biol.*, 15, (8) 702-713 available from: PM:15854902

Long, X., Ortiz-Vega, S., Lin, Y., & Avruch, J. 2005b. Rheb binding to mammalian target of rapamycin (mTOR) is regulated by amino acid sufficiency. *J.Biol.Chem.*, 280, (25) 23433-23436 available from: PM:15878852

Ma, X.M. & Blenis, J. 2009. Molecular mechanisms of mTOR-mediated translational control. *Nat.Rev.Mol.Cell Biol.*, 10, (5) 307-318 available from: PM:19339977

Manning, B.D. & Cantley, L.C. 2007. AKT/PKB signaling: navigating downstream. *Cell*, 129, (7) 1261-1274 available from: PM:17604717

Mayer, C., Zhao, J., Yuan, X., & Grummt, I. 2004. mTOR-dependent activation of the transcription factor TIF-IA links rRNA synthesis to nutrient availability. *Genes Dev.*, 18, (4) 423-434 available from: PM:15004009

McMahon, L.P., Yue, W., Santen, R.J., & Lawrence, J.C., Jr. 2005. Farnesylthiosalicylic acid inhibits mammalian target of rapamycin (mTOR) activity

both in cells and in vitro by promoting dissociation of the mTOR-raptor complex.

*Mol.Endocrinol.*, 19, (1) 175-183 available from: PM:15459249

Mita, M.M. & Tolcher, A.W. 2007. The role of mTOR inhibitors for treatment of sarcomas. *Curr.Oncol.Rep.*, 9, (4) 316-322 available from: PM:17588357

Mothe-Satney, I., Brunn, G.J., McMahon, L.P., Capaldo, C.T., Abraham, R.T., & Lawrence, J.C., Jr. 2000a. Mammalian target of rapamycin-dependent phosphorylation of PHAS-I in four (S/T)P sites detected by phospho-specific antibodies. *J.Biol.Chem.*, 275, (43) 33836-33843 available from: PM:10942774

Mothe-Satney, I., Yang, D., Fadden, P., Haystead, T.A., & Lawrence, J.C., Jr. 2000b. Multiple mechanisms control phosphorylation of PHAS-I in five (S/T)P sites that govern translational repression. *Mol.Cell Biol.*, 20, (10) 3558-3567 available from: PM:10779345

Murata, K., Wu, J., & Brautigan, D.L. 1997. B cell receptor-associated protein alpha4 displays rapamycin-sensitive binding directly to the catalytic subunit of protein phosphatase 2A. *Proc.Natl.Acad.Sci.U.S.A.*, 94, (20) 10624-10629 available from: PM:9380685

Panasyuk, G., Nemazanyy, I., Zhyvoloup, A., Filonenko, V., Davies, D., Robson, M., Pedley, R.B., Waterfield, M., & Gout, I. 2009. mTORbeta splicing isoform promotes cell proliferation and tumorigenesis. *J.Biol.Chem.*, 284, (45) 30807-30814 available from: PM:19726679

Pause, A., Belsham, G.J., Gingras, A.C., Donze, O., Lin, T.A., Lawrence, J.C., Jr., & Sonenberg, N. 1994. Insulin-dependent stimulation of protein synthesis by

phosphorylation of a regulator of 5'-cap function. *Nature*, 371, (6500) 762-767  
available from: PM:7935836

Pearce, L.R., Huang, X., Boudeau, J., Pawlowski, R., Wullschleger, S., Deak, M., Ibrahim, A.F., Gourlay, R., Magnuson, M.A., & Alessi, D.R. 2007. Identification of Protor as a novel Rictor-binding component of mTOR complex-2. *Biochem.J.*, 405, (3) 513-522 available from: PM:17461779

Peng, T., Golub, T.R., & Sabatini, D.M. 2002. The immunosuppressant rapamycin mimics a starvation-like signal distinct from amino acid and glucose deprivation. *Mol.Cell Biol.*, 22, (15) 5575-5584 available from: PM:12101249

Perry, J. & Kleckner, N. 2003. The ATRs, ATMs, and TORs are giant HEAT repeat proteins. *Cell*, 112, (2) 151-155 available from: PM:12553904

Peterson, R.T., Desai, B.N., Hardwick, J.S., & Schreiber, S.L. 1999. Protein phosphatase 2A interacts with the 70-kDa S6 kinase and is activated by inhibition of FKBP12-rapamycin-associated protein. *Proc.Natl.Acad.Sci.U.S.A*, 96, (8) 4438-4442  
available from: PM:10200280

Peterson, R.T. & Schreiber, S.L. 1998. Translation control: connecting mitogens and the ribosome. *Curr.Biol.*, 8, (7) R248-R250 available from: PM:9545190

Porstmann, T., Santos, C.R., Griffiths, B., Cully, M., Wu, M., Leever, S., Griffiths, J.R., Chung, Y.L., & Schulze, A. 2008. SREBP activity is regulated by mTORC1 and contributes to Akt-dependent cell growth. *Cell Metab*, 8, (3) 224-236 available from: PM:18762023

Pullen, N., Dennis, P.B., Andjelkovic, M., Dufner, A., Kozma, S.C., Hemmings,

B.A., & Thomas, G. 1998. Phosphorylation and activation of p70s6k by PDK1. *Science*, 279, (5351) 707-710 available from: PM:9445476

Pullen, N. & Thomas, G. 1997. The modular phosphorylation and activation of p70s6k. *FEBS Lett.*, 410, (1) 78-82 available from: PM:9247127

Richter, J.D. & Sonenberg, N. 2005. Regulation of cap-dependent translation by eIF4E inhibitory proteins. *Nature*, 433, (7025) 477-480 available from: PM:15690031

Rohde, J., Heitman, J., & Cardenas, M.E. 2001. The TOR kinases link nutrient sensing to cell growth. *J.Biol.Chem.*, 276, (13) 9583-9586 available from: PM:11266435

Rosen, E.D. & MacDougald, O.A. 2006. Adipocyte differentiation from the inside out. *Nat.Rev.Mol.Cell Biol.*, 7, (12) 885-896 available from: PM:17139329

Ruggero, D. & Pandolfi, P.P. 2003. Does the ribosome translate cancer? *Nat.Rev.Cancer*, 3, (3) 179-192 available from: PM:12612653

Sabatini, D.M., Barrow, R.K., Blackshaw, S., Burnett, P.E., Lai, M.M., Field, M.E., Bahr, B.A., Kirsch, J., Betz, H., & Snyder, S.H. 1999. Interaction of RAFT1 with gephyrin required for rapamycin-sensitive signaling. *Science*, 284, (5417) 1161-1164 available from: PM:10325225

Sabatini, D.M., Erdjument-Bromage, H., Lui, M., Tempst, P., & Snyder, S.H. 1994. RAFT1: a mammalian protein that binds to FKBP12 in a rapamycin-dependent fashion and is homologous to yeast TORs. *Cell*, 78, (1) 35-43 available from:

PM:7518356

Sabers, C.J., Martin, M.M., Brunn, G.J., Williams, J.M., Dumont, F.J., Wiederrecht, G., & Abraham, R.T. 1995. Isolation of a protein target of the FKBP12-rapamycin complex in mammalian cells. *J.Biol.Chem.*, 270, (2) 815-822 available from: PM:7822316

Saitoh, M., Pullen, N., Brennan, P., Cantrell, D., Dennis, P.B., & Thomas, G. 2002. Regulation of an activated S6 kinase 1 variant reveals a novel mammalian target of rapamycin phosphorylation site. *J.Biol.Chem.*, 277, (22) 20104-20112 available from: PM:11914378

Sancak, Y., Bar-Peled, L., Zoncu, R., Markhard, A.L., Nada, S., & Sabatini, D.M. 2010. Ragulator-Rag complex targets mTORC1 to the lysosomal surface and is necessary for its activation by amino acids. *Cell*, 141, (2) 290-303 available from: PM:20381137

Sancak, Y., Peterson, T.R., Shaul, Y.D., Lindquist, R.A., Thoreen, C.C., Bar-Peled, L., & Sabatini, D.M. 2008. The Rag GTPases bind raptor and mediate amino acid signaling to mTORC1. *Science*, 320, (5882) 1496-1501 available from: PM:18497260

Sancak, Y., Thoreen, C.C., Peterson, T.R., Lindquist, R.A., Kang, S.A., Spooner, E., Carr, S.A., & Sabatini, D.M. 2007. PRAS40 is an insulin-regulated inhibitor of the mTORC1 protein kinase. *Mol.Cell*, 25, (6) 903-915 available from: PM:17386266

Sarbassov, D.D., Ali, S.M., Kim, D.H., Guertin, D.A., Latek, R.R., Erdjument-Bromage, H., Tempst, P., & Sabatini, D.M. 2004. Rictor, a novel binding partner of

mTOR, defines a rapamycin-insensitive and raptor-independent pathway that regulates the cytoskeleton. *Curr.Biol.*, 14, (14) 1296-1302 available from: PM:15268862

Sarbassov, D.D., Ali, S.M., Sengupta, S., Sheen, J.H., Hsu, P.P., Bagley, A.F., Markhard, A.L., & Sabatini, D.M. 2006. Prolonged rapamycin treatment inhibits mTORC2 assembly and Akt/PKB. *Mol.Cell*, 22, (2) 159-168 available from: PM:16603397

Sarbassov, D.D., Guertin, D.A., Ali, S.M., & Sabatini, D.M. 2005. Phosphorylation and regulation of Akt/PKB by the rictor-mTOR complex. *Science*, 307, (5712) 1098-1101 available from: PM:15718470

Schaeffer, V. & Abrass, C.K. 2010. Mechanisms and control of protein translation in the kidney. *Am.J.Nephrol.*, 31, (3) 189-201 available from: PM:20029175

Schieke, S.M. & Finkel, T. 2006. Mitochondrial signaling, TOR, and life span. *Biol.Chem.*, 387, (10-11) 1357-1361 available from: PM:17081107

Schieke, S.M., Phillips, D., McCoy, J.P., Jr., Aponte, A.M., Shen, R.F., Balaban, R.S., & Finkel, T. 2006. The mammalian target of rapamycin (mTOR) pathway regulates mitochondrial oxygen consumption and oxidative capacity. *J.Biol.Chem.*, 281, (37) 27643-27652 available from: PM:16847060

Schmelzle, T. & Hall, M.N. 2000. TOR, a central controller of cell growth. *Cell*, 103, (2) 253-262 available from: PM:11057898

Schreiber, S.L. 1991. Chemistry and biology of the immunophilins and their immunosuppressive ligands. *Science*, 251, (4991) 283-287 available from:

PM:1702904

Sehgal, S.N. 2003. Sirolimus: its discovery, biological properties, and mechanism of action. *Transplant.Proc.*, 35, (3 Suppl) 7S-14S available from: PM:12742462

Sehgal, S.N., Baker, H., & Vezina, C. 1975. Rapamycin (AY-22,989), a new antifungal antibiotic. II. Fermentation, isolation and characterization. *J.Antibiot.(Tokyo)*, 28, (10) 727-732 available from: PM:1102509

Sekulic, A., Hudson, C.C., Homme, J.L., Yin, P., Otterness, D.M., Karnitz, L.M., & Abraham, R.T. 2000. A direct linkage between the phosphoinositide 3-kinase-AKT signaling pathway and the mammalian target of rapamycin in mitogen-stimulated and transformed cells. *Cancer Res.*, 60, (13) 3504-3513 available from: PM:10910062

Shaw, R.J. & Cantley, L.C. 2006. Ras, PI(3)K and mTOR signalling controls tumour cell growth. *Nature*, 441, (7092) 424-430 available from: PM:16724053

Shigemitsu, K., Tsujishita, Y., Hara, K., Nanahoshi, M., Avruch, J., & Yonezawa, K. 1999. Regulation of translational effectors by amino acid and mammalian target of rapamycin signaling pathways. Possible involvement of autophagy in cultured hepatoma cells. *J.Biol.Chem.*, 274, (2) 1058-1065 available from: PM:9873051

Shima, H., Pende, M., Chen, Y., Fumagalli, S., Thomas, G., & Kozma, S.C. 1998. Disruption of the p70(s6k)/p85(s6k) gene reveals a small mouse phenotype and a new functional S6 kinase. *EMBO J.*, 17, (22) 6649-6659 available from: PM:9822608

Sibanda, B.L., Chirgadze, D.Y., & Blundell, T.L. 2010. Crystal structure of DNA-PKcs reveals a large open-ring cradle comprised of HEAT repeats. *Nature*, 463,

(7277) 118-121 available from: PM:20023628

Stan, R., McLaughlin, M.M., Cafferkey, R., Johnson, R.K., Rosenberg, M., & Livi, G.P. 1994. Interaction between FKBP12-rapamycin and TOR involves a conserved serine residue. *J.Biol.Chem.*, 269, (51) 32027-32030 available from: PM:7528205

Thoreen, C.C., Kang, S.A., Chang, J.W., Liu, Q., Zhang, J., Gao, Y., Reichling, L.J., Sim, T., Sabatini, D.M., & Gray, N.S. 2009. An ATP-competitive mammalian target of rapamycin inhibitor reveals rapamycin-resistant functions of mTORC1. *J.Biol.Chem.*, 284, (12) 8023-8032 available from: PM:19150980

Thoreen, C.C. & Sabatini, D.M. 2009. Rapamycin inhibits mTORC1, but not completely. *Autophagy.*, 5, (5) 725-726 available from: PM:19395872

Tirado, O.M., Mateo-Lozano, S., Sanders, S., Dettin, L.E., & Notario, V. 2003. The PCPH oncoprotein antagonizes the proapoptotic role of the mammalian target of rapamycin in the response of normal fibroblasts to ionizing radiation. *Cancer Res.*, 63, (19) 6290-6298 available from: PM:14559816

Vander, H.E., Lee, S.I., Bandhakavi, S., Griffin, T.J., & Kim, D.H. 2007. Insulin signalling to mTOR mediated by the Akt/PKB substrate PRAS40. *Nat.Cell Biol.*, 9, (3) 316-323 available from: PM:17277771

Vezina, C., Kudelski, A., & Sehgal, S.N. 1975. Rapamycin (AY-22,989), a new antifungal antibiotic. I. Taxonomy of the producing streptomycete and isolation of the active principle. *J.Antibiot.(Tokyo)*, 28, (10) 721-726 available from: PM:1102508

Vilella-Bach, M., Nuzzi, P., Fang, Y., & Chen, J. 1999. The FKBP12-rapamycin-

binding domain is required for FKBP12-rapamycin-associated protein kinase activity and G1 progression. *J.Biol.Chem.*, 274, (7) 4266-4272 available from: PM:9933627

Vivanco, I. & Sawyers, C.L. 2002. The phosphatidylinositol 3-Kinase AKT pathway in human cancer. *Nat.Rev.Cancer*, 2, (7) 489-501 available from: PM:12094235

Vlahos, C.J., Matter, W.F., Hui, K.Y., & Brown, R.F. 1994. A specific inhibitor of phosphatidylinositol 3-kinase, 2-(4-morpholinyl)-8-phenyl-4H-1-benzopyran-4-one (LY294002). *J.Biol.Chem.*, 269, (7) 5241-5248 available from: PM:8106507

Wang, L., Harris, T.E., Roth, R.A., & Lawrence, J.C., Jr. 2007. PRAS40 regulates mTORC1 kinase activity by functioning as a direct inhibitor of substrate binding. *J.Biol.Chem.*, 282, (27) 20036-20044 available from: PM:17510057

Westphal, R.S., Coffee, R.L., Jr., Marotta, A., Pelech, S.L., & Wadzinski, B.E. 1999. Identification of kinase-phosphatase signaling modules composed of p70 S6 kinase-protein phosphatase 2A (PP2A) and p21-activated kinase-PP2A. *J.Biol.Chem.*, 274, (2) 687-692 available from: PM:9873003

Wiederrecht, G., Brizuela, L., Elliston, K., Sigal, N.H., & Siekierka, J.J. 1991. FKBP1 encodes a nonessential FK 506-binding protein in *Saccharomyces cerevisiae* and contains regions suggesting homology to the cyclophilins. *Proc.Natl.Acad.Sci.U.S.A*, 88, (3) 1029-1033 available from: PM:1704127

Wilson, K.F. & Cerione, R.A. 2000. Signal transduction and post-transcriptional gene expression. *Biol.Chem.*, 381, (5-6) 357-365 available from: PM:10937866

Withers, D.J., Ouwens, D.M., Nave, B.T., van der Zon, G.C., Alarcon, C.M., Cardenas, M.E., Heitman, J., Maassen, J.A., & Shepherd, P.R. 1997. Expression,

enzyme activity, and subcellular localization of mammalian target of rapamycin in insulin-responsive cells. *Biochem.Biophys.Res.Commun.*, 241, (3) 704-709 available from: PM:9434772

Wullschleger, S., Loewith, R., & Hall, M.N. 2006. TOR signaling in growth and metabolism. *Cell*, 124, (3) 471-484 available from: PM:16469695

Yang, Q., Inoki, K., Ikenoue, T., & Guan, K.L. 2006. Identification of Sin1 as an essential TORC2 component required for complex formation and kinase activity. *Genes Dev.*, 20, (20) 2820-2832 available from: PM:17043309

Yip, C.K., Murata, K., Walz, T., Sabatini, D.M., & Kang, S.A. 2010. Structure of the human mTOR complex I and its implications for rapamycin inhibition. *Mol.Cell*, 38, (5) 768-774 available from: PM:20542007

Yokogami, K., Wakisaka, S., Avruch, J., & Reeves, S.A. 2000. Serine phosphorylation and maximal activation of STAT3 during CNTF signaling is mediated by the rapamycin target mTOR. *Curr.Biol.*, 10, (1) 47-50 available from: PM:10660304

Young, D.A. & Nickerson-Nutter, C.L. 2005. mTOR--beyond transplantation. *Curr.Opin.Pharmacol.*, 5, (4) 418-423 available from: PM:15955739

Yu, K., Toral-Barza, L., Shi, C., Zhang, W.G., Lucas, J., Shor, B., Kim, J., Verheijen, J., Curran, K., Malwitz, D.J., Cole, D.C., Ellingboe, J., Ayral-Kaloustian, S., Mansour, T.S., Gibbons, J.J., Abraham, R.T., Nowak, P., & Zask, A. 2009. Biochemical, cellular, and in vivo activity of novel ATP-competitive and selective inhibitors of the mammalian target of rapamycin. *Cancer Res.*, 69, (15) 6232-6240

available from: PM:19584280